Transient stabilization of power systems : an unified approach

Diego Langarica Cordoba Langarica Ordoba

UNIVERSITE PARIS-SUD

ÉCOLE DOCTORALE
Sciences et Technologie de l'Information, des Télécommunications et des Systèmes
Laboratoire de *Signaux et Systems*

DISCIPLINE: Physique

THÈSE DE DOCTORAT

Soutenance prévue le 12/05/2014

par

Diego LANGARICA CORDOBA

Stabilisation Transitoire de Systèmes de Puissance: une approche unifiée

Transient Stabilization of Power Systems: An Unified Approach

UNIVERSITE PARIS-SUD

ÉCOLE DOCTORALE
Sciences et Technologie de l'Information, des Télécommunications et des Systèmes
Laboratoire des Signaux et Systèmes

DISCIPLINE: Physique

THÈSE DE DOCTORAT

Soutenance prévue le 12/05/2014

par

Diego LANGARICA CORDOBA

Stabilisation Transitoire de Systèmes de Puissance: une approche unifiée

Transient Stabilization of Power Systems: an unified approach

Composition du jury:

Directeur de thèse:	Romeo ORTEGA	Directeur de Recherche (LSS)
Rapporteurs:	Christophe PRIEUR	Directeur de Recherche (GIPSA-LAB)
	José CAÑEDO	Profeseur Chercheur (CINVESTAV)
Examinateurs:	Françoise LAMNABHI-LAGARRIGUE	Directeur de Recherche (LSS)
	Jean-Claude VANNIER	Professeur (SUPELEC)
	Daniele CASAGRANDE	Profesour Chercheur (UNIUD)
	Abdelkrim BENCHAIB	Chercheur (ALSTOM)
Membres invités:	Alejandro DONAIRE	Chercheur (U. NEWCASTLE)

Résumé

Un système de puissance électrique est un réseau complexe de composants électriques utilisés pour fournir, transmettre et utiliser l'énergie électrique. Son objectif final est d'offrir un service fiable, sécurisé et ininterrompu à l'utilisateur final, cela signifie, tension constante et fréquence constante en tout temps. Aujourd'hui, la tendance de la production d'électricité est vers un réseau interconnecté de lignes de transmission reliant la génération et les charges dans des grands systèmes intégrés. En fait, un réseau de système de puissance est considéré comme la machine la plus complexe et plus jamais construite par l'homme car elle peut s'étendre sur tout un continent. Pour cette raison, l'amélioration de la stabilité transitoire des réseaux électriques est d'une grande importance dans la société humaine, car si la stabilité est perdue, le collapse de la puissance peut se produire dans une grande zone peuplée et de graves dommages seront portées à l'économie régionale et les conforts des consommateurs.

Par conséquent, compte tenu de tous les problèmes présentés avant, ce travail de recherche aborde la stabilisation transitoire des systèmes de puissance multi-machines soumises à des perturbations du réseau à partir de deux approches: la centralisation, qui considère aucune limitation dans l'échange d'informations d'un réseau donné, et d'autre part, la décentralisation, qui suppose l'échange d'informations n'est pas disponible. À cette fin, d'abord, nous introduisons une nouvelle théorie de commande pour stabiliser globalement systèmes triangulaires non linéarisables globalement en utilisant une commande de rétroaction d'état dynamique non linéaire, qui diffère de backstepping puisque la forme stricte de rétroaction n'est plus nécessaire. Ensuite, sur la base de ces nouvelles idées, le problème de stabilisation transitoire des systèmes de puissance est résolu d'un point de vue centralisé, en assurant la stabilité asymptotique globale du point de fonctionnement, dans certaines conditions sur les paramètres physiques du système. Postérieurement, en utilisant uniquement les mesures locales disponibles avec la technologie existante, le contrôleur central précédent est transformé en un décentralisé, à condition que la dérivée de la puissance active à chaque générateur peut être appropriement estimée. La performance des deux contrôleurs est testée par des simulations numériques envisagent plusieurs scénarios de défaut en utilisant le système de 10 machines de Nouvelle-Angleterre. Contrairement aux solutions non linéaires ci-dessus, nous proposons une méthodologie basée sur observateur pour la stabilisation décentralisée des systèmes linéaires invariants dans le temps. L'originalité de ce travail repose sur le fait que chaque contrôleur local est fourni avec des mesures locales disponibles, il met en œuvre un observateur pour reconstruire l'état des autres sous-systèmes et utilise de manière équivalente ces estimations dans la loi de commande. Les observateurs sont conçus en suivant les principes de l'immersion et l'invariance. De plus, la classe des systèmes est identifiée par une solution d'une inégalité matricielle linéaire, à partir de laquelle on obtient les gains d'observateurs.

Mots clés: Systèmes de puissance, stabilisation non linéaire et linéaire décentralisée, inégalités matricielles linéaires , immersion et invariance, contrôle adaptatif et observateurs.

Abstract

An electric power system (EPS) is a complex network of electrical components used to *supply*, *transmit* and *use* electric power. Its final goal is to provide reliable, secure and uninterrupted service to the end-user, this means, constant voltage and frequency at all time. Nowadays, the trend in electric power production is toward an interconnected network of transmission lines linking generators and loads into large integrated systems. Actually, a power system network is considered the most complex and bigger machine ever built by man since it can span an entire continent. For this reason, improving power system *transient stability* is of great significance in human society, since if the stability is lost, power collapse may occur in a large populated area and serious damages will be brought to a regional economy and the consumer's comforts.

Therefore, considering all issues presented before, this research work tackles the transient stabilization of a multi-machine EPS subject to network disturbances from two approaches: *centralization* which considers no limitation in information exchange at any point of a given network, and on the other hand, *decentralization* which assumes the information exchange is not available. To this end, first we introduce a novel control theory to globally stabilize *non-globally linearizable triangular* systems employing a nonlinear dynamic state-feedback controller, which differs from standard backstepping since the strict-feedback form is no longer required. Then, based on these new ideas, the transient stabilization problem of EPS is solved from a centralized point of view ensuring, under some conditions on the physical parameters of the system, global asymptotic stability of the operating point. Subsequently, using only local measurements available with existing technology, the previous central controller is transformed into a truly decentralized one, provided that the derivative of the active power at each generator can be suitable estimated. Performance of both controllers is tested via numerical simulations considering several fault scenarios using the 10-machine New England benchmark. In contrast to the nonlinear solutions above, we offer an observer–based methodology for decentralized stabilization of large–scale linear time–invariant systems. The originality of this work relies on the fact that each local controller is provided with available local measurements, it implements a *deterministic* observer to reconstruct the state of the other subsystems and uses—in a *certainty–equivalent way*—these estimates in the control law. The observers are designed following the principles of immersion and invariance (I&I). Furthermore, the class of systems to which the design is applicable is identified via a linear matrix inequality solution, from which the observer gains are obtained.

Keywords: Electric power systems, decentralized nonlinear and linear stabilization, linear matrix inequalities, immersion and invariance, observer and adaptive control.

Contents

List of Figures

List of Tables

List of Simbols

$\mathbb{R}$	Set of real numbers.
$\mathbb{R}_+$	Set of real positive numbers.
u, v, ν	Referred as control inputs.
x_i	The i-th state variable of a given dynamical system.
$f(\cdot)$, $g(\cdot)$	Vector fields.
ξ	Controller/observer dynamical state.
x_2^d, x_3^d	Auxiliary controller signals.
$\mathcal{E}$	Equilibrium set.
V, $\mathcal{V}$	Lyapunov functions.
$\sigma(\cdot)$	A given odd function.
$h(\cdot)$	Nonlinear function present in triangular systems.
$\pi's$, $\beta's$	Controller gains.
$c's$	Lyapunov constants.
z	Estimation error.
δ	The rotor angle of a generator.
ω	Deviation from synchronous speed.
E	The voltage behind the transient reactance.
P	Normalized active power.
D	Normalized damping constant.
G	Normalied self-conductance.
V_B	Infinite bus voltage.
Y	Admittance value/matrix.
τ	Direct axis transient short circuit time constant.
E_f	Control constant voltage component applied to the field winding.
i, j, k	Indices.
N	Total number of machines/subsystems.
n	The order of subsystems.
$\bar{N}$	The set of all subsystems.
D_m	The Damping constant.
H	Inertia constant.
P_m	Mechanical power input.
G_m	Conductance.
x_d	Direct axis reactance.

x'_d	Direct axis transient reactance.
B_m	Susceptance.
ϵ	Controller gain.
A	Transition matrix.
B	Input matrix.
$\hat{x}_{j\Sigma_i}$	Estimate of the state x_j given in subsystem Σ_i.
$\xi_{j\Sigma_i}$	Observer state related to the estimation of x_j given in Σ_i.
F	Feedback matrix.
Λ	LMI matrix.
Ω	LMI matrix.
P, U	LMI matrices.
$K_{j\Sigma_i}$	Observer gain matrix.
P_e	Active power.
Q_e	Reactive power.
x_{ad}	Mutual reactance between the excitation and stator coils.
I_f	Field Current.
I_q	Quadrature axis current.
I_d	Direct axis current.
ε	Decaying term.
θ	Unknown parameter to be estimated.
γ	Filter gain.
κ	Filter gain
h^f, $\dot{h}^f$	Filtered function h and its derivative.

Abbreviations.

SMIB	Single Machine Infinite Bus system.
MAGLEV	Magnetic Levitation system.
I&I	Immersion and Invariance.
EPS	Electric Power System.
GAS	Global Asymptotic Stability.
LMI	Linear Matrix Inequality.

Resumé Detaillé

Cette étude de doctorat est consacrée à la *stabilisation transitoire* des systèmes de puissance électriques soumis à des perturbations du réseau. Par conséquent, ce chapitre d'introduction présente le cadre de l'application ainsi que la motivation, la revue de la littérature et des contributions apportées par ce travail. Egalement, ce chapitre comprend les parties principales de chacun des chapitres suivants.

Structure des systèmes de puissance électriques

Un système de puissance électrique est un réseau complexe de composants électriques utilisés pour *fournir*, *transmettre* et *utiliser* l'énergie électrique. Son but ultime est de fournir un service fiable, sécurisé et ininterrompu à l'utilisateur final, en d'autres termes, la tension et la fréquence constantes tout le temps. Dans un sens général, ce réseau est constitué par les éléments suivants [Kundur, 1994; El-Hawary, 2008]:

a) ***Unités de génération.*** Une composante essentielle des systèmes de puissance, qui utilise normalement des machines à courant alternatif triphasé, connues en tant que générateurs ou alternateurs synchrones, et qui transforme la puissance mécanique en une électrique. Les générateurs ont deux champs rotation synchrone, un champ produit par le rotor est entraîné à la vitesse synchrone et excité par un courant continu. L'autre champ est produit dans les enroulements de stator par les courants d'armature triphasés. La source de la puissance mécanique, communément connu comme le premier moteur, peut être turbines hydrauliques, turbines à vapeur dont l'énergie provient de la combustion du charbon, du gaz et du combustible nucléaire, les turbines à gaz ou moteurs à combustion interne [Bergen and Vital, 2000; Fardo and Patrick, 2009]. Dans les centrales électriques, plusieurs générateurs sont connectés en parallèle pour fournir la puissance totale nécessaire. Avec les préoccupations pour l'environnement, de nombreuses sources alternatives sont considérées. Par exemple l'énergie solaire, l'énergie géothermique, l'énergie éolienne, l'énergie marémotrice et la biomasse.

b) ***Systèmes de transmission et de distribution.*** Un réseau de transmission aérienne transfère l'énergie électrique à partir d'unités de production dans le système de distribution qui fournit finalement la charge. Les lignes de transmission interconnectent également les centrales voisines qui permettent l'envoi d'énergie entre les régions dans des conditions normales et d'urgence. Lignes de transmission à

haute tension sont terminés dans les sous-stations, qui sont appelés sous-stations haute tension ou sous-stations primaires. La fonction de certains sous-stations est de commutation des circuits dans et hors de service, ils sont considérés comme des stations de commutation. Aux sous-stations primaires, la tension est abaissée à une valeur plus appropriée pour la partie suivante du flux en direction de la charge. Très grands clients industriels peuvent être servis directement du système de transmission. La partie du système de transmission qui connecte les sous-stations haute tension par transformateurs abaisseurs aux sous-stations de distribution est appelé le réseau de transmission secondaire. Des banques de condensateurs et de réacteurs sont généralement installés dans les sous-stations pour le maintien de la tension de ligne de transmission.

Le système de distribution reliant les sous-stations de distribution à l'équipement de service d'entrée des consommateurs. Les lignes de distribution primaire alimentent la charge dans une zone géographique bien définie, où certains petits clients industriels sont servis. Le réseau de distribution secondaire réduit la tension pour utilisation par les consommateurs commerciaux et résidentiels. Les lignes et les câbles ne dépassant pas quelques centaines de mètres de longueur fournissent la puissance pour les consommateurs individuels. La distribution secondaire sert la plupart des clients à des niveaux de 120/240 V. Les systèmes de distribution utilisent les deux, conducteurs aériens et souterrains.

Un élément important dans EPS est le transformateur, qui transfère la puissance avec une très grande efficacité d'un niveau de tension à l'autre. La puissance transférée au secondaire est pratiquement la même que le première, à l'exception des pertes internes dans le transformateur. L'utilisation d'un transformateur élévateur de tension permettra de réduire les pertes dans la ligne, ce qui permet la transmission d'énergie sur de longues distances possibles. A la fin de la réception des lignes de transmission transformateurs abaisseurs sont utilisés pour réduire la tension à des valeurs appropriées pour la distribution ou l'utilisation. L'électricité dans les systèmes de puissance peut rencontrer quatre ou cinq transformations entre les unités de production et les consommateurs.

La majorité des systèmes de puissance comptent sur courant alternatif triphasé, le standard pour la transmission d'électricité à grande échelle et la distribution dans le monde moderne. Néanmoins, systèmes spécialisés qui comptent sur la puissance à courant continu se trouvent dans les systèmes d'aéronef, les systèmes de chemin de fer électrique, les systèmes haute tension à courant continu, les lignes de transmission sous-marins et les voitures.
fourniture

c) ***Centres de charge.*** Charges électriques sont divisés en secteurs industriel, commercial, et résidentiel. Charges industrielles sont charges composés, et les moteurs à induction forment une forte proportion de ceux-ci. Normalement, les charges composés sont en fonction de la tension et de la fréquence et forment une partie

importante de la charge du système. Charges commerciales et résidentielles sont constituées en grande partie de l'éclairage, le chauffage et la cuisine. Ces charges sont indépendants de la fréquence et consomment petite puissance réactive. La charge varie tout au long de la journée, et la puissance doit être toujours disponible pour les consommateurs à la demande.

Par exemple, La figure 1.1 donne un aperçu général des entités susmentionnées et leurs interconnexions. De plus, cette recherche considère le paradigme de flux d'énergie d'une direction au même temps que les prochaines fonctionnalités du système:

- ***Alimentation***: générateurs synchrones à courant alternatif triphasé,
- ***Transmission***: lignes de transmission modélisées en utilisant le modèle π, [Kundur, 1994; El-Hawary, 2008],
- ***Utilisation***: charges de puissance active et réactive supposés comme impédances constantes.

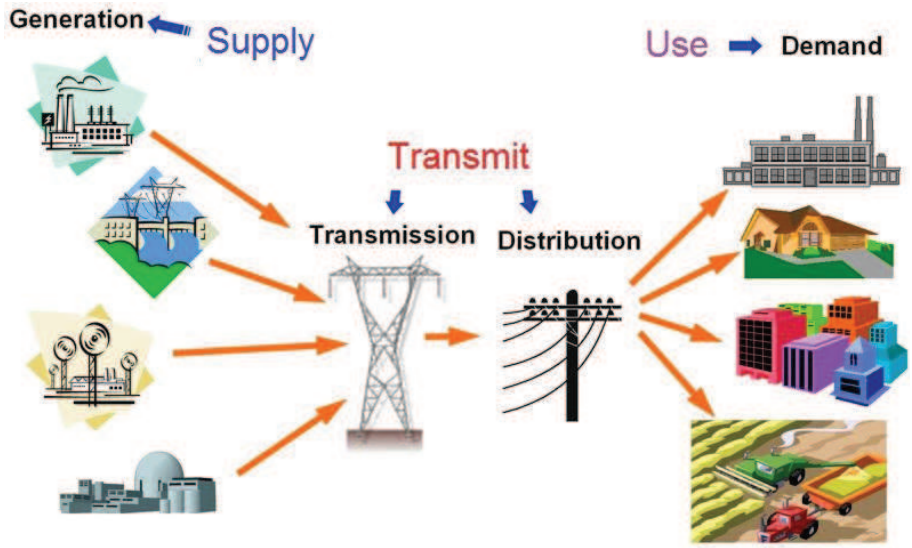

Figure 1: Composants du système de puissance électrique.

Motivation

Depuis la révolution industrielle, la demande et la consommation d'énergie a augmenté de façon constante et systèmes de puissance très complexes ont été construits pour répondre à cette demande croissante. L'évolution de la production d'énergie électrique est vers un réseau interconnecté de lignes de transmission reliant les producteurs et les charges en grands systèmes intégrés. En fait, un réseau de système de puissance est considérée comme la machine la plus complexe et plus jamais construite par l'homme car elle peut s'étendre sur tout un continent [Anderson and Fouad, 2003].

Le fonctionnement correct et sûr de ces systèmes complexes dépend largement de la capacité de l'opérateur du système à fournir un service fiable et continu aux charges. Idéalement, les charges doivent être alimentées à une tension et fréquence constante à tout moment. En termes pratiques, cela signifie que la tension et la fréquence doivent être maintenues dans des tolérances étroites afin que l'équipement du consommateur peut fonctionner de manière satisfaisante. Par exemple, une chute de tension de 10 % à 15 % ou une réduction de la fréquence du système de seulement quelques hertz peut conduire à caler les charges de moteur sur le système. Ainsi, on peut dire que l'opérateur du système électrique doit maintenir un très haut niveau de service électrique sécurisé.

Stabilité transitoire

La sécurité du système de puissance en général, peut être définie comme la robustesse du système à fonctionner en un état d'équilibre dans des conditions normales et des conditions perturbé. La sécurité du système de puissance couvre une grande variété d'aspects, habituellement subdivisé en phénomènes statiques et dynamiques. La stabilité du système de puissance fait actuellement référence à la partie dynamique de la sécurité. En outre, la notion de stabilité peut être défini de façon générale comme propriété d'un système de puissance qui lui permet de rester dans un état d'équilibre stable dans des conditions normales de fonctionnement et de retrouver un état d'équilibre acceptable après avoir été soumis à une perturbation [Kundur, 1994; Pavella et al., 2000; IEEE/CIGRE, 2004].

Il s'agit d'un problème complexe en fonction d'une variété de facteurs, tel que: laps de temps qui doit être pris en considération afin d'évaluer la stabilité, la taille de la perturbation considéré et la nature physique de l'instabilité qui en résulte. Par conséquent, même si une classification rigoureuse entre différents types de stabilités est difficile, une classification pratique souvent accepté s'appuie sur les facteurs ci-dessus. Ainsi, en référence à l'intervalle de temps du phénomène, on distingue la stabilité à court terme de la stabilité à long terme. En référence à la taille de la perturbation considérée, on distingue la stabilité de petit perturbation de la stabilité à grande perturbation: le premier peut être manipulé par linéarisation des équations dynamiques du mouvement, tandis que le second nécessite des approches non linéaires. En outre, à la fois la stabilité de petite perturbation et la stabilité de grande perturbation peut être subdivisée en ceux de tension et d'angle. La Figure 1.2 illustre cette classification. On peut constater que la stabilité de l'angle à grande perturbation est la stabilité dite transitoire; c'est l'un des deux aspects qui constituent ce qu'on appelle la sécurité dynamique; l'autre aspect est la stabilité de la tension de grande perturbation

La présente monographie est consacrée à la stabilité transitoire des réseaux électriques multi-machine et cette caractéristique se réfère à la capacité de maintenir un fonctionnement synchrone des machines lorsqu'ils sont soumis à une forte perturbation. L'apparition de ces perturbations peut conduire à des grandes excursions d'angles de rotor et, chaque fois que des mesures correctives ne fonctionnent pas, perte de synchronisme entre les machines existe. En général, la perte de synchronisme se développe en quelques secondes après de la présence des perturbations. En fait, parmi les phénomènes considérés dans la Figure 1.2, la stabilité transitoire est le plus rapide à se développer. Le caractère non

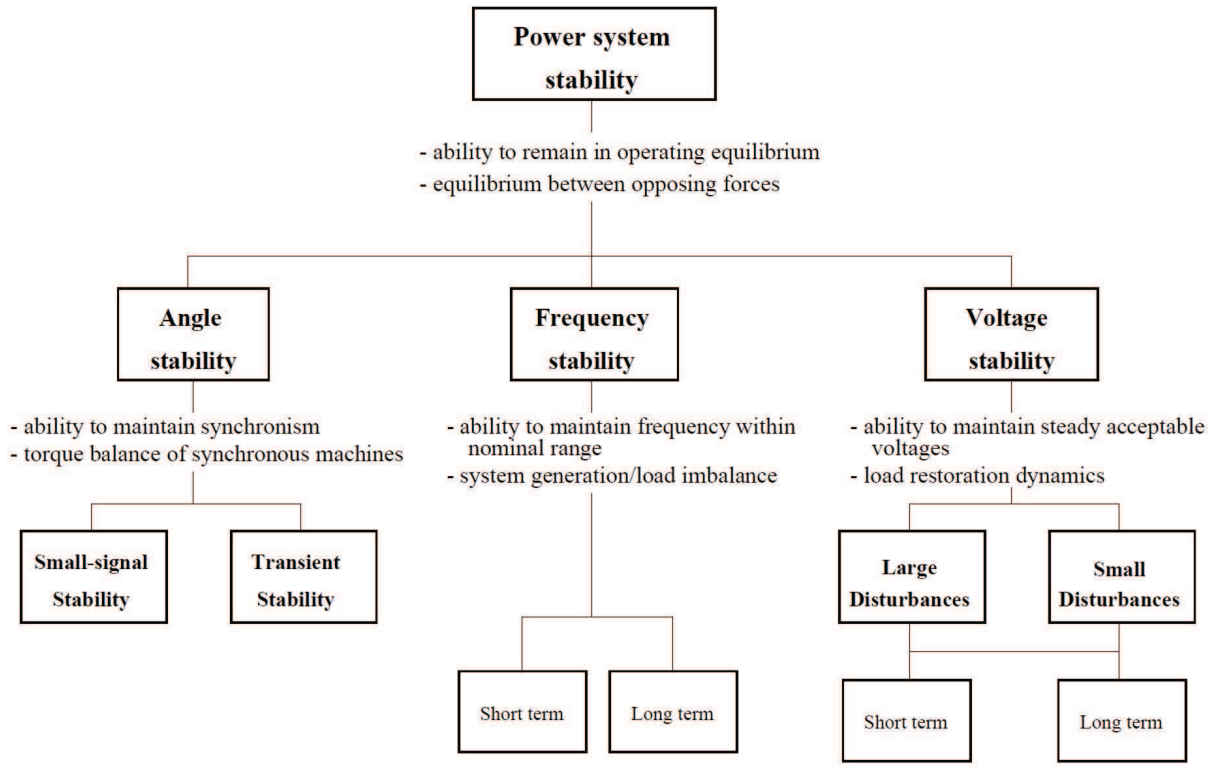

Figure 2: Types de phénomènes de stabilité des réseaux électriques.

linéaire de la stabilité transitoire, son évolution rapide et ses implications pratiques désastreuses font l'un des plus importants et en même temps la question la plus problématiques pour évaluer et encore plus à contrôler, surtout aujourd'hui, avec les pratiques de déréglementation émergents du secteur électrique dans de nombreux pays.

En effet, le secteur de l'énergie électrique déréglementé en Europe et dans beaucoup d'autres parties du monde appelle des gestionnaires de réseau indépendants à être responsable du réseau de transmission. Le secteur de l'électricité se déplace donc dans un nouveau régime de réglementation, où les nouveaux centres de contrôle devront surveiller et de contrôler les réseaux beaucoup plus importants que ceux qui existent déjà et de suivre en beaucoup plus courts horizons temporels beaucoup plus de transactions d'énergie qu'aujourd'hui: grande taille du réseau , des quantités plus importantes de flux d'énergie, et des horizons plus courts sont susceptibles d'influer sur la stabilisation transitoire et le rendre encore plus complexe et indispensable que dans le passé.

l'Amélioration de la stabilité transitoire est d'une grande importance dans la société humaine, car si la stabilité est perdue, l'effondrement d'énergie peut se produire dans une grande zone peuplée et des graves dommages seront portés à l'économie régionale et les conforts des consommateurs. Par conséquent,considérant tous les problèmes présentés avant, ce travail aborde la stabilisation transitoire d'un système soumis à des perturbations du réseau à partir deux approches: la centralisation, qui considère aucune limitation à l'échange d'informations à n'importe quel point d'un réseau donné, et d'autre part, la

décentralisation, qui suppose l'échange d'informations n'est pas disponible. Le premier n'est justifiée que par l'utilisation d'unités de mesure de phaseur (PMU) et de la technologie de communication actuelle, où les variables d'intérêt comme la tension, la fréquence et le courant peuvent être acquises en temps réel pour être traitées par le centre de contrôle. Notez que cette approche est sensible aux échecs sur des canaux de communication, mais est bien acceptée par la pratique moderne et ouvre à des nouveaux défis dans le domaine du contrôle de tolérance aux pannes.

Au contraire, l'approche de la décentralisation est apparue récemment à partir la nécessité d'opérer les systèmes de puissance lorsque l'échange de l'information n'est pas disponible ou partiellement disponible. Comme indiqué précédemment, le marché libéralisé de l'énergie a ouvert de nouveaux horizons dans le domaine de contrôle en matière d'intégration de la production d'énergie renouvelable dans l'infrastructure électrique actuelle. De plus, l'ancien paradigme où les centres de production sont situés à longue distance loin des centres de consommation a été remplacé par l'approche de la production distribuée, qui permet de petites et micro-centrales de production de contribuer puissance afin de répondre à la demande actuelle d'électricité collectivement. Par conséquent, cette nouvelle génération distribuée présente un phénomène de flux d'énergie bidirectionnel, qui conduit à effets négatifs à la fiabilité et la stabilité du réseau existant.

Revue de la littérature

Au cours de cette recherche, les prochains sujets ont été revisités.

Modélisation des systèmes de puissance

La théorie de la machine synchrone pour la modélisation des systèmes électriques de puissance a été largement étudiée dans plusieurs livres de texte comme [Elgerd, 1982; Pai, 1989; Kundur, 1994; Bergen and Vital, 2000; Anderson and Fouad, 2003], où l'analyse de état stationnaire et les caractéristiques de performance transitoire sont développés en détail. Les lois de Kirchhoff et les principes physiques sont utilisés pour formuler un modèle complet en trois phases. Cette description capture les deux dynamiques électriques et mécaniques d'un générateur synchrone en utilisant un total de huit variables d'etats; six pour la partie électrique et deux pour la partie mécanique. Pourtant, en raison de la nature sinusoidale de la tension et des courants dans cette description mathématique, il est souvent appliqué la transformation de *Park* et, par conséquent, des quantités non-oscillatoire dans la trame de référence $d-q$ sont utilisés au lieu pour l'analyse et le contrôle.

Une autre approche différente a été signalé dans [Zonetti, 2011; Zonetti et al., 2012], où en utilisant représentations bond-graph individuelles des générateurs synchrones, des lignes de transmission et des charges, un modèle à ports hamiltonien pour un système de puissance de trois phases est dérivé sans aucune hypothèse de simplification. Ce modèle équivalent conduit à une description basée sur l'énergie du système, où tous les éléments conservent leur interprétation physique d'origine, ouvrant la voie à l'analyse fondée sur l'énergie. Malheureusement, pour un cas multi-machine ce modèle n'est pas encore défini

dans un cadre de référence $d-q$ car un angle doit être sélectionné comme référence pour les autres afin d'appliquer une telle transformation.

Modèles simplifiés ont également été dérivée pour gérer les deux une seule machine et multi-machines représentations. Par exemple, considérons le modèle classique de troisième ordre signalés dans [Pai, 1989; Chiang et al., 1995a; Lu et al., 2001]. Tandis que le modèle complet en trois phases utilise six variables d'état pour représenter le sous-système électrique, ce modèle simplifié emploie juste une variable d'état pour le même but. Cette variable d'état électrique artificielle est nommé *tension derrière la réactance transitoire* et malgré les simplifications, cette représentation a la capacité d'inclure ou non les pertes de puissance dues à la conductance de réseau, caractéristique importante qui a conduit à plusieurs conceptions de contrôle de stabilisation. Les contrôleurs détaillées dans cette thèse sont basés dans cette représentation simplifiée pour systèmes électriques en tenant compte d'un réseau avec des pertes de puissance. Néanmoins, quelques résultats numériques en utilisant le modèle complet en trois phases sont réalisées, montrant la robustesse du contrôleur faisant face à la dynamique non linéaire non modélisée.

Stabilisation des systèmes de puissance

En raison du grand complexité, la stabilité transitoire dans les systèmes de puissance est souvent analysée considérant la représentation d'une seule machine. Par conséquent, chaque unité de production est considérée séparément, tandis que l'ensemble des autres machines sont considérées comme un bus infini, fonctionnant à tension et fréquence constante par rapport à la machine considéré. Dans cette approche, plusieurs résultat basé sur des techniques non linéaires et spécialisés ont été publiés sur ces dernières années. Par exemple, les contrôleurs de linéarisation par rétroaction ont été signalés dans [Lu et al., 2001] and [Fusco and Russo, 2011], la technique de mode glissant est détaillé dans [Loukianov et al., 2011], immersion et invariance (I&I), adaptative robuste H_∞ et backstepping en [Manjarekar et al., 2012; Sun et al., 2009; Fu and Zhao, 2005], respectivement.

Le travail de thèse de doctorat en [Galaz, 2003] a publié ses résultats dans [Ortega et al., 2001; Galaz et al., 2001, 2004]. De plus, en utilisant le contrôle basé dans la passivité, ces résultats abordent le problème de l'élargissement de la région de l'attraction de l'équilibre dans les systèmes électriques décrits par la représentation d'une seule machine. Ensuite, la notion du contrôle basé en passivité, est étendue à un cas multi-machine en [Ortega et al., 2005] pour prouver l'existence d'une loi de commande de rétroaction d'état non-linéaire statique qui assure la stabilité asymptotique du point de fonctionnement, avec une estimation bien définie du domaine d'attraction. Malheureusement, une expression explicite pour le contrôleur est donnée seulement pour les cas de un, deux et trois machine. De plus, pour établir le résultat de l'existence de plus de trois machines les hypothèses strictes que tous les inerties du générateur sont égaux, et que les pertes en ligne sont suffisamment petites, sont faites.

Après, la thèse de doctorat réalisés dans [Dib, 2009] ramasse les résultats donnés par [Dib et al., 2009a,b,c, 2011]. Ces résultats sont également consacrés au problème de

l'élargissement de la région de l'attraction, mais au contraire, ils proposent une nouvelle loi de stabilisation basée sur l'énergie pour le contrôle de l'excitation des alternateurs synchrones et considère des modèles plus naturelles et les plus populaires de préservation de structure qui préservent l'identité des composants du réseau, permettant un traitement plus réaliste des charges. Tout d'abord, ces résultats ont introduit la méthode des moments pour la réduction du ordre des systèmes non linéaires avec le but d'estimer les états non mesurés et de construire des lois de contrôle simplifiées. Ensuite, la méthode I&I est utilisée pour stabiliser un système d'énergie multi-machine où la formulation du problème de commande est ajusté pour répondre aux exigences de stabilité transitoire pratiques (convergence de l'angle de rotor).

Dans le travail [Casagrande et al., 2011b], une nouvelle théorie du contrôle pour stabiliser globalement systèmes triangulaires qui ne sont pas totalement linéarisables est introduit. Cette théorie emploie un contrôleur par retour d'état dynamique non linéaire et contraste avec la technique de backstepping normale car l'exigence d'une structure stricte de rétroaction dans les systèmes triangulaires est détendu, par conséquent, une loi de commande est alors explicitement obtenu. En conséquence, en [Casagrande et al., 2012, 2014] la théorie est étendue efficacement aux systèmes de puissance multi-machines où un contrôleur centralisé qui stabilise globalement et asymptotiquement, avec une fonction de Lyapunov bien défini pour une ligne de transmission avec pertes est synthétisé. L'efficacité et la performance de la solution est illustrée en simulant le problème de la récupération de l'équilibre après un défaut, aussi bien dans le cas du système d'ordre simplifiée et dans le cas d'un modèle de huitième ordre plus précise avec les signaux d'entrée saturés.

Car les systèmes de puissance couvrent normalement grandes régions géographiques, il est naturel de les faire fonctionner d'une manière décentralisée, en d'autres termes, considérant la limitation sur l'échange d'informations entre les unités de production. Selon cette approche, le processus de décentralisation redistribue ou disperse la tâche de commande à chaque contrôleur local agissant sur les centres de production correspondants. Évidemment, cette action de contrôle est basée uniquement sur des mesures locales. En début des années 70, la perspective donnée par [Wang and Davison, 1973], commencé formellement la recherche sur le contrôle décentralisé. Ils ont démontré que un système peut être stabilisée avec un contrôleur décentralisé (statique ou dynamique) si et seulement s'il ne possède pas de modes fixes décentralisés instables, voir aussi [Lunze, 1992]. Le scénario typique de stabilisation décentralisés de systèmes suppose que la matrice d'entrée est plein et vise à trouver la sortie locale telle que la boucle fermée est stable. Les enquêtes et les évolutions les plus récentes sur ce problème peuvent être trouvés dans [Lavaei and Aghdam, 2008; Lam and Davison, 2010; Miller and Davison, 2012; Song et al., 2013]. Une autre approche est présentée dans [Šiljak and Zečević, 2005] où un nouveau schéma basé sur les inégalités matricielles linéaires est conçu pour la stabilisation robuste décentralisé d'un systèmes de puissance de 10 machines. Les non-linéarités du système sont considérées comme incertitude, mais limitée par une inégalité quadratique. Sur la base de cette hypothèse, le problème de stabilisation est traduit en un problème de solvabilité des inégalités matricielles linéaires pour obtenir finalement des gains de rétroaction appropriés. Ces notions sont inspirées par les livres [Šiljak, 1991; Boyd et al., 1994; Zečević and Šiljak, 2010].

Enfin, plusieurs références ont été étudiés en ce qui concerne la stabilisation décentralisée des systèmes non linéaires. Même peu de résultats sur le contrôle décentralisé des systèmes électriques traitent avec rigueur la dynamique non linéaire du système. Deux exceptions notables sont [Guo et al., 2000] et [Yan et al., 2010], où il est constaté que la technologie actuelle permet la mesure locale de signaux supplémentaires, à savoir, la puissance active, la puissance réactive et le courant de champ à chaque générateur. En [Guo et al., 2000] les termes de couplage du système de puissance sont considérés comme une perturbation additive de l'équation mécanique. En supposant que, les limites de cette perturbation sont connus et l'état complet de chaque générateur est disponible pour la mesure, un schéma de backstepping décentralisée qui réduit (à un certain niveau) le gain $\mathcal{L}_2$ de l'opérateur à partir de la perturbation à la fréquence de puissance est proposé. En [Yan et al., 2010] les mêmes mesures que [Guo et al., 2000] sont supposés, et un contrôleur de backstepping adaptatif qui assure bornitude ultime de l'Etat est proposé. En ajoutant l'adaptation, les auteurs parviennent à détendre l'hypothèse de la connaissance de borne supérieure dans les perturbations.

Contributions

Les principales contributions de ce travail sont énumérés ci-dessous.

- Légères modifications à la théorie proposée dans [Casagrande et al., 2011b] sont détaillées ici au chapitre 2. Ces modifications impliquent l'introduction de gains de commande ayant pour objectif une meilleure performance dynamique en boucle fermée. En outre, la technique proposée est appliquée aux systèmes Maglev et SMIB pour stabiliser un point d'équilibre donné, ces résultats ne sont pas signalés dans toute autre référence de la littérature.

- Un contrôleur centralisé qui stablizes globalement et asymptotiquement systèmes de puissance considérant des lignes transmissions avec pertes est rapporté ici. Au meilleur de notre connaissance, c'est le premier résultat relatif dans la littérature. De plus, l'efficacité du schéma proposé est testé faisant face à une dynamique non linéaire non modélisés et d'ordre élevé, étant donné que le contrôleur est synthétisé à partir d'un modèle de troisième ordre, mais à la place est appliqué à un modèle de huit ordre pour obtenir des résultats numériques satisfaisants incluant plusieurs scénarios de défaut.

- Ainsi également, une nouvelle méthode pour stabiliser des systèmes linéaires interconnectés à grande échelle via un contrôle décentralisé basé sur observateur est détaillé ici. La restriction d'échange limitée de l'information entre les sous-systèmes a été surmonté en utilisant observateurs I&I que, c'est bien connu, ont une nouvelle structure consistant en une partie intégrale et une partie proportionnelle. De plus, les gains d'observation sont obtenues grâce à une solution des inégalités matricielles linéaires et les valeurs propres du observateur sont placés dans une région circulaire souhaitée.

- Enfin, une version adaptative décentralisée du contrôleur centralisé pour systèmes de puissance multi-machine avec des lignes de transmission à pertes est rapporté dans ce travail. Ce nouveau schéma est décentralisée dans le sens où il n'y a pas d'échange en information entre les contrôleurs de chaque machine. La décentralisation est réalisée en utilisant les mesures des variables d'etat locales, la puissance active et la puissance réactive, qui sont disponibles avec la technologie existante. En plus, le schéma proposé utilise d'une manière équivalente l'estimation de la différence entre la réactance de l'axe direct et la réactance transitoire de l'axe direct, soit $x_d - x'_d$ dans la loi de commande, apportant robustesse au terme de linéarisation partielle de boucle interne .

Présentation de la thèse

Dans le **Chapitre 2**, nous introduisons une nouvelle théorie de contrôle pour stabiliser globalement *systèmes triangulaires non globalement linéarisables* utilisant un contrôleur d'état de rétroaction dynamique non linéaire. Afin d'aider à une meilleure compréhension, le matériau est exposé augmentant le degré de complexité dans chaque section. Ce cadre théorique comprend seulement les systèmes représentés par deux ou trois états et son applicabilité est testé par deux systèmes physiques, c'est à dire, une machine unique bus infini et un système de lévitation magnétique.

En **Chapitre 3**, une solution non linéaire globale pour le problème de système d'alimentation électrique multi-machine avec des conductances de transfert non négligeable est présentée. Cette schéma est *centralisé* dans le sens que tous les états de la machine sont disponibles pour la mesure et il n'ya pas de contraintes sur l'échange d'informations. Bien que ce soit le contrôleur est inspiré de celui présenté dans le chapitre 2, quelques manipulations sont détaillées afin de résoudre une boucle algébrique. Enfin, des simulations en tenant compte de plusieurs défauts de réseau en utilisant le le 10 machines.

Chapitre 4 détails la stabilisation des systèmes linéaires temps-invariant à grande échelle à partir d'un point de vue *décentralisé*. Ce schéma met en œuvre un observateur de type déterministe utilisant idées d'immersion et invariance en combinaison avec le cadre des inégalités linéaires de matricielle pour reconstruire les États d'autres sous-systèmes et utilise de manière équivalente ces estimations dans la loi de commande. Des résultats numériques sont offertes pour un système de deux machines et pour un système académique de quatre sous-systèmes.

Dans le **Chapitre 5**, nous présentons un contrôleur dynamique *décentralisé* non linéaire qui stabilise le point d'équilibre d'un système de puissance donné. Cette partie est une extension naturelle de celle présentée dans le **Chapitre 3**, où, en revanche, certaines hypothèses sur les mesures soient prises afin de parvenir à un fonction *décentralisé*. De la même manière, le système d'alimentation de 10-machines de Nouvelle Anglaterre est utilisée pour tester l'efficacité du dispositif de commande via plusieurs scénarios de simulation.

Finalement, le **Chapitre 6** présente les conclusions de la recherche et propose également

des travaux futurs.

Publications

Ce travail de thèse a fourni trois publications des revues et deux actes de congrès, ce sont:

Articles dans des revues

- Daniele Casagrande, Alessandro Astolfi, **Diego Langarica**, Romeo Ortega. Transient Stability Problem for Multimachine Power Systems: a Theoretical Solution and its Applicability. *IET, Generation, Transmission and Distribution*, 2014.
- **Diego Langarica** and Romeo Ortega. An Observer–Based Scheme for Decentralized Stabilization of Large-Scale Systems with Application to Power Systems, *Asian Journal of Control* 2013.
- **Diego Langarica Cordoba**, Romeo Ortega, Daniele Casagrande, Alessandro Astolfi. Transient Stability of Multimachine Power Systems: Towards a Global Decentralized Solution. *Automatica* 2014, Submitted.

Actes de congrès

- D. Zonetti, S. Fiaz, R. Ortega, A. Van Der Schaft, **D. Langarica**, J. Scherpen. Du Bond Graph au Modèle Hamiltonien à Ports d'un Système de Puissance. *Conférence Internationale Francophone d'Automatique*, Grenoble, France, July 2012,
- Daniele Casagrande, Alessandro Astolfi, Romeo Ortega, **Diego Langarica**. A Solution to the Problem of Transient Stability of Multimachine Power Systems. *IEEE 51st Annual Conference on Decision and Control (CDC)*, December 2012, 1703-1708.

Chapter 1

Introduction

This research concerns to *transient stabilization* of Electric Power Systems (EPS) subject to network disturbances. Therefore, this introductory chapter presents the framework of the application along with the motivation, the literature review and the contributions made by this work.

1.1 Power systems structure

An electric power system is a complex network of electrical components used to *supply*, *transmit* and *use* electric power. Its final goal is to provide reliable, secure and uninterrupted service to the end-user, this means, constant voltage and frequency at all time. In a general sense, this network is formed by the next elements [Kundur, 1994; El-Hawary, 2008]:

a) ***Generation units.*** An essential component of power systems which normally uses three-phase alternating current (AC) machines known as synchronous generators or alternators to transform the mechanical power into electrical one. Generators have two synchronously rotating fields, one field is produced by the rotor driven at synchronous speed and excited by direct current (DC). The other field is produced in the stator windings by the three-phase armature currents. The source of the mechanical power, commonly known as the prime mover, may be hydraulic turbines, steam turbines whose energy comes from the burning of coal, gas and nuclear fuel, gas turbines, or occasionally internal combustion engines [Bergen and Vital, 2000; Fardo and Patrick, 2009]. In power stations, several generators are connected in parallel to provide the total power needed. With concerns for the environment, many alternative sources are considered. For instance solar power, geothermal power, wind power, tidal power, and biomass.

b) ***Transmission and distribution systems.*** An overhead transmission network transfers electric power from generating units to the distribution system which ultimately supplies the load. Transmission lines also interconnect neighboring utilities which allow the dispatch of power within regions during normal and emergency conditions. High voltage transmission lines are terminated in substations, which are called high-voltage substations or primary substations. The function of some substations is switching circuits in and out of service, they are referred to as switching stations. At the primary substations, the voltage is stepped down to a value

more suitable for the next part of the flow toward the load. Very large industrial customers may be served directly from the transmission system. The portion of the transmission system that connects the high-voltage substations through step-down transformers to the distribution substations is called the subtransmission network. Capacitor banks and reactor banks are usually installed in the substations for maintaining the transmission line voltage.

The distribution system connects the distribution substations to the consumer's service-entrance equipment. The primary distribution lines supply the load in a well-defined geographical area where some small industrial customers are served. The secondary distribution network reduces the voltage for utilization by commercial and residential consumers. Lines and cables not exceeding a few hundred meters in length deliver power to the individual consumers. The secondary distribution serves most of the customers at levels of 240/120 V. Distribution systems utilize both overhead and underground conductors.

An important element in EPS is the transformer, which transfers power with very high efficiency from one level of voltage to another. The power transferred to the secondary is almost the same as the primary, except for internal losses in the transformer. Using a step-up transformer will reduce losses in the line, which makes the transmission of power over long distances possible. At the receiving end of the transmission lines step-down transformers are used to reduce the voltage to suitable values for distribution or utilization. The electricity in an EPS may undergo four or five transformations between generation units and consumers.

The majority of EPS systems rely upon three-phase AC power, the standard for large-scale power transmission and distribution across the modern world. However, specialized EPS that rely upon DC power are found in aircraft systems, electric railway systems, High Voltage DC systems, submarine transmission lines and automobiles.

c) ***Load centers.*** Electric loads are divided into industrial, commercial, and residential. Industrial loads are composite loads, and induction motors form a high proportion of these. Normally composite loads are functions of voltage and frequency and form a major part of the system load. Commercial and residential loads consist largely of lighting, heating, and cooking. These loads are independent of frequency and consume negligibly small reactive power. The load varies throughout the day, and power must be always available to consumers on demand.

For instance, Figure 1.1 gives a general insight of the aforementioned entities and their interconnections. Furthermore, this research considers the *one-direction power flow* paradigm along with the next features in EPS:

- ***Supply***: three-phase AC synchronous generators,

- ***Transmit***: transmission lines modeled using the π model [Kundur, 1994; El-Hawary, 2008],
- ***Demand***: active and reactive power loads assumed as constant impedances.

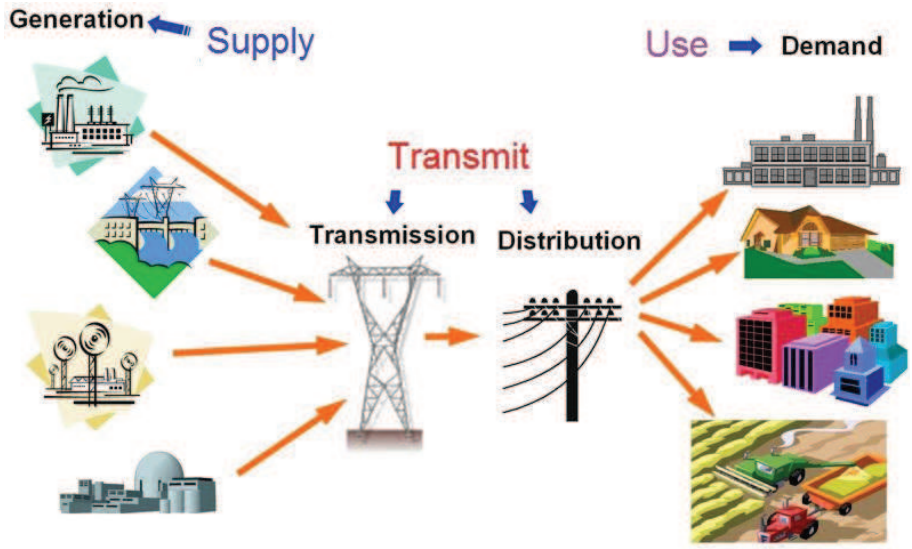

Figure 1.1: Electric power system components.

1.2 Motivation

Since the industrial revolution demand and consumption of energy has increased steadily and very complex EPS have been built to satisfy this increasing demand. The trend in electric power production is toward an interconnected network of transmission lines linking generators and loads into large integrated systems. Actually a power system network is considered the most complex and bigger machine ever built by man since it can span an entire continent [Anderson and Fouad, 2003].

Successful and secure operation of such complex systems depends largely on the system operator's ability to provide reliable and uninterrupted service to the loads. Ideally, the loads must be fed at constant voltage and frequency at all times. In practical terms, this means that both voltage and frequency must be held within close tolerances so that the consumer's equipment may operate satisfactorily. For example, a drop in voltage of 10% to 15% or a reduction of the system frequency of only a few hertz may lead to stalling the motor loads on the system. Thus, it can be accurately stated that the power system operator must maintain a very high standard of secure electrical service.

1.2.1 Transient stability

Power system security in general may be defined as the system robustness to operate in an equilibrium state under normal and perturbed conditions. Power system security

covers a wide range of aspects, usually subdivided into *static* and *dynamic* phenomena. Power system *stability* currently refers to the *dynamic* part of security. In addition, the *stability* concept may be defined broadly as that property of a power system that enables it to remain in a stable equilibrium state under normal operating conditions and to regain an acceptable equilibrium state after being subjected to a disturbance [Kundur, 1994; Pavella et al., 2000; IEEE/CIGRE, 2004] .

This is a multifaceted problem depending upon a variety of factors, such as: the *time span* that must be taken into consideration in order to assess stability, the *size of the disturbance* considered and the *physical nature* of the resulting instability. Hence, although a rigorous classification among distinct types of stabilities is difficult, a practical classification often accepted relies on the above factors. Thus, with reference to the *time span* of the phenomena, one distinguishes *short-term* from *long-term stability*. With reference to the *size of the disturbance* considered, one distinguishes *small-disturbance* from *large-disturbance* stability: the former may be handled via *linearization* of the dynamic equations of motion, while the latter requires *nonlinear* approaches. Further, both the small-disturbance and large-disturbance stability phenomena may be subdivided into *voltage* and *angle* ones. Figure 1.2 illustrates this classification. One can see that the angle large-disturbance stability is the so-called ***transient stability***; this is one of the two aspects making up what is called *dynamic security*; the other aspect is large disturbance voltage stability.

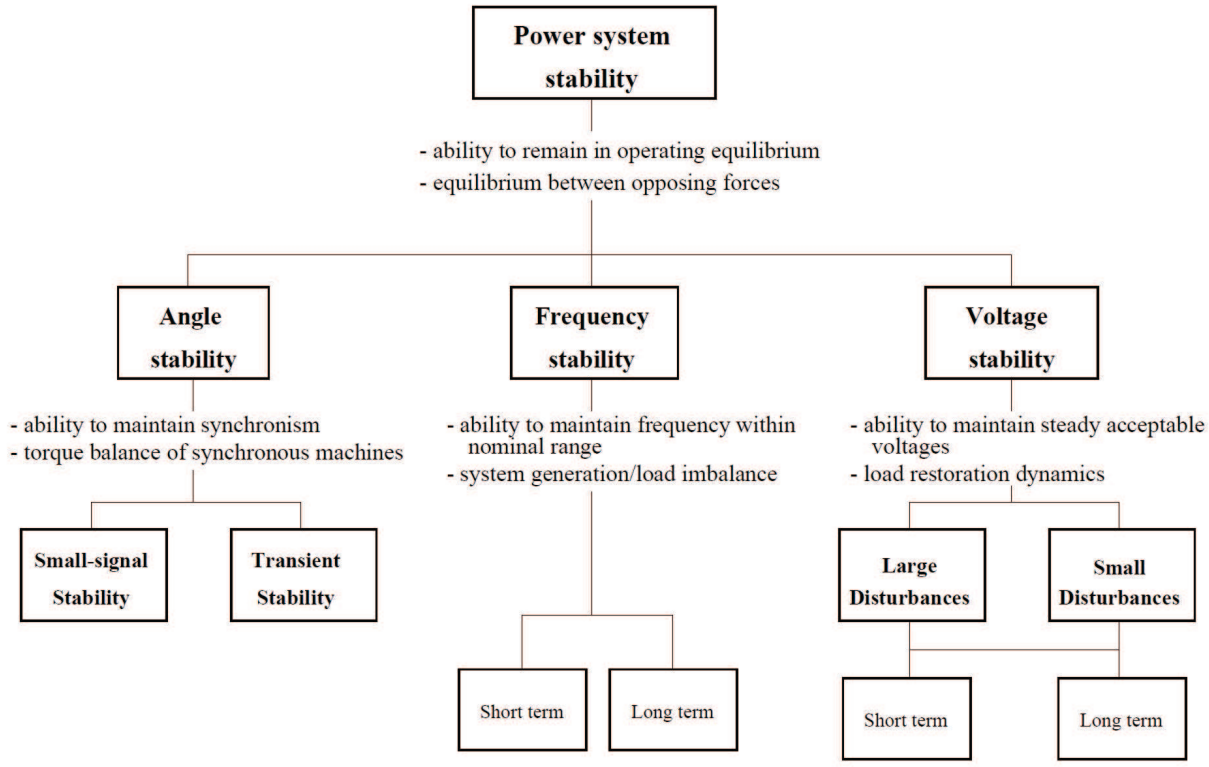

Figure 1.2: Types of power systems stability phenomena.

This monograph is devoted to *transient stability* of multi-machine EPS and this feature

refers to the ability to maintain synchronous operation of the machines when subjected to a large disturbance. The occurrence of such disturbance may result in large excursions of the system machine rotor angles and, whenever corrective actions fail, loss of synchronism results among machines. Generally, the loss of synchronism develops in very few seconds after the disturbance presence. Actually, among the phenomena considered in Figure 1.2 *transient stability* is the fastest to develop. The nonlinear character of *transient stability*, its fast evolution and its disastrous practical implications make it one of the most important and at the same time most problematic issues to assess and even more to control, especially today, with the emerging deregulation practices of the electric sector in many countries.

Indeed, the deregulated electric energy sector in Europe and in many other parts of the world will call for distributed independent system operators to be responsible for the transmission network. The electric utility industry is thus moving into a new regulatory regime, where the new control centers will have to monitor and control networks significantly larger than the existing ones and to track in much shorter time horizons many more energy transactions than today: larger network size, more important amounts of power flows, and shorter time horizons are likely to impact *transient stabilization* and to make it even more intricate and indispensable than in the past.

Improving power system *transient stability* is of great significance in human society, since if the stability is lost, power collapse may occur in a large populated area and serious damages will be brought to a regional economy and the consumer's comforts. Therefore, considering all issues presented before, this work tackles the transient stabilization of a multi-machine EPS subject to network disturbances from two approaches: *centralization* which considers no limitation in information exchange at any point of a given network, and on the other hand, *decentralization* which assumes the information exchange is not available. The former is only justified by the use of phasor measurement units (PMU) and current communication technology, where interest variables as voltage, frequency and current can be acquired in real-time to be processed by the control center. Note that this approach is sensitive to communication channels failures, yet is well accepted by modern practice and opens new challenges in fault tolerant control area.

On the contrary, *decentralization* approach has emerged recently from the need to operate EPS when information exchange is not available or partially available. As stated before, deregulated energy market has opened new horizons in control research regarding integration of renewable energy production into current electric infrastructure. What's more, the old paradigm where generation centers were located long distance away from consumer centers has been replaced by distributed generation approach, which allows small and micro generation facilities to contribute power in order to meet current electricity demand collectively. Consequently, this new distributed generation introduces a *bidirectional power flow* phenomenon resulting in adverse effects to the reliability and stability of the existing network.

1.3 Literature review

During this research the next topics were revisited.

1.3.1 Power systems modeling

Synchronous machine theory for EPS modeling have been extensively studied in several text books like [Elgerd, 1982; Pai, 1989; Kundur, 1994; Bergen and Vital, 2000; Anderson and Fouad, 2003], where steady state analysis and transient performance characteristics are developed in detail. Kirchhoff laws and physical principles are used to formulate a complete three-phase model. This description captures both electrical and mechanical dynamics of a synchronous generator using in total eight states variables; six for the electrical part and two for the mechanical one. However, due to sinusoidal nature of voltage and currents in this three-phase mathematical description, it is often applied *Park's* transformation and consequently, non-oscillatory quantities in the so-called $d-q$ reference frame are used instead for analysis and control.

Another different approach has been reported in [Zonetti, 2011; Zonetti et al., 2012], where using individual bond–graph representation of synchronous generators, transmission lines and loads, a *port-Hamiltonian* model for a full three-phase EPS is derived without any simplifying assumptions. This equivalent model leads to an energy–based description of the full system, where all elements preserve their original physical interpretation, paving the road for the energy–based analysis. Unfortunately, for a multi-machine case, this model is not yet defined in a $d-q$ reference frame since one machine angle must be selected as reference to the others in order to apply such transformation.

Simplified models have also been derived to handle both single machine and multi-machine representations. For instance, consider the classical third-order model with flux decay dynamics reported in [Pai, 1989; Chiang et al., 1995a; Lu et al., 2001]. Whereas the complete three-phase model uses six states variables to represent the electrical subsystem, this simplified model employs just one state variable for the same purpose. This artificial electrical state variable is named the *voltage behind the transient reactance* and although simplifications, this representation has the capability to include or not power losses due to network conductances, important feature that has led to several stabilizing control designs. The controllers detailed in this thesis are based in this simplified representation for EPS considering a lossy network. However, some numerical results using the complete three-phase model are carried out, showing controller robustness to high-order and unmodelled nonlinear dynamics.

1.3.2 Stabilization of power systems

Due to high complexity, *transient stability* in EPS is often analyzed considering the single machine infinite bus (SMIB) representation. Consequently, each generating unit is considered separately, while the set of the other machines and components are considered an infinite bus running at constant voltage and frequency with respect to the machine

under consideration. Under this approach, several result based on nonlinear and specialized techniques have been published on recent years. For instance, feedback linearization controllers were reported in [Lu et al., 2001] and [Fusco and Russo, 2011], sliding-mode technique is detailed in [Loukianov et al., 2011], immersion and invariance (I&I), adaptive robust H_∞ and backstepping like techniques in [Manjarekar et al., 2012; Sun et al., 2009; Fu and Zhao, 2005], respectively.

The PhD thesis work in [Galaz, 2003] has published its results in [Ortega et al., 2001; Galaz et al., 2001, 2004]. Furthermore, via passivity based control and energy shaping these results tackle the problem of enlarging the region of attraction of equilibrium in power systems described by a SMIB representation. Afterwards, the passivity based control notion is extended to a multi-machine case in [Ortega et al., 2005] to prove the existence of a nonlinear static state–feedback control law that ensures asymptotic stability of the operating point, with a well-defined estimate of the domain of attraction. Unfortunately, an explicit expression for the controller is given only for the single, two and three machine cases. Moreover, to establish the existence result for more than three machines the stringent assumptions that all generator inertias are equal, and that the line losses are sufficiently small, are made.

Latter, the PhD research made in [Dib, 2009] gather the results given by [Dib et al., 2009a,b,c, 2011]. These results are also devoted to the problem of enlarging the region of attraction, but in contrast, propose a new energy-based stabilizing law for excitation control of synchronous generators and considers a more natural and widely popular structure-preserving models that preserve the identity of the network components, allowing a more realistic treatment of the loads. First, these results introduced the method of *moment* for nonlinear systems order reduction aiming to estimate unmeasured states and to construct simplified control laws. Then, I&I methodology is used to stabilize a multi-machine power system where the formulation of the control problem is adjusted to meet the practical transient stability requirements (rotor angle convergence).

In the work [Casagrande et al., 2011b], a new control theory to globally stabilize *non-globally linearizable triangular* systems employing a nonlinear dynamic state-feedback controller is introduced. This theory contrast with standard backstepping technique because the strict-feedback structure requirement in triangular systems is relaxed, consequently a control law is then explicitly obtained. As a result, in [Casagrande et al., 2012, 2014] the theory is extended effectively to multi-machine power systems where a globally asymptotically *centralized* stabilizing controller, with a well–defined Lyapunov function, for the lossy transmission line is synthesized. The effectiveness and the performance of the solution is illustrated by simulating the problem of recovering the equilibrium after a fault, both in the case of the reduced order simplified system and in the case of a more precise eighth-order model with saturated input signals.

Since power systems normally span large geographical regions, it is natural to operate them in a *decentralized* manner, in other words, considering limitation on information exchange between generation units. Under this approach, the *decentralization* process redistributes or disperse the control task to each local controller acting upon corresponding

generation centers. Obviously this control action is based only on local measurements. In the early 70's, the perspective given by [Wang and Davison, 1973], started formally the research on *decentralized* control. They proved that a system can be stabilized with a *decentralized* controller (static or dynamic) if and only if it does not have unstable *decentralized* fixed modes, see also [Lunze, 1992]. The typical scenario of decentralized stabilization of linear time–invariant (LTI) systems assumes that the input matrix is *full* and aims at finding local output feedbacks such the closed–loop is stable. Surveys and more recent developments on this problem may be found in [Lavaei and Aghdam, 2008; Lam and Davison, 2010; Miller and Davison, 2012; Song et al., 2013]. Another approach is presented in [Šiljak and Zečević, 2005] where a new scheme is designed for robust *decentralized* stabilization of a 10-machine power systems, based on linear matrix inequalities (LMI). System nonlinearities are considered to be uncertain, but bounded by a quadratic inequality. Based on this assumption, the stabilization problem is translated to a LMI solvability problem to finally obtain suitable feedback gains. These notions are inspired by the books [Šiljak, 1991; Boyd et al., 1994; Zečević and Šiljak, 2010].

Finally, several references where investigated regarding to *decentralized* stabilization of nonlinear systems. Very few results on *decentralized* control of power systems rigorously deal with the systems nonlinear dynamics. Two notable exceptions are [Guo et al., 2000] and [Yan et al., 2010], where it is observed that current technology permits the local measurement of additional signals—namely, active and reactive power and field winding current at each generator. In [Guo et al., 2000] the coupling terms of the power system are viewed as an additive disturbance to the mechanical equation. Assuming that, besides the aforementioned measurement, bounds on this disturbance are known and the full state of each generator is available for measurement, a decentralized backstepping scheme that reduces (to a certain level) the $\mathcal{L}_2$ gain of the operator from the disturbance to the power frequency is proposed. In [Yan et al., 2010], the same measurements as [Guo et al., 2000] are assumed, and an adaptive backstepping controller that ensures ultimate boundedness of the full state is proposed. Adding the adaptation the authors manage to relax the assumption of knowledge of known upperbound in the disturbances.

1.4 Scope and contributions

The major contributions of this work are listed below.

- Slight modifications to the theory given in [Casagrande et al., 2011b] is detailed here in Chapter 2. These modifications involve introduction of control gains aiming to provide better closed-loop dynamic performance. In addition, the proposed technique is applied to SMIB and MAGLEV systems to stabilize a given equilibrium point, these results are not reported in any other literature reference whatsoever.

- An explicit globally asymptotically stabilizing *centralized* controller for EPS considering lossless transmissions lines is reported here. To the best of our knowledge, this is the very first result concerning in the literature. Furthermore, the effectiveness of the proposed scheme is tested facing high order and unmodeled nonlinear dynamics,

since the controller is synthesized from a third order model but instead is applied to an eight order model to obtain satisfactory numerical results including several fault scenarios.

- Thus also, a new methodology to stabilize large-scale interconnected linear time invariant systems via *decentralized* observer-based control is detailed here. The restriction of limited exchange information between subsystems has been overcome using I&I observers that, is well known, have a novel structure consisting of an integral part and a proportional part. What's more, observer gains are obtained via a LMI solution and observer eigenvalues are placed in a desired LMI circular region.

- Finally, an adaptive *decentralized* version of the GAS *centralized* controller for multi-machine power systems with lossy transmission lines is reported in this work as well. This novel scheme is *decentralized* in the sense that there is no on-line information exchange between machine controllers. The decentralization is carried out using the local measurements of the local state variables, the active and the reactive power, which are available with existing technology. Additionally, the proposed scheme uses in a certainty equivalent way the estimate of the difference between the direct axis reactance and the direct axis transient reactance, namely $x_d - x'_d$ in the control law, providing robustness to the inner-loop partial linearizing term.

1.5 Thesis overview

This report is organized in the following manner:

In **Chapter 2**, we introduce a novel control theory to globally stabilize *non-globally linearizable triangular* systems employing a nonlinear dynamic state-feedback controller. To assist a better understanding, the material is exhibited increasing the degree of complexity in each section. This theory framework comprise just systems represented by two or three states and its applicability is tested through two physical systems, *i.e.*, a single machine infinite bus and a magnetic levitation system.

In **Chapter 3**, a global nonlinear solution to the problem of multi-machine power system with non-negligible transfer conductances is presented. This scheme is *centralized* in the sense that all machine states are available for measurement and there is no constraints on information exchange. Although this controller is inspired from the one presented in Chapter 2, some manipulations are detailed in order to solve an algebraic loop. Finally, some simulations considering several network faults in the 10-machine New England bench mark are carried out.

Chapter 4 details the stabilization of large-scale linear time-invariant systems from a *decentralized* point of view. This scheme implements a deterministic-type observer using immersion and invariance ideas in combination with linear matrix inequalities framework to reconstruct other subsystems states and uses in a certainty equivalent way these estimates in the control law. Numerical results are offered for a two-machine system and

academic case study of four subsystems.

In **Chapter 5**, we present a *decentralized* nonlinear dynamic controller which stabilizes the equilibrium point of a given power system. This scheme is a natural extension of the one presented in **Chapter 3**, where in contrast, some assumptions on measurements are made in order to achieve a *decentralized* feature. In the same way, the 10-machine New England power system is used to test the effectiveness of the controller via several simulation scenarios.

Finally, **Chapter 6** provides the conclusions of the research and also proposes some future work.

1.6 Publications

This thesis research has provide three journal publications and two conference papers, these are:

Journal papers

- Daniele Casagrande, Alessandro Astolfi, **Diego Langarica**, Romeo Ortega. Transient Stability Problem for Multimachine Power Systems: a Theoretical Solution and its Applicability. *IET, Generation, Transmission and Distribution*, 2014.
- **Diego Langarica** and Romeo Ortega. An Observer–Based Scheme for Decentralized Stabilization of Large-Scale Systems with Application to Power Systems, *Asian Journal of Control* 2013.
- **Diego Langarica Cordoba**, Romeo Ortega, Daniele Casagrande, Alessandro Astolfi. Transient Stability of Multimachine Power Systems: Towards a Global Decentralized Solution. *Automatica* 2014, Submitted.

Conference papers

- D. Zonetti, S. Fiaz, R. Ortega, A. Van Der Schaft, **D. Langarica**, J. Scherpen. Du Bond Graph au Modèle Hamiltonien à Ports d'un Système de Puissance. *Conférence Internationale Francophone d'Automatique*, Grenoble, France, July 2012,
- Daniele Casagrande, Alessandro Astolfi, Romeo Ortega, **Diego Langarica**. A Solution to the Problem of Transient Stability of Multimachine Power Systems. *IEEE 51st Annual Conference on Decision and Control (CDC)*, December 2012, 1703-1708.

Chapter 2

Stabilization of Non-Globally Linearizable Triangular Systems

Nonlinear dynamical systems in triangular form have been widely studied in control literature. For instance, standard backstepping technique has been successful to globally stabilize a given lower triangular systems in strict-feedback form [Krstić et al., 1995; Janković et al., 1997; Khalil, 2000; Marquez, 2003]. Nevertheless, this technique fails when such system does not present a strict-feedback structure. As a result, the term *non-globally linearizable triangular* has been coined for this type of systems. Several works are dedicated to stabilization of such triangular systems that are only locally feedback linearizable, see e.g. [Tsinias, 1997; Čelikovský and Arande-Bricaire, 1999; Čelikovský and Nijmijer, 1996; Korobov and Pavlichkov, 2008; Pavlichkov and Ge, 2009; Lin and Qian, 2002; Qian and Lin, 2001; Tsinias and Karafyllis, 1999]. All these works either provide only existence results for a stabilizing control law, or require additional assumptions in order to compute an explicit control law. The main contribution of this chapter is precisely to offer a solution to overcome the aforementioned problem. This solution relies on a nonlinear dynamic state-feedback controller which indeed globally stabilize the equilibrium of a *non-globally linearizable triangular* system.

The results listed here are taken from [Casagrande et al., 2011a], but in contrast, some changes are made to complete the analysis and improve the controller performance by adding some gains to the scheme. In addition, the theory developed in this chapter is applied to two physical systems represented by a set of nonlinear differential equations with triangular structure, namely, a single machine infinite bus (SMIB) system and magnetic levitation (MAGLEV) system.

The remaining of the chapter is organized as follows. To facilitate the understanding of the general methodology the material is presented in increasing degrees of complexity. First, a simple example is considered in Section 2.1. Then, Sections 2.2 and 2.3 are devoted to the extensions to two- and three-dimensional systems, respectively. The applicability of the proposed scheme is presented in Section 2.4, while finally Section 2.5 contains a simplified version (numerical results included), which will be used in the following chapters.

2.1 Motivating example

The main goal of this example is to show in a simple way the stabilization problem for a specific triangular system, and equally important, to initially present the controller to be developed in this chapter. Let's begin with the triangular system described by the equations

$$\begin{aligned} \dot{x}_1 &= 1 - x_2^2 \\ \dot{x}_2 &= u\,, \end{aligned} \tag{2.1}$$

where $x_1, x_2 \in \mathbb{R}$ are the states and $u \in \mathbb{R}$ is the control signal. For our convenience, the system (2.1) will be presented in the standard form

$$\begin{bmatrix} \dot{x}_1 \\ \dot{x}_2 \end{bmatrix} = \begin{bmatrix} 1 - x_2^2 \\ 0 \end{bmatrix} + \begin{bmatrix} 0 \\ 1 \end{bmatrix} u = f(x) + g(x)u \tag{2.2}$$

where $x \in \mathbb{R}^2$. As in a standard backstepping procedure, the main idea is to use the control signal u to control x_2 and, in turn, to use x_2 to control x_1. Notice that this system does not fit the strict-feedback form [Khalil, 2000], and consequently standard backstepping technique can not be applied for stabilization purposes. However, it is possible to apply a local feedback linearization around each equilibrium point, which are included in the set

$$\mathcal{E} = \{(x_1, x_2) \in \mathbb{R}^2 \ : \ |x_2| = 1\}.$$

For instance, let's define the equilibrium point to be stabilized as $(x_1, x_2) = (0, 1)$, in order to get a local feedback linearization law, we seek a transformation $T = [T_1, T_2]^\top$ such that the next conditions hold:

$$i)\ \frac{\partial T_1}{\partial x} g = 0, \quad ii)\ \frac{\partial T_1}{\partial x} f(x) = T_2 \quad \text{and} \quad iii)\ \frac{\partial T_2}{\partial x} g \neq 0. \tag{2.3}$$

In this case, the first condition implies that

$$\frac{\partial T_1}{\partial x} g = \begin{bmatrix} \frac{\partial T_1}{\partial x_1} & \frac{\partial T_1}{\partial x_2} \end{bmatrix} \begin{bmatrix} 0 \\ 1 \end{bmatrix} = \frac{\partial T_1}{\partial x_2} = 0,$$

so that T_1 can be selected independent of x_2. Taking into account the second and the third condition simultaneously,

$$\frac{\partial T_1}{\partial x} f(x) = \begin{bmatrix} \frac{\partial T_1}{\partial x_1} & \frac{\partial T_1}{\partial x_2} \end{bmatrix} \begin{bmatrix} 1 - x_2^2 \\ 0 \end{bmatrix} = \frac{\partial T_1}{\partial x_1}(1 - x_2^2) = T_2$$

and

$$\frac{\partial T_2}{\partial x} g = \begin{bmatrix} \frac{\partial T_2}{\partial x_1} & \frac{\partial T_2}{\partial x_2} \end{bmatrix} \begin{bmatrix} 0 \\ 1 \end{bmatrix} = \frac{\partial}{\partial x_2} \left[\frac{\partial T_1}{\partial x_1}(1 - x_2^2) \right] \neq 0,$$

suggest the selection of $T_1 = x_1$, which yields to $T_2 = 1 - x_2^2$, fulfilling the conditions (2.3) above.

Furthermore, using the new variables $z_1 = x_1$ and $z_2 = 1 - x_2^2$ a new equivalent dynamical system can be defined as

$$\begin{bmatrix} \dot{z}_1 \\ \dot{z}_2 \end{bmatrix} = \begin{bmatrix} 0 & 1 \\ 0 & 0 \end{bmatrix} z + \begin{bmatrix} 0 \\ -2x_2 \end{bmatrix} u, \tag{2.4}$$

where $z = [z_1 \;\; z_2]^\top \in \mathbb{R}^2$. Observe that a stabilizing control law can be obtained as

$$u = -\frac{1}{2x_2}v,$$

and selecting $v = -z_1 - z_2$, yields finally to the local feedback linearizing law

$$u = -\frac{1}{2x_2}(-x_1 - 1 + x_2^2). \tag{2.5}$$

Notice that the control law (2.5) is not defined when $x_2 = 0$, therefore this solution offers only a local stabilization. What's more is that this control law does not distinguish between the equilibrium points $(0, 1)$ and $(0, -1)$. For this purpose, in the following part of this section, a global dynamic nonlinear stabilization controller is proposed as a solution to overcome the limitations presented above.

To this end, we define a new variable as

$$x_2^d = \frac{1 + \sigma(x_1)}{\xi}, \tag{2.6}$$

where $\xi \in \mathbb{R}^+$ is the controller state defined below in (2.8) and $\sigma : \mathbb{R} \to \mathbb{R}$ has the odd sign property if $\sigma(y)y > 0$ for $y \neq 0$ and $\sigma(0) = 0$. To render the desired equilibrium point $(0, 1)$ attractive, we need an input $u(t)$ such that

$$\lim_{t\to\infty} |x_2^d(t) - x_2(t)| = 0, \quad \lim_{t\to\infty} |\xi(t) - x_2(t)| = 0, \quad \lim_{t\to\infty} |x_2(t)| = 1.$$

For this reason, the next Lyapunov function is then proposed as

$$V(x_1, x_2, \xi) = \frac{1}{2}(x_1^2 + (\xi - x_2)^2 + (x_2 - x_2^d)^2),$$

which is obviously introduced by our desire to drive x_1 to zero and by the objectives given above. Note that the equilibrium of x_1 can take any value in $\mathbb{R}$. Subsequently, the time derivative of V is initially obtained as

$$\dot{V} = x_1(1 - x_2^2) + (\xi - x_2)(\dot{\xi} - u) + (x_2 - x_2^d)(u - \dot{x}_2^d), \tag{2.7}$$

where the dynamics of ξ selected to be

$$\dot{\xi} = u + x_2 - \xi - x_1 x_2^d, \tag{2.8}$$

yields to

$$\dot{V} = -x_1\sigma(x_1) - x_1x_2(x_2 - x_2^d) - (\xi - x_2)^2 + (x_2 - x_2^d)(u - \dot{x}_2^d).$$

Additionally the control law is proposed as

$$u = \dot{x}_2^d + x_1x_2 - (x_2 - x_2^d), \tag{2.9}$$

to render $\dot{V}$ as

$$\dot{V} = -x_1\sigma(x_1) - (\xi - x_2)^2 - (x_2 - x_2^d)^2 \tag{2.10}$$

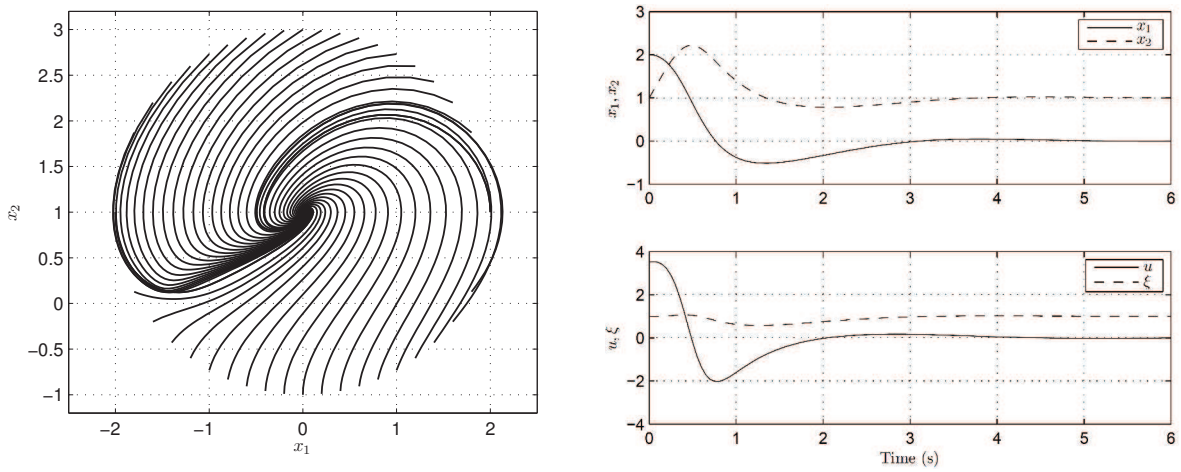

Figure 2.1: Phase portrait (left) for initial conditions on the circle $x_1^2 + (x_2 - 1)^2 = 4$ and close-loop system trajectories (right) for initial conditions $(x_1(0), x_2(0), \xi(0)) = (2, 1, 1)$.

Since the term $x_1\sigma(x_1) > 0$ when $x_1 \neq 0$, it follows that, $\dot{V} \leq 0$ and $\dot{V} = 0$ when $x_1 = 0$, $\xi = x_2$ and $x_2^* = x_2$. Applying La Salle's invariance principle, when $x_1 \equiv 0$ we have $x_2 \in \{-1, 1\}$. Since V is radially unbounded in $\mathbb{R}^2 \times \mathbb{R}^+$ and positive definite with respect to $(0, 1, 1)$, if the initial condition for ξ is chosen in $\mathbb{R}^+$, we have $\xi(t) \to 1$ and hence $x_2(t) \to 1$. The first advantage obtained by introducing the variable ξ is that we can assure that x_2 tends to 1. Moreover, the choice of the function $\sin(x_1)$ ensures that the input signal is defined for all possible trajectories.

Indeed, replacing x_2^d defined by (2.6) in (2.9), the control signal can be written in the compact form

$$u(x_1, x_2, \xi) = \frac{\xi^2 \widetilde{u}(x_1, x_2, \xi)}{\xi^2 + 1 + \sigma(x_1)}, \tag{2.11}$$

where

$$\widetilde{u}(x_1, x_2, \xi) = x_1 x_2 - (x_2 - x_2^d)^2 + \frac{1}{\xi}\frac{\partial \sigma}{\partial x_1}(1 - x_2^2) - \frac{1}{\xi^2}(1 + \sigma(x_1))(x_2 - \xi - x_1 x_2^d),$$

where the denominator is always positive and the control law is well defined, in contrast to the solution given by (2.5).

To illustrate the proposed solution, simulation results for the closed-loop system given by equation (2.1), (2.8) and (2.11) are shown in Figure 2.1 along with the monotonically decreasing Lyapunov function V in Figure 2.2. For all cases the initial condition for $\xi(0)$ is selected as 1 and $\sigma(x_1) = \tanh(x_1)$. As depicted in the phase portrait, the equilibrium $(0, 1)$ is attractive to all initial conditions, even for the trajectories starting from the other equilibrium point $(0, -1)$. Also, it is demostrated that the controller state ξ remains in $\mathbb{R}^+$ as stated above.

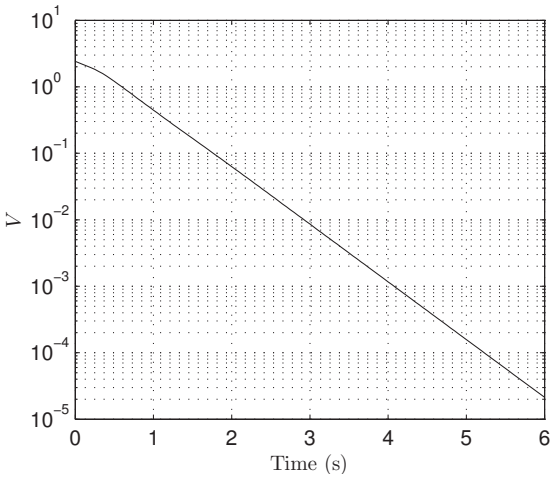

Figure 2.2: Lyapunov Function V.

2.2 The second-order case

In this section, a generalization of the ideas given before is presented as a methodology to stabilize triangular systems. To begin with, consider the second order system of the form

$$\begin{aligned} \dot{x}_1 &= f(x_1, x_2) \\ \dot{x}_2 &= u, \end{aligned} \tag{2.12}$$

where $x_1, x_2 \in \mathbb{R}$, $u \in \mathcal{U} \subset \mathbb{R}$ and $f : \mathbb{R}^2 \to \mathbb{R}$ assumed smooth. Then, suppose the origin $(x_1, x_2) = (0, 0)$ is an equilibrium, such that $f(0, 0) = 0$.

Definition 2.2.1. *A function $\sigma : \mathbb{R} \to \mathbb{R}$ has the odd sign property if $\sigma(y)y > 0$ for $y \neq 0$ and $\sigma(0) = 0$.*

Meanwhile in [Casagrande et al., 2011a] the function $\sigma(\cdot)$ has been selected as $\sigma(x_1) = \tanh(x_1)$, here we have defined this odd function as $\sigma(x_1) = \sin(x_1)$. From the last definition we can assure that the origin of (2.12) can be rendered attractive if there exist a signal $u(t)$ such that

$$\lim_{t\to\infty} |f(x_1(t), x_2(t)) + \sigma(x_1(t))| = 0, \quad \lim_{t\to\infty} |x_2(t)| = 0.$$

To this end, f needs to fulfill the next conditions.

Assumption 2.2.1. *The function f can be splitted into two functions $k : \mathbb{R} \to \mathbb{R}$ and $h : \mathbb{R}^2 \to \mathbb{R}$, with $k(0) > 0$, such that f can be written as*

$$f(x_1, x_2) = k(x_1) - h(x_1, x_2)(x_2 + \lambda), \tag{2.13}$$

for some nonzero constant $\lambda \in \mathbb{R}$.

Note that the condition $k(0) > 0$ implies that $h(0, 0) \neq 0$. Furthermore, we extend the state space by adding the controller state such that the dynamics of the closed-loop system

are

$$\begin{aligned} \dot{x}_1 &= k(x_1) - h(x_1, x_2)(x_2 + \lambda) \\ \dot{x}_2 &= u \\ \dot{\xi} &= \dot{h} + (h(x_1, x_2) - \xi) - x_1(x_2^d + \lambda), \end{aligned} \tag{2.14}$$

where $\xi \in \mathbb{R}^{sgn(h)}$ with $\xi(0) = \xi_0 \in \mathbb{R}^{sgn(h)}$ and x_2^d the solution of

$$(x_2^d + \lambda)\xi = \sigma(x_1) + k(x_1). \tag{2.15}$$

Note that the controller state ξ is introduced in the analysis to cope the effect of the function h. In addition, the notation $\mathbb{R}^{sgn(h)}$ is a compact form to denote $\mathbb{R}^+$ when $h(0,0) > 0$ and $\mathbb{R}^-$ when $h(0,0) < 0$.

Considering that in steady state $\xi = h(0,0)$, then the point in the extended space

$$(x_1, x_2, \xi) = (0, 0, h(0,0)) = \mathcal{E},$$

is an equilibrium point of (2.14), if u is a *static* state feedback verifying that $u|_{\mathcal{E}} = 0$.

Similar to the previous example, the equilibrium $\mathcal{E}$ can be asymptotically stabilized in such way that the region of attraction is $\mathbb{R}^2 \times \mathbb{R}^{sgn(h)}$. The next statements are necessary to establish the stability result.

Lemma 2.2.1. *The controllability condition for the system (2.12) at* $(0,0)$ *is*

$$h(0,0) \neq -\lambda \frac{\partial h}{\partial x_2}(0,0)\,. \tag{2.16}$$

Proof 2.2.1. *At the origin (0,0) the denominator of the explicit control law (remark 2.2.1 below) must be different from zero, this is*

$$\xi^2 + (\sigma(x_1) + k(x_1))\frac{\partial h}{\partial x_2} \neq 0.$$

To probe is indeed defined at (0,0), first we recall that at the origin we have defined that

$$\xi = h(0,0), \quad \sigma(0) = 0$$

and because $f(0,0) = 0$*, from (2.13) we get*

$$0 = k(0) - h(0,0)\lambda,$$

then evaluating (2.2.1) at the origin, results in

$$h^2(0,0) + \lambda h(0,0)\frac{\partial h}{\partial x_2}(0,0) \neq 0,$$

factorizing $h(0,0)$ *yields*

$$h(0,0)\left(h(0,0) + \lambda \frac{\partial h}{\partial x_2}(0,0)\right) \neq 0,$$

since we have already defined that $h(0,0) \neq 0$*, finally, we can state that the control law is defined at the origin if*

$$h(0,0) + \lambda \frac{\partial h}{\partial x_2}(0,0) \neq 0$$

or

$$h(0,0) \neq -\lambda \frac{\partial h}{\partial x_2}(0,0)$$

holds.

■

Lemma 2.2.2. *The Lyapunov function*

$$V(x_1, x_2, \xi) = \frac{1}{2}\left(x_1^2 + (x_2 - x_2^d)^2 + (\xi - h)^2\right), \tag{2.17}$$

with the relation between x_2^d *and* ξ *defined by (2.15), is radially unbounded in* $\mathbb{R}^2 \times \mathbb{R}^{sgn(h)}$ *if and only if*

$$\lim_{x_2 \to \infty} h(x_1, x_2) = \infty, \tag{2.18}$$

uniformly in x_1*.* □

Theorem 2.2.3. *Suppose that system (2.12) verifies Assumption 2.2.1, the controllability condition* (2.16) *and the growth condition* (2.18)*. There exists a function* σ *with the odd sign property and a neighborhood of the equilibrium* $\mathcal{E}$ *of the augmented system (2.14) such that the control law*

$$u = \dot{x}_2^d + x_1 h(x_1, x_2) - (x_2 - x_2^d), \tag{2.19}$$

with x_2^d *given by (2.15), is well-defined, and asymptotically stabilizes* $\mathcal{E}$ *with region of attraction* $\mathbb{R}^2 \times \mathbb{R}^{sgn(h)}$*.* □

Proof 2.2.2. *Considering the Lyapunov function given by (2.17) its time derivative results in the next expression*

$$\dot{V} = x_1(k(x_1) - (x_2 + \lambda)h) + (x_2 - x_2^d)(u - \dot{x}_2^d) + (\xi - h)(\dot{\xi} - \dot{h}),$$

where from (2.14) and (2.19) we get

$$\begin{aligned} \dot{\xi} - \dot{h} &= (h - \xi) - x_1(x_2^d + \lambda) \\ u - \dot{x}_2^d &= x_1 h - (x_2 - x_2^d) \end{aligned}$$

and in combination of (2.15), the equation of $\dot{V}$ *is finally computed as*

$$\dot{V} = -x_1\sigma(x_1) - (\xi - h)^2 - (x_2 - x_2^d)^2.$$

■

Remark 2.2.1. *The controllability rank condition in Theorem 2.2.3 is necessary since the explicit computation of the control law (2.19) yields, after some manipulations, to*

$$u(x_1, x_2, \xi) = \frac{\xi^2 \tilde{u}(x_1, x_2, \xi)}{\xi^2 + (\sigma(x_1) + k(x_1))\dfrac{\partial h}{\partial x_2}},$$

where

$$\tilde{u} = \tilde{u}_1 + x_1 h(x_1, x_2) - (x_2 - x_2^d),$$

with

$$\tilde{u}_1 = \frac{1}{\xi}\left(\frac{\partial \sigma}{\partial x_1} + \frac{\partial k}{\partial x_1}\right) f(x_1, x_2) - \frac{1}{\xi^2}(\sigma + k)\left(\frac{\partial h}{\partial x_1} f(x_1, x_2) + (h - \xi) - x_1(x_2^d + \lambda)\right).$$

Corollary 2.2.4. *If $\partial h/\partial x_2 > 0$ for all x_1 and all x_2 and if, for some $\eta \in \mathbb{R}^+$, $k(x_1) > \eta$, then there exists a function σ with the odd sign property such that $\sigma(x_1) + k(x_1) > 0$, with u given by (2.19), the equilibrium $\mathcal{E}$ of (2.14) is locally asymptotically stable and the region of attraction is $\mathbb{R}^2 \times \mathbb{R}^{sgn(h)}$, consequently the equilibrium $x_1 = 0$, $x_2 = 0$ is globally asymptotically stable.*

Example: Consider again the triangular system of Section 2.1. The selected equilibrium point $(0, 1) = (\bar{x}_1, \bar{x}_2)$ is now shifted to the origin by the error coordinates

$$\begin{aligned} \tilde{x}_1 &= x_1 - \bar{x}_1 = x_1 \\ \tilde{x}_2 &= x_2 - \bar{x}_2 = x_2 - 1. \end{aligned} \tag{2.20}$$

Consequently, the system (2.1) is transformed into

$$\begin{aligned} \dot{\tilde{x}}_1 &= 1 - (\tilde{x}_2 + 1)(\tilde{x}_2 + 1) \\ \dot{\tilde{x}}_2 &= u, \end{aligned} \tag{2.21}$$

which $\dot{\tilde{x}}_1$ is of the form (2.13) with $k(\tilde{x}_1) = 1$, $\lambda = \bar{x}_2 = 1$ and $h(\tilde{x}_1, \tilde{x}_2) = (\tilde{x}_2 + 1)$. Moreover, $h(0, 0) = 1 \neq 0$ and the controllability rank condition holds. Finally, we have $\partial h/\partial \tilde{x}_2 = 1 > 0$ and the hypotheses of Corollary 2.2.4 are fulfilled. Therefore, the function $\sigma(\tilde{x}_1) = \sin(\tilde{x}_1)$ is such that the control law locally asymptotically stabilizes the equilibrium and the region of attraction is $\mathbb{R}^2 \times \mathbb{R}^+$. Equivalent numerical results to those in Figures 2.1 and 2.2 may be obtained for this example with the equilibrium shifted to the origin.

2.3 The third-order case

For our purpose, the result described in the previous section is now extended to a system with three states in triangular form. Specifically, we consider systems of the form

$$\begin{aligned} \dot{x}_1 &= f_1(x_1, x_2) \\ \dot{x}_2 &= f_2(x_1, x_2, x_3) \\ \dot{x}_3 &= u\,, \end{aligned} \tag{2.22}$$

where $x_1, x_2, x_3 \in \mathbb{R}$, $f_1 : \mathbb{R}^2 \to \mathbb{R}$ and $f_2 : \mathbb{R}^3 \to \mathbb{R}$ assumed smooth vector fields and $(0,0,0)$ is an equilibrium. Therefore, to render these equilibrium point $(0,0,0)$ attractive, we need an input $u(t)$ such that

$$\lim_{t\to\infty} |x_1(t)| = 0, \quad \lim_{t\to\infty} |x_2(t) - x_2(t)^d| = 0, \quad \lim_{t\to\infty} |x_3(t) - x_3^d(t)| = 0,$$

$$\lim_{t\to\infty} |\xi_1(t) - h_1(t)| = 0, \quad \lim_{t\to\infty} |\xi_2(t) - h_2(t)| = 0,$$

where $\xi_1 \in \mathbb{R}$ and $\xi_2 \in \mathbb{R}$ are the controller states and $x_2^d \in \mathbb{R}$ and $x_3^d \in \mathbb{R}$ are auxiliary signals, all them defined below. To this end, f_1 and f_2 are required to have the next structure.

Assumption 2.3.1. *There exist some smooth functions $k_1 : \mathbb{R} \to \mathbb{R}$, $k_2 : \mathbb{R}^2 \to \mathbb{R}$, $h_1 : \mathbb{R}^2 \to \mathbb{R}$ and $h_2 : \mathbb{R}^3 \to \mathbb{R}$, verifying $k_1(0) > 0$ and $k_2(0,0) > 0$, such that, we can split each f_1 and f_2 as*

$$\begin{aligned} f_1(x_1, x_2) &= k_1(x_1) - (x_2 + \lambda_1)h_1(x_1, x_2) \\ f_2(x_1, x_2, x_3) &= k_2(x_1, x_2) - (x_3 + \lambda_2)h_2(x_1, x_2, x_3), \end{aligned} \tag{2.23}$$

with some nonzero constants λ_1, $\lambda_2 \in \mathbb{R}$.

Note that since $f_1(0,0) = 0$ and $f_2(0,0,0) = 0$, we have $k_1(0) = \lambda_1 h_1(0,0)$ and $k_2(0,0) = \lambda_2 h_2(0,0,0)$. Moreover the requirements on k_1 and k_2 imply $h_1(0,0) \neq 0$ and $h_2(0,0,0) \neq 0$, respectively.

As presented before, we make use of the functions x_2^d and x_3^d defined by the relationships

$$\begin{aligned} (x_2^d + \lambda_1)\xi_1 &= \sigma(x_1) + k_1(x_1) \\ (x_3^d + \lambda_2)\xi_2 &= \sigma(x_2 - x_2^d) - x_1 h_1(x_1, x_2) + k_2(x_1, x_2) - \dot{x}_2^d, \end{aligned} \tag{2.24}$$

where we introduced the controller states ξ_1 and ξ_2 to cope with the nonlinearities h_1 and h_2, respectively. In any case, we have only defined one function $\sigma(\cdot)$ with the odd sign property for analysis simplification. In the following, arguments will be omitted for brevity.

Now, consider the augmented system

$$\begin{aligned} \dot{x}_1 &= k_1 - (x_2 + \lambda_1)h_1 \\ \dot{x}_2 &= k_2 - (x_3 + \lambda_2)h_2 \\ \dot{x}_3 &= u \\ \dot{\xi}_1 &= \dot{h}_1 + \pi_1(h_1 - \xi_1) - \pi_2 x_1(x_2^d + \lambda_1) \\ \dot{\xi}_2 &= \dot{h}_2 + \pi_3(h_2 - \xi_2) - \pi_4(x_3^d + \lambda_2)(x_2 - x_2^d), \end{aligned} \tag{2.25}$$

where π_1 to π_4 are positive real constants to be selected. Afterwards, define the point

$$(x_1, x_2, x_3, \xi_1, \xi_2) = (0, 0, 0, h_1(0,0), h_2(0,0,0)) := \mathcal{E},$$

and note that, if u is a *static* state feedback verifying $u|_{\mathcal{E}} = 0$, then $\mathcal{E}$ is an equilibrium of (2.25).

Lemma 2.3.1. *The system (2.22) can be stabilized to* $(0,0,0)$*, if the controllability condition*

$$\begin{aligned} h_1(0,0) &\neq -\lambda_1 \frac{\partial h_1}{\partial x_2}(0,0) \\ h_2(0,0,0) &\neq -\lambda_2 \frac{\partial h_2}{\partial x_3}(0,0,0), \end{aligned} \tag{2.26}$$

holds

Lemma 2.3.2. *The Lyapunov function*

$$V(x_1,x_2,x_3,\xi_1,\xi_2) = \frac{1}{2}(c_1x_1^2+c_2(\xi_1-h_1)^2+c_3(\xi_2-h_2)^2+c_4(x_2-x_2^d)^2+c_5(x_3-x_3^d)^2), \tag{2.27}$$

with x_2^d *and* x_3^d *defined by (2.24) and* c_1 *to* c_5 *positive real constants, is radially unbounded in* $\mathbb{R}^3 \times \mathbb{R}^{sgn(h_1)} \times \mathbb{R}^{sgn(h_2)}$ *if and only if*

$$\lim_{x_2\to\infty} h_1(x_1,x_2) = \infty, \quad \lim_{x_3\to\infty} h_2(x_1,x_2,x_3) = \infty, \tag{2.28}$$

uniformly in x_1*, and in* x_1 *and* x_2*, respectively.*

Theorem 2.3.3. *Consider the system (2.22) verifying Assumption 2.3.1, the controllability rank condition (2.26), and the growth condition* (2.28)*. There exist a function* σ*, with the odd sign property, and a neighborhood of the equilibrium* $\mathcal{E}$ *of the augmented system (2.25) such that the control law*

$$u = \dot{x}_3^d + \pi_5 h_2(x_2 - x_2^d) - \pi_6(x_3 - x_3^d)\,, \tag{2.29}$$

with π_5 *and* π_6 *positive real constants, is well-defined, and asymptotically stabilizes* $\mathcal{E}$ *with region of attraction* $\mathbb{R}^3 \times \mathbb{R}^{sgn(h_1)} \times \mathbb{R}^{sgn(h_2)}$*.* □

Proof 2.3.1. *Consider the positive real constants* π_1*,* π_3*,* π_6*,* c_3 *and* c_5 *as free variables, fixing* $\pi_2 = 1$*, selecting freely* $c_1 = c_2 = c_4$ *and defining* $\pi_4 = c_1/c_3$ *and* $\pi_5 = c_1/c_5$*, after some computations the time derivative of* V *results in*

$$\begin{aligned} \dot{V} = &-c_2\pi_2 x_1\sigma(x_1) - c_3\pi_4(x_2 - x_2^d)\sigma(x_2 - x_2^d) - \\ &- c_5\pi_6(x_3 - x_3^d)^2 - c_2\pi_1(\xi_1 - h_1)^2 - c_3\pi_3(\xi_2 - h_2)^2. \end{aligned} \tag{2.30}$$

It follows that, $\dot{V} \leq 0$ *and* $\dot{V} = 0$ *when* $x_1 = 0$*,* $x_2 = x_2^d$*,* $x_3 = x_3^d$*,* $\xi_1 = h_1$ *and* $\xi_2 = h_2$*.* ■

Remark 2.3.1. *The controllability rank condition in Theorem 2.3.3 is necessary since the explicit computation of the control law (2.29) yields, after some manipulations, to*

$$u = \frac{\xi_2^2 \tilde{u}}{\xi_2^2 + \Phi_2 \dfrac{\partial h_2}{\partial x_3}}\,,$$

where

$$\tilde{u} = \frac{1}{\xi_2}\Phi_1 - \frac{1}{\xi_2^2}\Phi_2\Gamma + \pi_5 h_2(x_2 - x_2^d) - \pi_6(x_3 - x_3^d),$$

with

$$\Gamma = \frac{\partial h_2}{\partial x_1}\dot{x}_1 + \frac{\partial h_2}{\partial x_2}\dot{x}_2 + \pi_3(h_2 - \xi_2) - \pi_4(x_3^d + \lambda_2)(x_2 - x_2^d),$$

$$\Phi_1 = \dot{\sigma}(x_2 - x_2^d) - x_1\dot{h}_1 - \dot{x}_1 h_1 + \dot{k}_2 - \ddot{x}_2^d,$$

and finally

$$\Phi_2 = \sigma(x_2 - x_2^d) - x_1 h_1(x_1, x_2) + k_2(x_1, x_2) - \dot{x}_2^d.$$

Corollary 2.3.4. *If $\partial h_2/\partial x_3 > 0$ and if, for some $\eta \in \mathbb{R}^+$, $\Phi_2 > \eta$ for all x_1 and all x_2, then there exists a function σ with the odd property such that the control law (2.29) locally asymptotically stabilizes $\mathcal{E}$ and the region of attraction is $\mathbb{R}^3 \times \mathbb{R}^{sgn(h_1)} \times \mathbb{R}^{sgn(h_2)}$. Hence the original equilibrium $x_1 = 0$, $x_2 = 0$ and $x_3 = 0$ is globally asymptotically stable.*

2.4 Applicability examples

The goal of this section is to show how the theory developed in this chapter is applied to physical systems modeled by a set of nonlinear differential equations in triangular form. To this end, a single machine infite bus (SMIB) system and a magnetic levitation (MAGLEV) system are considered and some simulation results are also given. Note that in this exercise, we assume all parameters known and all state variables available for measurement for both SMIB and MAGLEV systems.

2.4.1 Single machine infinite bus system

Electric power is produced at generation stations (normally three-phase synchronous machines) and transmitted to consumers via an interconnected complex network of individual components [Kundur, 1994; Anderson and Fouad, 2003]. Due to the high complexity of power systems, their stability properties are often analyzed by considering separately each generating units, while the set of the other machines and components are then considered an infinite bus (running at constant voltage and frequency) with respect to the machine under consideration. This infinite bus is connected to the generator through transformers, transmission lines and loads, which have an equivalent admittance Y as depicted in Figure 2.3.

The SMIB electrical and mechanical dynamics are represented by the set of nonlinear differential equations (2.31) as in [Ortega et al., 2005]

$$\begin{aligned} \dot{\delta} &= \omega \\ \dot{\omega} &= -D\omega + P - GE^2 - EV_B Y \sin(\delta + \alpha) \\ \dot{E} &= -aE + bV_B Y \cos(\delta + \alpha) + \frac{1}{\tau}(E_f + \nu), \end{aligned} \tag{2.31}$$

where the states variables are the rotor angle $\delta \in [0, \pi)$ in rad, the angular speed deviation $\omega \in \mathbb{R}$ in rad/sec and the quadrature axis internal voltage $E \in \mathbb{R}^+$ in $p.u.$ (also called the voltage behind the transient reactance), respectively. The control input is the field

excitation signal ν in *p.u.*

The normalized parameters D and P stands for the friction factor and the mechanical power, the last assumed constant. G is the normalized generator self-conductance. V_B is the bus voltage in *p.u.* normally assumed as one, Y and α are related with the conductance and susceptance of the network (admittance matrix). The constants a and b are related with the synchronous and transient reactances of the direct-axis, as well as the self-susceptance of the machine. The constant τ is the direct-axis transient time constant in *sec.* E_f represents the constant voltage component of the field excitation. The reader is kindly referred to [Ortega et al., 2005] and the bibliography therein for more details about the system parameters.

The set of equations (2.31) refers also to the classical three-dimensional flux decay model in which lossy transmission line is supposed. In this case, the presence of transfer conductance reflected in the term GE^2 is explicitly taken into account. Due to this nonlinearity, the model is called the *lossy* model of the SMIB system and standard backstepping technique can not be applied since the lossy model does not present a strict-feedback structure.

To derive the proposed controller, it is convenient first to apply a partial linearizing feedback law to cancel nonlinearities presented in the third component of the set of equations (2.31), *i.e.*,

$$\nu = \tau[u + aE - bV_B Y \cos(\delta + \alpha)] - E_f, \tag{2.32}$$

where u is the new control input. Then, the equilibrium point $(\bar{\delta}, 0, \bar{E})$ of the resulting system is shifted to the origin by using the error coordinates,

$$x_1 := \delta - \bar{\delta}, \quad x_2 := \omega, \quad x_3 := E - \bar{E}, \tag{2.33}$$

therefore, we obtain an equivalent system

$$\begin{aligned} \dot{x}_1 &= x_2 \\ \dot{x}_2 &= -Dx_2 + P - (x_3 + \bar{E})\left[G(x_3 + \bar{E}) + V_B Y \sin(x_1 + \bar{\delta} + \alpha)\right] \\ \dot{x}_3 &= u \end{aligned} \tag{2.34}$$

where analogously to (2.22) and accordingly to assumption 2.3.1, we get

$$\begin{aligned} \lambda_1 &= -1, & \lambda_2 &= \bar{E}, \\ k_1(x_1) &= 1, & k_2(x_1, x_2) &= -Dx_2 + P, \\ h_1(x_1, x_2) &= -1, & h_2(x_1, x_2, x_3) &= G(x_3 + \bar{E}) + V_B Y \sin(x_1 + \bar{\delta} + \alpha). \end{aligned} \tag{2.35}$$

Moreover, defining the odd function as $\sigma(\cdot) = \sin(\cdot)$, the control law (2.29) described in the last section is then defined and applied to the SMIB to stabilize the equilibrium point $(\bar{\delta}, 0, \bar{E})$. All system parameters and controller gains are gathered in Table 2.1 and 2.2, respectively. The initial conditions are $\delta(0) = 0.9838$ *rad*, $\omega(0) = 0.2$ *rad/sec* and $E(0) = 0.8440$ *p.u.*. The controller initial conditions are $\xi_1(0) = -1$ and $\xi_2(0) = 33.8$, both selected equal to $h_1(0, 0)$ and $h_2(0, 0, 0)$ respectively.

Parameter	Value
G	0.1
α	0.5
Y	34.29
D	0.1
b	0.0043
a	0.3341
E_f	0.3266
P	35.7259
$\bar{\delta}$	0.8944
$\bar{E}$	1.055
V_B	1

Table 2.1: SMIB system parameters.

In Figure 2.4 the time histories of the augmented system states are shown. It is evident that the error coordinates converge to zero, been the error x_2 the most representative signal since it has stronger oscillatory behavior than the other two, phenomenon inherent to EPS. Simultaneously, the controller states ξ_1 and ξ_2 barely move from their equilibriums. All these signals converge their steady states at 8 seconds approximately. In Figure 2.5 the control signal ν and the Lyapunov function are presented, where the last, accordingly to theory, present a monotonically decreasing behavior proving global asymptotic stability.

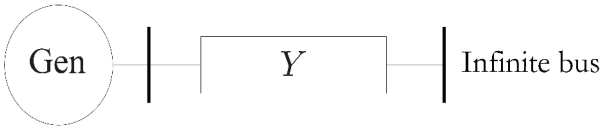

Figure 2.3: SMIB system.

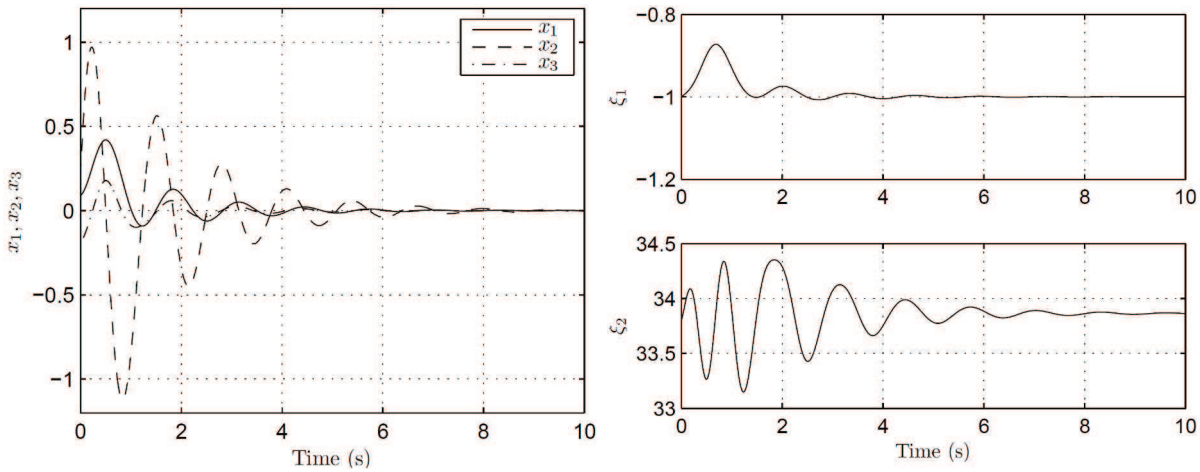

Figure 2.4: States of the augmented system for the SMIB.

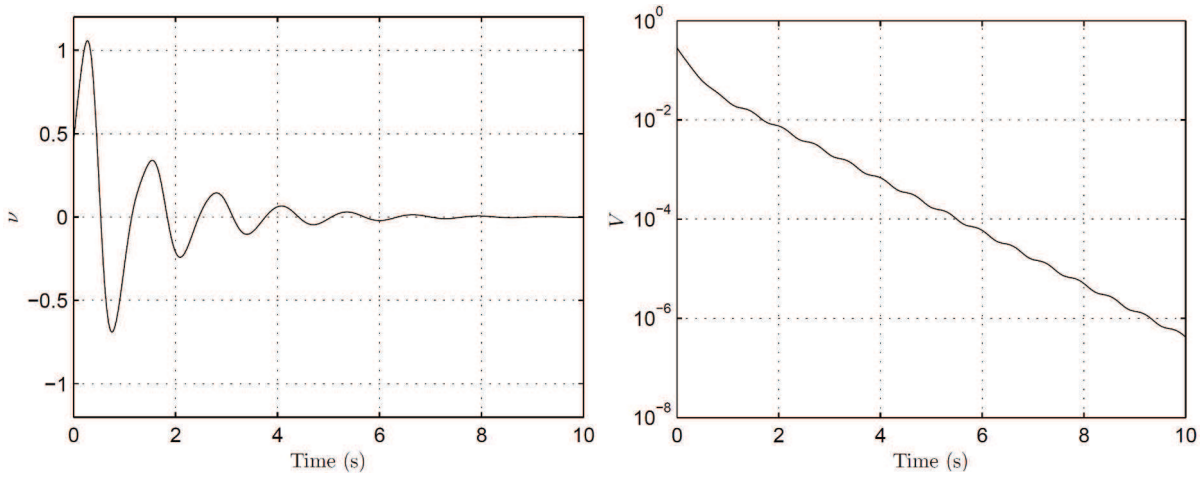

Figure 2.5: Control Signal and Lyapunov function for the SMIB.

Gain	SMIB	MAGLEV
π_1	4	3.5
π_2	1	1
π_3	2.5	2.5
π_4	0.035	1
π_5	0.02	0.5
π_6	0.001	0.1
c_1, c_2, c_4	0.07	0.5
c_3	2	0.5
c_5	3.5	1

Table 2.2: Controller gains.

2.4.2 Magnetic levitation system

This kind of systems are a familiar setup that is receiving increasing attention in applications where it is essential to reduce friction force due to mechanical contact. Magnetic suspension systems are commonly encountered in high-speed trains and magnetic bearings, as well as in gyroscopes and accelerometers. The basic configuration is shown in Figure 2.6, where m is the mass of the ball, y is the distance between the ball and the electromagnet, i is the current passing through the coil and v is the voltage applied to the coil.

In order to keep *levitating* the ball in the air, an electromagnetic force due to current must be generated by the electromagnet with the same magnitude and opposite direction as the force due to gravity. Nevertheless, since the ball is required to levitate at a desired position, a controller is needed for this task.

To begin with, a state space model for this system can be formulated by the set of

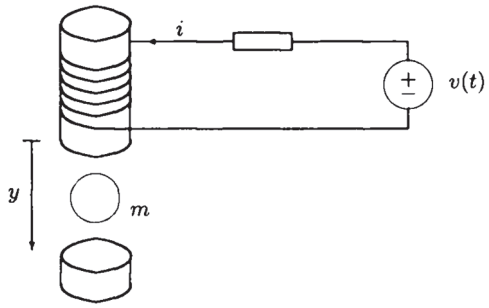

Figure 2.6: MAGLEV system.

equations

$$\begin{aligned}\dot{y}_1 &= y_2 \\ \dot{y}_2 &= g - \frac{D}{m}y_2 - \frac{\lambda_L \mu_L y_3^2}{2m(1+\mu_L y_1)^2} \\ \dot{y}_3 &= \frac{1+\mu_L y_1}{\lambda_L}\left[-Ry_3 + \frac{\lambda_L \mu_L}{(1+\mu_L y_1)^2}y_2 y_3 + v + v_f\right],\end{aligned} \tag{2.36}$$

where we renamed the position of the ball $y = y_1$, the speed of the ball $\dot{y} = y_2$ and the current $i = y_3$. g stands for the gravity constant, D is the viscous friction coefficient, λ_L and μ_L are positive constants related to the inductance L which is position dependent. R is the coil electrical resistance and v_f is the voltage constant component to keep the ball at a desired position. For further details about the obtention of this model, the interested reader is referred to [Marquez, 2003], where some physical laws are used to get the dynamics above.

The main goal here is to fit the model (2.36) with the structure given by (2.22). Again, we use a partial linearizing control law

$$v = \frac{\lambda_L}{1+\mu_L y_1}u + Ry_3 - \frac{\lambda_L \mu_L}{(1+\mu_L y_1)^2}y_2 y_3 - v_f, \tag{2.37}$$

with the new control signal u, such that in combination with the error coordinates

$$x_1 := y_1 - \bar{y}_1, \quad x_2 := y_2, \quad x_3 := y_3 - \bar{y}_3 \tag{2.38}$$

where $\bar{y}_1$ is the desired ball position, meanwhile $\bar{y}_3$ is the required current for such desired position, yield the equivalent system

$$\begin{aligned}\dot{x}_1 &= x_2 \\ \dot{x}_2 &= g - \frac{D}{m}x_2 - (x_3 + \bar{y}_3)\frac{\lambda_L \mu_L (x_3 + \bar{y}_3)}{2m(1+\mu_L(x_1+\bar{y}_1))^2} \\ \dot{x}_3 &= u,\end{aligned} \tag{2.39}$$

where analogously to (2.22) and accordingly to assumption 2.3.1, we get

$$\begin{array}{rclrcl} \lambda_1 & = & -1, & \lambda_2 & = & \bar{y}_3, \\ k_1(x_1) & = & 1, & k_2(x_1,x_2) & = & g - \frac{D}{m}x_2, \\ h_1(x_1,x_2) & = & -1, & h_2(x_1,x_2,x_3) & = & \frac{\lambda_L \mu_L (x_3+\bar{y}_3)}{2m(1+\mu_L(x_1+\bar{y}_1))^2}. \end{array} \tag{2.40}$$

Again, defining the odd function as $\sigma(\cdot) = \sin(\cdot)$, the control law (2.29) is then defined and applied to the MAGLEV to stabilize the equilibrium point $(\bar{y}_1, 0, \bar{y}_3)$. All system parameters and controller gains are gathered in Table 2.3 and 2.2, respectively. The initial conditions are $y_1(0) = 0.05\ m$, $y_2(0) = 0\ m/sec$ and $y_3(0) = 3\ A$.. The controller state initial conditions are $\xi_1(0) = -1$ and $\xi_2(0) = 3.1$, both selected equal to $h_1(0, 0)$ and $h_2(0, 0, 0)$ respectively.

Parameter	Value
m	0.05
g	9.81
λ_L	1
μ_L	0.1
D	0.001
R	1.2
v_f	3.7961
$\bar{y}_1$	0.1
$\bar{y}_1$	3.1634

Table 2.3: MAGLEV system parameters.

In Figure 2.7 the time histories of the augmented system states are shown. Meanwhile all error signals converge to zero, the error x_2 is the most representative signal since it has stronger oscillatory behavior than the other two. Simultaneously, the controller states ξ_1 and ξ_2 barely move from their equilibriums. All these signals converge their steady states around $t = 6$ seconds. In Figure 2.5 the control signal v and the Lyapunov function are presented, where the last, accordingly to theory, present a monotonically decreasing behavior, desired feature, reflecting GAS.

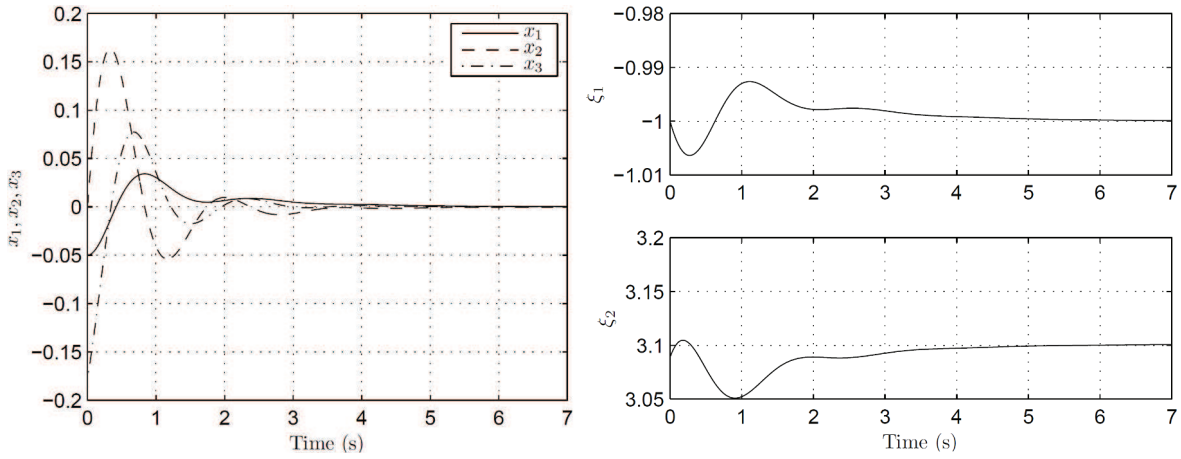

Figure 2.7: States of the augmented system for the MAGLEV.

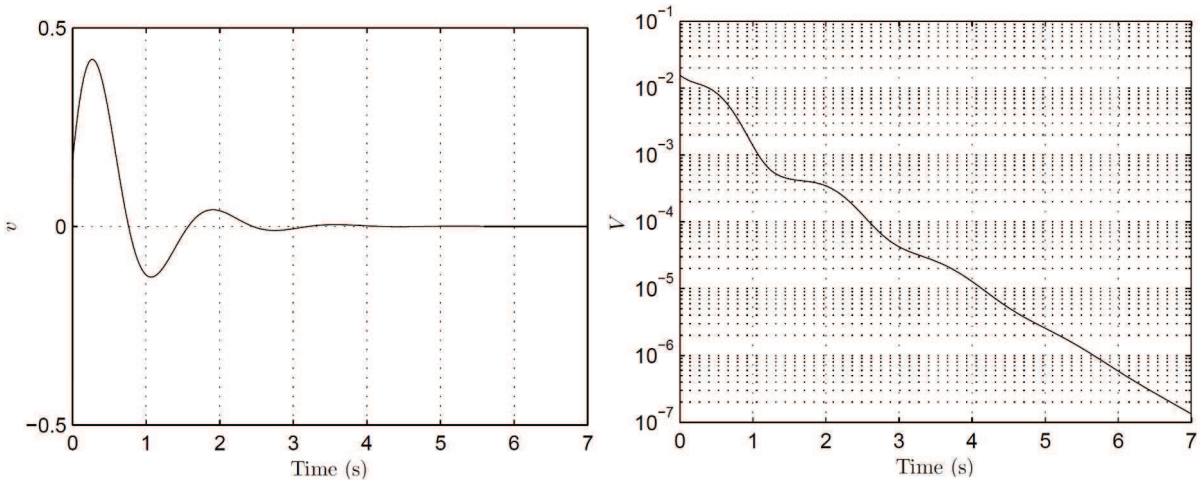

Figure 2.8: Control Signal and Lyapunov function for the MAGLEV.

2.5 Simplified controller

In this section, in contrast with the previous one, we present the formalization of a *simplified* controller as presented in [Casagrande et al., 2011a]. This simplified version arises from the need to properly fit the theory to the application which is the stabilization of power systems, as it will be present in the following chapters. To this end, consider the system

$$\begin{aligned} \dot{x}_1 &= f_1(x_2) \\ \dot{x}_2 &= f_2(x_1, x_2, x_3) \\ \dot{x}_3 &= u \end{aligned} \tag{2.41}$$

where $x_1, x_2, x_3 \in \mathbb{R}$, $u \in \mathcal{U} \subset \mathbb{R}$, $f_1 : \mathbb{R} \to \mathbb{R}$ and $f_2 : \mathbb{R}^3 \to \mathbb{R}$ are smooth vector fields and the origin $(0, 0, 0)$ is an equilibrium.

From the last definition we can assure that the origin of (2.41) is rendered attractive if the there exist a signal $u(t)$ such that

$$\lim_{t\to\infty} |x_1(t)| = 0, \quad \lim_{t\to\infty} |x_2(t)| = 0, \quad \lim_{t\to\infty} |x_3(t) - x_3^d(t)| = 0,$$

$$\lim_{t\to\infty} |\xi(t) - h(t)| = 0,$$

where $\xi \in \mathbb{R}$ is the controller state and $x_3^d \in \mathbb{R}$ is an auxiliary signal, redefined below. To this end, f_2 need to fulfill the next conditions.

Assumption 2.5.1. *There exist functions $k : \mathbb{R} \to \mathbb{R}$ and $h : \mathbb{R}^2 \to \mathbb{R}$, verifying $f_1(0) = 0$, $k(0) = p > 0$ and $h(0, 0) > 0$, such that*

$$f_2(x_1, x_2, x_3) \;=\; k(x_2) - (x_3 + \lambda)h(x_1, x_3), \tag{2.42}$$

for some real constant $\lambda \neq 0$.

Since $f_2(0,0,0) = 0$, in the equilibrium we have $k(0) = p = \lambda h(0,0)$. Note that in this case, the controller uses only one dynamical state ξ because only one function h is taken into consideration. Subsequently, we introduce the relationship

$$(x_3^d + \lambda)\xi = \sigma(x_1) + k(0), \tag{2.43}$$

and the augmented system results in

$$\begin{aligned} \dot{x}_1 &= f_1(x_2) \\ \dot{x}_2 &= k(x_2) - (x_3 + \lambda)h(x_1, x_3) \\ \dot{x}_3 &= u \\ \dot{\xi} &= \dot{h} + \pi_1(h - \xi) - \pi_2 x_2(x_3^d + \lambda) - \epsilon\sigma(x_1)(x_3 + \lambda), \end{aligned} \tag{2.44}$$

where $\xi \in \mathbb{R}^{sgn(h)}$ with $\xi(0) = \xi_0 \in \mathbb{R}^{sgn(h)}$, and π_1, π_2, ϵ as positive constants. Define the point

$$(x_1, x_2, x_3, \xi) = (0, 0, 0, h(0,0)) := \mathcal{E},$$

and note that, if u is a static state feedback verifying $u|_{\mathcal{E}} = 0$, then $\mathcal{E}$ is an equilibrium of (2.44).

Lemma 2.5.1. *The controllability condition for the system (2.41) is then*

$$h(0,0) \quad \neq \quad -\lambda \frac{\partial h}{\partial x_3}(0,0)\,. \tag{2.45}$$

Lemma 2.5.2. *The Lyapunov function*

$$V = c_1 \int_0^{x_1} \sigma(\eta)\mathrm{d}\eta + c_2\epsilon x_2\sigma(x_1) + \frac{1}{2}\left[c_3 x_2^2 + c_4(\xi - h)^2 + c_5(x_3 - x_3^d)^2\right], \tag{2.46}$$

with c_i, for $i = 1, 2, \ldots, 5$ are positive constant gains and x_3^d defined by (2.43), is radially unbounded in $\mathbb{R}^3 \times \mathbb{R}^{sgn(h)}$ if and only if

$$\lim_{x_3 \to \infty} h(x_1, x_3) = \infty, \tag{2.47}$$

uniformly in x_1.

Theorem 2.5.3. *Consider the system (2.41) verifying Assumption 2.5.1, the controllability rank condition (2.45), and the growth condition* (2.47)*. There exist a function σ, with the odd sign property, and a neighborhood of the equilibrium $\mathcal{E}$ of the augmented system (2.44) such that the control law*

$$u = \dot{x}_3^d + \pi_3 h x_2 - \pi_4(x_3 - x_3^d) + \epsilon\sigma(x_1)\xi, \tag{2.48}$$

with π_3 and π_4 as positive constants gains and x_3^d given by (2.43), is well-defined, and asymptotically stabilizes $\mathcal{E}$ with region of attraction $\mathbb{R}^3 \times \mathbb{R}^{sgn(h)}$. □

Remark 2.5.1. *The controllability rank condition in Theorem 2.5.3 is necessary since the explicit computation of the control law (2.48) yields, after some manipulations, to the explicit form*

$$u(x_1, x_2, \xi) = \frac{\xi^2 \tilde{u}(x_1, x_2, x_3, \xi)}{\xi^2 + (\sigma(x_1) + k(0))\dfrac{\partial h}{\partial x_3}},$$

where

$$\tilde{u} = \tilde{u}_1 + \pi_3 x_2 h(x_1, x_2) - \pi_4(x_3 - x_3^d) + \epsilon\sigma(x_1)\xi,$$

with

$$\tilde{u}_1 = \frac{1}{\xi}\frac{\partial \sigma}{\partial x_1} f_1 - \frac{1}{\xi^2}\left(\sigma(x_1) + k(0)\right)\left(\frac{\partial h}{\partial x_1} f_1 + \pi_1(h - \xi) - \pi_2 x_2(x_3^d + \lambda) - \sigma(x_1)\epsilon(x_3 + \lambda)\right).$$

Corollary 2.5.4. *If $\partial h/\partial x_3 > 0$ and if, for some $p \in \mathbb{R}^+$, $k(0) = p$, then there exists a function σ with the odd property such that $\sigma(x_1) + p > 0$ for all x_1, then the control law (2.48) locally asymptotically stabilizes $\mathcal{E}$ and the region of attraction is $\mathbb{R}^3 \times \mathbb{R}^{sgn(h)}$. Hence the original equilibrium $x_1 = 0$, $x_2 = 0$ and $x_3 = 0$ is globally asymptotically stable.*

In the next, simulation results for the SMIB and MAGLEV systems are presented using the *simplified* controller (2.48) and comments are given camparing these results with those using the *complete* controller (2.29).

SMIB

Recalling the expression (2.34) and repeated here for convenience

$$\begin{aligned} \dot{x}_1 &= x_2 \\ \dot{x}_2 &= -Dx_2 + P - (x_3 + \bar{E})\left[G(x_3 + \bar{E}) + V_B Y \sin(x_1 + \bar{\delta} + \alpha)\right] \\ \dot{x}_3 &= u, \end{aligned} \tag{2.49}$$

where analogously to (2.41) and accordingly to assumption 2.5.1, we identify the functions

$$\begin{aligned} \lambda &= \bar{E}, \\ k(x_2) &= -Dx_2 + P, \\ h(x_1, x_3) &= G(x_3 + \bar{E}) + V_B Y \sin(x_1 + \bar{\delta} + \alpha), \end{aligned} \tag{2.50}$$

and defining again the odd function as $\sigma(\cdot) = \sin(\cdot)$, the control law (2.48) is then defined and applied to the SMIB to stabilize the equilibrium point $(\bar{\delta}, 0, \bar{E})$. All controller gains for this case are gathered in Table 2.4.

Figures 2.9 and 2.10 show the interest variables for this case. For instance, the error variables oscillate less and converge faster to the origin than those corresponding to the *complete* controller in Figure 2.4. On the other hand, the control signal ν here is stronger than the one presented in Figure 2.5. It is important to mention that this *simplified* controller uses only one state, for that reason, we present only the state ξ in Figure 2.9, which can be compared with ξ_2 in Figure 2.4. Finally, as stated by theory the Lyapunov function is monotonically decreasing at all time.

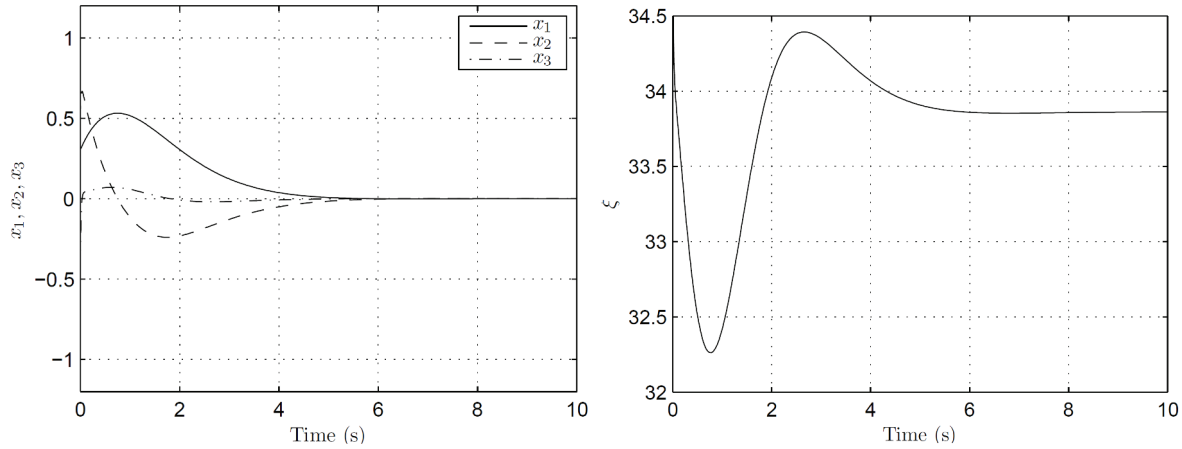

Figure 2.9: States of the augmented system for the SMIB, simplified controller.

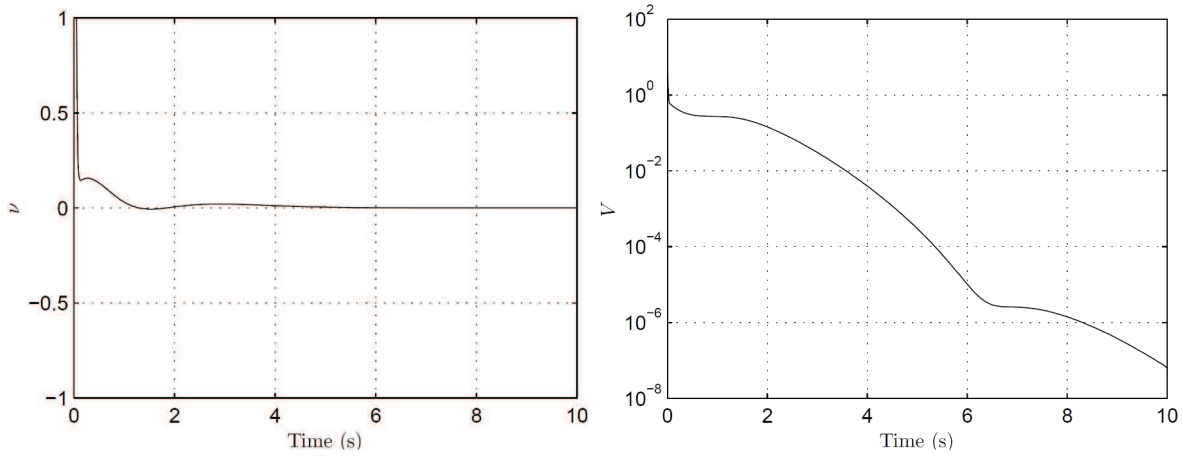

Figure 2.10: Control signal and Lyapunov function for the SMIB, simplified controller.

MAGLEV

Recalling the expression (2.39) and repeated here for convenience

$$\begin{aligned} \dot{x}_1 &= x_2 \\ \dot{x}_2 &= g - \frac{D}{m}x_2 - (x_3 + \bar{y}_3)\frac{\lambda_L \mu_L (x_3 + \bar{y}_3)}{2m(1 + \mu_L(x_1 + \bar{y}_1))^2} \\ \dot{x}_3 &= u \end{aligned} \tag{2.51}$$

where analogously to (2.41) and accordingly to assumption 2.5.1, we get

$$\begin{aligned} \lambda &= \bar{y}_3, \\ k(x_1, x_2) &= g - \tfrac{D}{m}x_2, \\ h(x_1, x_2, x_3) &= \tfrac{\lambda_L \mu_L (x_3 + \bar{y}_3)}{2m(1+\mu_L(x_1+\bar{y}_1))^2}, \end{aligned} \tag{2.52}$$

and defining the odd function as $\sigma(\cdot) = \sin(\cdot)$, the control law (2.48) is then defined and applied to the MAGLEV system to stabilize the equilibrium point $(\bar{\delta}, 0, \bar{E})$. All controller

gains for this case are gathered in Table 2.4.

Figures 2.11 and 2.12 show the interest variables for this case. Comparatively, the error variables have less amplitude and converge faster to the origin than those corresponding to the *complete* controller in Figure 2.7. On the other hand, the control signal v here is stronger than the one presented in Figure 2.8. What's more, the Lyapunov function is monotonically decreasing at all time clamming asymptotic stability of the closed-loop system.

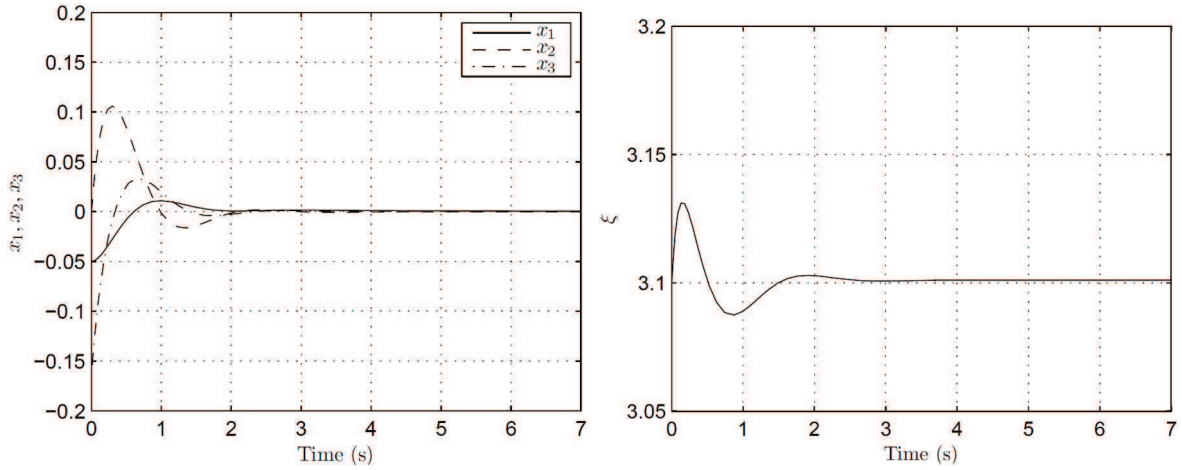

Figure 2.11: States of the augmented system for the MAGLEV, simplified controller.

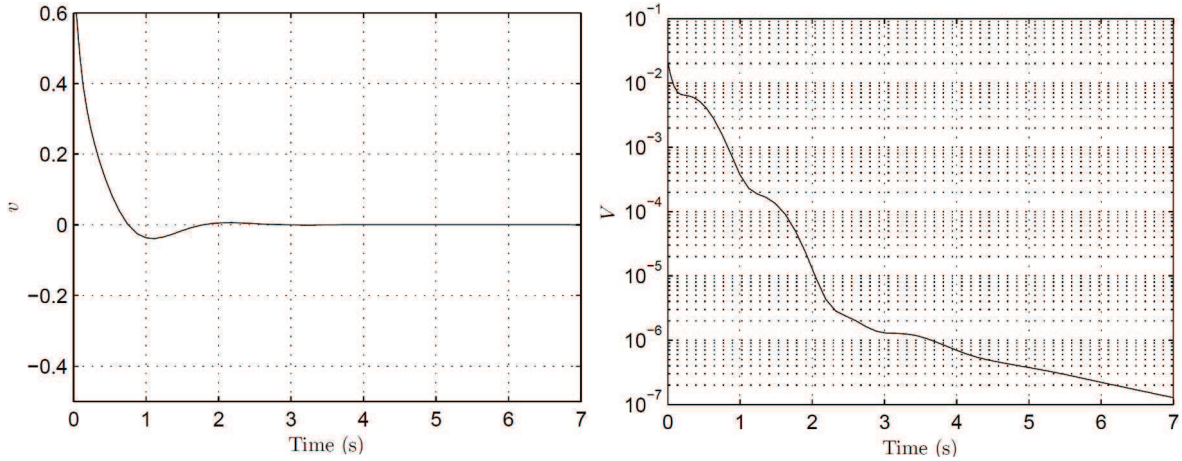

Figure 2.12: Control Signal and Lyapunov function for the MAGLEV, simplified controller.

Gain	SMIB	MAGLEV
π_1	70	3
π_2	0.1	1
π_3	0.1	1
π_4	70	10
c_1	2	1
c_3	2	1
c_2, c_4, c_5	20	1
ϵ	0.0049	0.001

Table 2.4: Simplified controller gains.

Chapter 3

Global Nonlinear Centralized Stabilization

In the current chapter, a solution to the problem of transient stabilization for multi-machine power systems, with transfer conductances different from zero, is given. The $3N$–dimensional (reduced order) model of the N-generator system, with lossy transmission lines, nonlinear loads, is then used to construct a nonlinear dynamic state-feedback control law ensuring, under some conditions on the physical parameters, global asymptotic stability of the operating point. To date, only few results are available for this problem with the restrictive assumption of uniform inertia in all network generators, inference far from realistic. The remaining of the chapter is organized as follows. In Section II the system model and the problem formulation are presented. Section III contains some discussion regarding the main assumptions. Subsequently, the controller and main stability result are given in Section IV. Finally, Section V presents simulation results on the 10-machine New England power system benchmark.

3.1 System model and problem formulation

The dynamics of the power system, consisting of N machines, loads and transmission lines, may be described by the aggregated reduced model equations (see [Chiang et al., 1995b; Ortega et al., 2005])

$$\dot{\delta}_i = \omega_i \tag{3.1}$$

$$\dot{\omega}_i = -D_i\omega_i + P_i - G_iE_i^2 - E_i \sum_{j=1,j\neq i}^{N} E_jY_{ij}\sin(\delta_i-\delta_j+\alpha_{ij}) \tag{3.2}$$

$$\dot{E}_i = -a_iE_i + b_i \sum_{j=1,j\neq i}^{N} E_j\cos(\delta_i-\delta_j+\alpha_{ij}) + E_{f_i}/\tau_i + \nu_i/\tau_i \tag{3.3}$$

with $i \in \bar{N} := \{1, 2, \ldots, N\}$ and where

- $\delta_i(t) \in [0, 2\pi)$, measured in radians, is the rotor angle of the i-th machine;
- $\omega_i(t) \in \mathbb{R}$, measured in radians per seconds, is the angular velocity deviation;
- $E_i(t) \in \mathbb{R}_+$, measured in p.u., is the generator quadrature internal voltage;
- $D_i = D_{mi}/M_i$, with D_{mi} the damping constant (measured in p.u.), $M_i = 2H_i$ and H_i the inertia constant (measured in seconds);

- $P_i = \omega_0 P_{mi}/M_i$, with P_{mi} the constant mechanical input power in p.u. and ω_0 the synchronous speed (measured in radians per second);
- $G_i = \omega_0 G_{mi}/M_i$, with G_{mi} the self-conductance (measured in p.u.);
- τ_i, measured in seconds, is the transient short circuit time constant;
- $\nu_i(t) \in \mathbb{R}$, measured in p.u., is the control voltage input;
- E_{fi}, measured in p.u., is the control constant voltage component applied to the field winding.

The positive constants a_i and b_i are defined as

$$a_i = \frac{1}{\tau_i}(1 - (x_{di} - x'_{di})B_{mi}), \quad b_i = \frac{1}{\tau_i}(x_{di} - x'_{di}), \tag{3.4}$$

where x_{di} is the direct axis reactance in p.u., x'_{di} is the direct axis transient reactance in p.u. and B_{mi} is the self-susceptance of the internal machine bus in p.u.. We assume $x_{di} - x'_{di} > 0$. The parameters Y_{ij} and α_{ij}, with $i \neq j$, are constants depending on the topology and physical properties of the network and of the loads. Consistently with physical constraints, we assume that, for all i, $P_i > 1$. The need for this assumption will become mathematically clear in the sequel, besides that we also assume the generators are always transforming mechanical energy into electrical power.

Assumption 3.1.1. *To formulate, and solve, the transient stability problem we assume that all states are measurable and all parameters are exactly known.*

Assuming that all states are measurable was practically unreasonable a few years back. However, with the increasing utilization of measuring and telemetering devices (in particular, the Phasor Measurement Units [Karlsson et al., 2004]) this is becoming a feasible possibility [Prioste and e Silva, 2007].

The equilibrium to be stabilized is defined as

$$\mathcal{E} := (\bar{\boldsymbol{\delta}}, \mathbf{0}, \bar{\mathbf{E}}) \in S^N \times \mathbb{R}^N \times \mathbb{R}^N_+, \tag{3.5}$$

where $S := [0, 2\pi)$, $\bar{\boldsymbol{\delta}} := \mathrm{col}(\bar{\delta}_i)$ and $\bar{\mathbf{E}} := \mathrm{col}(\bar{E}_i)$ and we make the following assumption.

Assumption 3.1.2. *The equilibrium $\bar{\boldsymbol{\delta}}$ is such that (3.3), with $\omega_i = 0$ and $\delta_i = \bar{\delta}_i$, for all i, has a unique solution in $\mathbf{E} = \mathrm{col}(E_i)$, with $E_i > 0$.*

To derive the proposed controller it is convenient to apply a partial linearizing feedback to the system system (3.1)-(3.3), *i.e.*,

$$\nu_i = \tau_i \left(u_i + a_i E_i - b_i \sum_{\substack{j=1 \\ j \neq i}}^{N} E_j \cos(\delta_i - \delta_j + \alpha_{ij}) \right) - E_{f_i}, \tag{3.6}$$

where $u_i(t) \in \mathbb{R}$, for $i \in \bar{N}$, are the new control inputs. And then, express the resulting system in error coordinates, *i.e.*

$$\mathbf{x}_1 := \mathrm{col}(\delta_i) - \bar{\boldsymbol{\delta}}, \quad \mathbf{x}_2 := \mathrm{col}(\omega_i), \quad \mathbf{x}_3 := \mathrm{col}(E_i) - \bar{\mathbf{E}}, \tag{3.7}$$

This yields the equations

$$\begin{aligned} \dot{\mathbf{x}}_1 &= \mathbf{x}_2 \,, \\ \dot{\mathbf{x}}_2 &= -\mathrm{diag}\{D_i\}\mathbf{x}_2 + \mathbf{P} - \mathrm{diag}\{x_{3,i} + \bar{E}_i\}\mathbf{h}(\mathbf{x}_1, \mathbf{x}_3) \,, \\ \dot{\mathbf{x}}_3 &= \mathbf{u} \,, \end{aligned} \tag{3.8}$$

where

$$\mathbf{P} := \mathrm{col}(P_i) \,, \;\; \mathbf{h}(\mathbf{x}_1, \mathbf{x}_3) := \mathrm{col}(h_i(\mathbf{x}_1, \mathbf{x}_3)) \,, \;\; \mathbf{u} := \mathrm{col}(u_i) \tag{3.9}$$

with

$$h_i(\mathbf{x}_1, \mathbf{x}_3) := G_i(x_{3,i} + \bar{E}_i) + \sum_{j=1, j\neq i}^{N} (x_{3,j} + \bar{E}_j) Y_{ij} \sin(\mu_{ij}(\mathbf{x}_1)), \tag{3.10}$$

where, for $i \neq j$, we define

$$\mu_{ij}(\mathbf{x}_1) := x_{1,i} + \bar{\delta}_i - x_{1,j} - \bar{\delta}_j + \alpha_{ij}, \tag{3.11}$$

and, for $k = 1, 2, 3$,

$$\mathbf{x}_k = [x_{k,1}, x_{k,2}, \ldots, x_{k,N}]^\top . \tag{3.12}$$

We want to design a dynamic control law stabilizing the equilibrium of system (3.8). As explained below, some conditions on the system parameters must be imposed to ensure that the controller is defined for all ξ_i and all $x_{1,i}$. To express these conditions in a compact form we define the $N \times N$ matrices

$$L := \begin{pmatrix} L_{1,1} & \cdots & L_{1,N} \\ \vdots & \ddots & \vdots \\ L_{N,1} & \cdots & L_{N,N} \end{pmatrix} , \tag{3.13}$$

and

$$Q(\mathbf{x}_1, \boldsymbol{\xi}) := \begin{pmatrix} Q_{1,1} & \cdots & Q_{1,N} \\ \vdots & \ddots & \vdots \\ Q_{N,1} & \cdots & Q_{N,N} \end{pmatrix} , \tag{3.14}$$

with

$$L_{i,j} = \begin{cases} P_i/\bar{E}_i + G_i \bar{E}_i & \text{if } i = j \,, \\ Y_{ij} \bar{E}_j \sin(\bar{\delta}_i - \bar{\delta}_j + \alpha_{ij}) & \text{otherwise,} \end{cases} \tag{3.15}$$

and

$$Q_{i,j} = \begin{cases} \xi_i^2/[\sin(x_{1,i}) + P_i] + G_i & \text{if } i = j \,, \\ Y_{ij} s_{ij}(\mathbf{x}_1) & \text{otherwise,} \end{cases} \tag{3.16}$$

where

$$s_{ij}(\mathbf{x}_1) := \sin(\mu_{ij}(\mathbf{x}_1)) \,, \tag{3.17}$$

for $i \neq j$, and $\boldsymbol{\xi} := \mathrm{col}(\xi_i)$ is the state of the dynamic controller. Note that, given that we assume $P_i > 1$ for all i, the matrix $\mathbf{Q}(\mathbf{x}_1, \boldsymbol{\xi})$ is well–defined.

The aforementioned assumption on the system parameters, now, reads as follows.

Assumption 3.1.3. *The parameters P_i, G_i, Y_{ij} and α_{ij} are such that the matrix L is invertible.*

Problem Formulation Consider the system (3.8) verifying Assumptions 3.1.1–3.1.3. Find a dynamic state–feedback control law such that the equilibrium of the closed-loop system, namely of the extended system consisting in the system (3.8) and in the dynamic controller, is asymptotically stable and admits a well–defined domain of attraction. Also, give conditions that ensure global asymptotic stability.

3.2 Discussion

The following remarks regarding the problem formulation and the assumptions are in order. To carry out the discussion, it is convenient to recall the physical interpretation of some of the parameters of the reduced model (3.1)-(3.3). (See [Lu et al., 2001; Kundur, 1994] for additional details.) Namely, for $j \neq i$,

$$Y_{ij} := \sqrt{G_{ij}^2 + B_{ij}^2}\,, \qquad \alpha_{ij} := \arctan(\frac{G_{ij}}{B_{ij}})\,, \tag{3.18}$$

where G_{ij}, B_{ij} are the (normalized) conductance and susceptance of the generator, respectively. If it is assumed that the line is *lossless*, which is often done in power system studies, $G_{ij} = 0$—and, consequently also $\alpha_{ij} = 0$. In this case $Y_{ij} = B_{ij}$, that is usually small compared to G_i, which is the self–conductance of the generator. Assumption 3.1.2 requires that the equilibrium angles $\bar{\delta}_i$ be such that the quadratic equations

$$G_i E_i^2 + E_i \sum_{j=1, j\neq i}^{N} E_j Y_{ij} \sin(\bar{\delta}_i - \bar{\delta}_j + \alpha_{ij}) - P_i = 0, \tag{3.19}$$

have a unique positive solution for $E_i > 0$. Under the assumption of lossless line the second left–hand term is small compared to G_i, particularly so if $\bar{\delta}_i \approx \bar{\delta}_j$. Then, the equations take the form $G_i E_i^2 \approx P_i$ that, clearly, have unique solutions for $E_i > 0$, for $i \in \bar{N}$.

Assumption 3.1.3 holds if the Y_{ij}'s are sufficiently small compared with the G_i's. Given the discussion above, this is the case for lossless line systems. Actually, a simple (conservative) sufficient condition for this assumption to hold stems from direct application of Gershgorin circle's theorem [Varga, 2009]. Factoring from the right the full–rank matrix $\mathrm{diag}\{\bar{E}_i\}$ and recalling that $P_i > 0$, a direct application of the theorem shows that if

$$G_i \geq \sum_{j=1, j\neq i}^{N} Y_{ij} |\sin(\bar{\delta}_i - \bar{\delta}_j + \alpha_{ij})|, \tag{3.20}$$

then the matrix $\mathbf{L}$ has all its eigenvalues on the open right-hand plane, hence is full rank. Note that a sufficient condition for (3.20) to hold is $G_i \geq \sum_{j=1,j\neq i}^{N} Y_{ij}$.

The latter also guarantees that the matrix $\mathbf{Q}(\mathbf{x}_1, \boldsymbol{\xi})$ is invertible for all $\mathbf{x}_1 \in S^N$, $\boldsymbol{\xi} \in \mathbb{R}^N$—a condition that is imposed in the proposition below for global stability. Finally, because of physical constraints, the angle δ_i and the quadrature axis internal voltage E_i are restricted to belong to $[0, 2\pi)$ and $\mathbb{R}_+$, respectively [Kundur, 1994]. Since our interest is to obtain global results, the latter restriction is not considered in the paper. Therefore we assume $\mathbf{x}_3(t) \in \mathbb{R}^N$. Note that, in contrast with most of the controllers proposed in the literature, including the one given in [Casagrande et al., 2011b], the restriction of $\mathbf{x}_1(t) \in S^N$ is enforced.

3.3 Main result

In this section we design a feedback control law and give conditions on the parameters of the machines and the network to ensure stability properties for the closed-loop system. The control law, the dynamics of the augmented state and the Lyapunov function (see equations (3.21), (3.22) and (3.37) below), as well as the proof of the effectiveness of the controller, are based on the results described in [Casagrande et al., 2011b] and [Casagrande et al., 2012]. To prove the stability properties we make use of the following classical result [Isidori, 1995].

Theorem 3.3.1. *Consider the dynamical system $\dot{\mathbf{x}} = \mathbf{f}(\mathbf{x})$, where $\mathbf{x}(t) \in \mathbb{R}^n$, and suppose that $\mathbf{x}_0$ is an equilibrium point, namely that $\mathbf{f}(\mathbf{x}_0) = \mathbf{0}$. If there exists a radially unbounded function $V : \mathbb{R}^n \to \mathbb{R}$ (called* Lyapunov function*) such that*

- *$V(\mathbf{x}) > 0$ for all $\mathbf{x} \neq \mathbf{x}_0$, and $V(\mathbf{x}_0) = 0$,*
- *$\nabla V(\mathbf{x})^\top \mathbf{f}(\mathbf{x}) < 0$ for all $\mathbf{x} \neq \mathbf{x}_0$, and $\nabla V(\mathbf{x}_0)^\top \mathbf{f}(\mathbf{x}_0) = 0$*

then the equilibrium $\mathbf{x}_0$ is locally asymptotically stable in the sense of Lyapunov, namely

- *for all $\rho_1 > 0$ there exist $\rho_2 > 0$ such that if $\|\mathbf{x}(0) - \mathbf{x}_0\| < \rho_2$ then $\|\mathbf{x}(t) - \mathbf{x}_0\| < \rho_1$, for all $t > 0$, and*
- *there exist a neighborhood U of $\mathbf{x}_0$ such that if $\mathbf{x}(0) \in U$ then*

$$\lim_{t\to\infty} \mathbf{x}(t) = \mathbf{x}_0 \,.$$

□

To begin with, we define the function $\mathbf{u} : S^N \times \mathbb{R}^{3N} \to \mathbb{R}^N$ as $\mathbf{u} = \mathrm{col}(u_i)$, where u_i, is implicitly defined by the relations

$$u_i(\mathbf{x}(t), \boldsymbol{\xi}(t)) = \dot{x}^d_{3,i}(t) + \beta_{1,i}\, h_i(\mathbf{x}_1(t), \mathbf{x}_3(t)) x_{2,i}(t) - \beta_{2,i}\,(x_{3,i}(t) - x^d_{3,i}(t)) + \epsilon_i \xi_i(t) \sin(x_{1,i}(t))\,, \tag{3.21}$$

where $\beta_{1,i} > 0$, $\beta_{2,i} > 0$ and $0 < \epsilon_i < 1$, for all i, $\boldsymbol{\xi} = (\xi_1 \ \cdots \ \xi_N)^\top$ is the controller state the dynamics of which are defined by

$$\dot{\xi}_i = \beta_{3,i} \ (h_i(\mathbf{x}_1, \mathbf{x}_3) - \xi_i) - \beta_{4,i} \ (x_{3,i}^d + \bar{E}_i)x_{2,i} + \dot{h}_i(\mathbf{x}_1, \mathbf{x}_3, \mathbf{u}) - \epsilon_i(x_{3,i} + \bar{E}_i)\sin(x_{1,i}), \tag{3.22}$$

$$\dot{h}_i(\mathbf{x}_1, \mathbf{x}_3, \mathbf{u}) = G_i u_i + \sum_{j=1, j\neq i}^{N} [u_j Y_{ij} \sin(\mu_{ij}(x_{1,i})) + (x_{3,j} + \bar{E}_j)Y_{ij}(x_{2,i} - x_{2,j})\cos(\mu_{ij}(x_{1,i}))] \tag{3.23}$$

with $\mu_{ij}(\mathbf{x}_1)$ as in (3.11), $\beta_{3,i} > 0$, $\beta_{4,i} > 0$ and

$$x_{3,i}^d = [\sin(x_{1,i}) + P_i]/\xi_i - \bar{E}_i \, . \tag{3.24}$$

Proposition 3.3.2. *Consider system (3.8) and suppose it verifies Assumptions 3.1.1 to 3.1.3.*

i) The function $\mathbf{u}$ *in (3.21) is well-defined in a neighborhood of*

$$\mathcal{E}_0 := (\mathbf{0}, \mathbf{h}(\mathbf{0}, \mathbf{0})) \in S^N \times \mathbb{R}^{3N} \, . \tag{3.25}$$

ii) There exists ϵ^* *such that if* $\epsilon_i \in (0, \epsilon^*)$ *for all* i *then* $(\mathbf{x}, \boldsymbol{\xi}) = \mathcal{E}_0$ *is the unique equilibrium of the closed-loop system (3.8), (3.21), (3.22), and it is locally asymptotically stable.*

iii) The domain of attraction of $\mathcal{E}_0$ *contains all initial conditions such that, along the corresponding trajectories of the closed–loop system, the matrix* $\mathbf{Q}(\mathbf{x}_1(t), \boldsymbol{\xi}(t))$*, defined in* (3.14)*, is invertible for all* t*.*

iv) If the matrix $\mathbf{Q}(\mathbf{x}_1, \boldsymbol{\xi})$ *is invertible for all* $\mathbf{x}_1 \in S^N$ *and for all* $\boldsymbol{\xi} \in \mathbb{R}^N$*, then* $\mathcal{E}_0$ *is a* globally asymptotically stable *equilibrium.* □

Proof 3.3.1. *i) First, note that the control signal* u_i *appears—through equations (3.22) and (3.23)—on the right hand side of (3.21) and must, therefore, be made explicit. Substituting (3.23) and (3.22) in the expression of* $\dot{x}_3^d$ *that can be computed from (3.24), namely*

$$\dot{x}_{3,i}^d = \frac{x_{2,i}\cos(x_{1,i})}{\xi_i} - \frac{\sin(x_{1,i}) + P_i}{\xi^2}\dot{\xi}_i \, , \tag{3.26}$$

we obtain

$$\dot{x}_{3,i}^d = \frac{g_{1,i}}{\xi_i} + \frac{g_{2,i}}{\xi_i^2}\left(\sum_{j=1}^{N}[H_{ij}u_j + K_{ij}] + \beta_{3,i}(h_i - \xi_i) + \frac{g_{3,i}}{\xi_i} + g_{4,i}\right), \tag{3.27}$$

where

$$\begin{aligned} g_{1,i} &= x_{2,i}\cos(x_{1,i}) \, , \\ g_{2,i} &= -[\sin(x_{1,i}) + P_i] \, , \\ g_{3,i} &= -\beta_{4,i}[\sin(x_{1,i}) + P_i]x_{2,i} \, , \\ g_{4,i} &= -\epsilon_i(x_{3,i} + \bar{E}_i)\sin(x_{1,i}) \, , \end{aligned} \tag{3.28}$$

$H_{ii} = G_i$ *for all* $i \in \bar{N}$, $H_{ij} = Y_{ij}s_{ij}(\boldsymbol{x}_1)$, $j \in \bar{N}$, $i \neq j$, $K_{ii} = 0$, *and*

$$K_{ij} = (x_{3,j} + \bar{E}_j)Y_{ij}(x_{2,i} - x_{2,j})\cos(\mu_{ij}(x_{1,i}))\,, \tag{3.29}$$

with $i \neq j$. *In the sequel the arguments of the functions are omitted for brevity wherever this does not generate confusion.*

Evaluating at $\mathbf{x} = \mathbf{0}$ *the second equation in (3.8) we have* $h_i(\mathbf{0}, \mathbf{0}) > 0$. *Moreover, from* (3.24) *we see that, at the equilibrium* $\boldsymbol{\xi}$ *and* $\mathbf{h}$ *coincide, hence* $\xi_i > 0$, *in some neighborhood of* $\mathcal{E}_0$. *Therefore, (3.21) can be rewritten as*

$$u_i = g_{5,i} + \sum_{j=1}^{N} \frac{g_{2,i}H_{ij}u_j}{\xi_i^2}\,, \tag{3.30}$$

where

$$g_{5,i} = \frac{g_{1,i}}{\xi_i} + \frac{g_{2,i}}{\xi_i^2}\left(\sum_{j=1}^{N} K_{ij} + \beta_{3,i}(h_i - \xi_i) + \frac{g_{3,i}}{\xi_i} + g_{4,i}\right) + \beta_{1,i}h_i x_{2,i} - \beta_{2,i}(x_{3,i} - x_{3,i}^d) + \epsilon_i\xi_i\sin(x_{1,i}) \tag{3.31}$$

is defined in this neighborhood. Let $\mathbf{g}_5 := col(g_{5,i})$, *let* I_N *be the identity matrix of dimension* N, *and let* $\widetilde{L}$ *be the matrix with entries*

$$\widetilde{L}_{ij} = \frac{g_{2,i}H_{ij}}{\xi_i^2}\,. \tag{3.32}$$

We may rewrite equation (3.21) as

$$\mathbf{u} = (I_N - \widetilde{L})^{-1}\mathbf{g}_5. \tag{3.33}$$

Explicit computations yield

$$I_N - \widetilde{L} = diag\left\{\frac{\sin(x_{1,i}) + P_i}{\xi_i^2}\right\}\mathbf{Q}(\mathbf{x}_1, \boldsymbol{\xi}). \tag{3.34}$$

Therefore, since $P_i > 1$ *and* $\xi_i > 0$, $I_N - \widetilde{L}$ *is invertible if and only if* $\mathbf{Q}(\mathbf{x}_1, \boldsymbol{\xi})$ *is invertible. Finally, since*

$$\mathbf{Q}(\mathbf{0}, \mathbf{h}(\mathbf{0}, \mathbf{0})) = L\ diag\{\bar{E}_i\}, \tag{3.35}$$

Assumption 3.1.3 implies that the control law is well-defined in $\mathcal{E}_0$ *and, by continuity, in a neighborhood of* $\mathcal{E}_0$.

ii) Uniqueness of the equilibrium is immediately proven by substitution, as long as the control law $\mathbf{u}$ *is well-defined. The proof of stability relies on the existence of a Lyapunov function [Isidori, 1995]. Consider the function* $V : S^N \times \mathbb{R}^{3N} \to \mathbb{R}$ *defined by*

$$\begin{aligned} V(\mathbf{x}, \boldsymbol{\xi}) = \sum_{i=1}^{N}\left(c_{1,i}\int_0^{x_{1,i}} \sin(\eta)\mathrm{d}\eta + c_{2,i}\epsilon_i x_{2,i}\sin(x_{1,i})\right) + \\ + \frac{1}{2}\left(c_{3,i}\|\mathbf{x}_2\|^2 + c_{4,i}\|\boldsymbol{\xi} - \mathbf{h}\|^2 + c_{5,i}\|\mathbf{x}_3 - \mathbf{x}_3^d\|^2\right) \end{aligned} \tag{3.36}$$

with $\mathbf{x}_3^d := col(x_{3,i}^d)$ *and where* $c_{k,i}$*, for* $k = 1, 2, \ldots, 5$ *are positive constant gains such that, for all* i*,* $c_{1,i} \geq 1$*,* $c_{2,i} \geq 1$ *and* $c_{3,i} \geq 1$*. It is shown below that the control design is simplified if some relations among the gains* $c_{k,i}$*, as well as some relations between the gains* $c_{k,i}$ *and the parameters* β*'s, hold (see equations (3.43)). However, for the moment we prefer to write the Lyapunov function in the form (3.36). Note that* V *can be rewritten as*

$$V(\mathbf{x}, \boldsymbol{\xi}) = \frac{1}{2}c_{4,i}\|\boldsymbol{\xi}-\mathbf{h}\|^2+\frac{1}{2}c_{5,i}\|\mathbf{x}_3-\mathbf{x}_3^d\|^2+\sum_{i=1}^{N}[c_{1,i}(1-\cos(x_{1,i}))+\frac{c_{3,i}x_{2,i}^2}{2}+c_{2,i}\epsilon_i x_{2,i}\sin(x_{1,i})]. \tag{3.37}$$

If the terms in parenthesis are non–negative, V *is positive definite—with respect to the point*

$$(\mathbf{x}_1, \mathbf{x}_2, \mathbf{x}_3, \boldsymbol{\xi}) = (\mathbf{0}, \mathbf{0}, \mathbf{x}_3^d, \mathbf{h}(\mathbf{0}, \mathbf{0}))\,. \tag{3.38}$$

To establish this fact, note that, since $c_{1,i} > 0$*, the Young's inequality [Evans, 2010]*

$$c_{2,i}\epsilon_i x_{2,i}\sin(x_{1,i}) \geq -\frac{c_{2,i}^2\epsilon_i^2 x_{2,i}^2}{2c_{1,i}} - \frac{c_{1,i}\sin^2(x_{1,i})}{2} \tag{3.39}$$

holds. Using the inequality above and choosing $c_{3,i}c_{1,i} > c_{2,i}^2\epsilon_i^2$ *we obtain*

$$c_{1,i}(1-\cos(x_{1,i}))+c_{2,i}\epsilon_i x_{2,i}\sin(x_{1,i})+c_{3,i}x_{2,i}^2/2 \geq 0\,. \tag{3.40}$$

This proves that V *is positive definite. Observe now that* (3.21) *yields*

$$\dot{x}_{3,i} - \dot{x}_{3,i}^d = \beta_{1,i}h_i x_{2,i} - \beta_{2,i}(x_{3,i} - x_{3,i}^d) + \epsilon_i\xi_i\sin(x_{1,i})\,, \tag{3.41}$$

and that from (3.23) *and* (3.22) *one obtains*

$$\begin{aligned}\dot{\xi}_i - \dot{h}_i &= \beta_{3,i}(h_i - \xi_i) - \beta_{4,i}(x_{3,i}^d + \bar{E}_i)x_{2,i} - \epsilon_i(x_{3,i} + \bar{E}_i)\sin(x_{1,i}) \\ &= \beta_{3,i}(h_i - \xi_i) - \beta_{4,i}[\sin(x_{1,i}) + P_i]\frac{x_{2,i}}{\xi_i} - \epsilon_i(x_{3,i} + \bar{E}_i)\sin(x_{1,i}),\end{aligned} \tag{3.42}$$

where we have substituted (3.24) *in the second identity. Therefore, selecting*

$$\begin{aligned}\beta_{1,i} &= \beta_{4,i}\,, \\ c_{1,i} &= c_{3,i}\,, \\ c_{2,i} &= c_{4,i} = c_{5,i}, \\ c_{1,i} &= c_{2,i}\beta_{1,i},\end{aligned} \tag{3.43}$$

the time-derivative of V *along the trajectories of the closed-loop system* (3.8), (3.21), (3.22) *can be written as*

$$\dot{V} = -c_{4,i}\beta_{3,i}\|\boldsymbol{\xi}-\mathbf{h}\|^2-c_{5,i}\beta_{2,i}\|\mathbf{x}_3-\mathbf{x}_3^d\|^2-\sum_{i=1}^{n}[x_{2,i} \quad \sin(x_{1,i})]M_i(x_{1,i})\begin{bmatrix} x_{2,i} \\ \sin(x_{1,i}) \end{bmatrix}, \tag{3.44}$$

where

$$M_i(x_{1,i}) := \begin{pmatrix} c_{3,i}D_i - c_{2,i}\epsilon_i\cos(x_{1,i}) & \frac{c_{2,i}\epsilon_i D_i}{2} \\ \frac{c_{2,i}\epsilon_i D_i}{2} & c_{2,i}\epsilon_i \end{pmatrix}. \tag{3.45}$$

Now, if

$$0 < \epsilon_i < \frac{4c_3 D}{c_2(4+D)} \tag{3.46}$$

then

$$c_{3,i} D_i - c_{2,i}\epsilon_i \cos(x_{1,i}) > 0\,, \tag{3.47}$$

$$c_{2,i}\epsilon_i \left(c_{3,i} D_i - c_{2,i}\epsilon_i \cos(x_{1,i})\right) - \frac{c_{2,1}^2 \epsilon_i^2 D_i^2}{4} > 0\,, \tag{3.48}$$

and hence the matrix $M_i(x_{1,i})$ is positive definite. Moreover, since $\epsilon_i > 0$ then $M_i(x_{1,i}) \geq \rho_i I_2 > 0$ for some $\rho_i > 0$ and, consequently,

$$\dot{V} \leq -\sum_{i=1}^{n} \rho_i [x_{2,i}^2 + \sin^2(x_{1,i})] - c_{4,i}\beta_{3,i}\|\boldsymbol{\xi} - \mathbf{h}\|^2 - c_{5,i}\beta_{2,i}\|\mathbf{x}_3 - \mathbf{x}_3^d\|^2 \leq 0. \tag{3.49}$$

Therefore all trajectories converge to the set (3.38)*. Assumption 3.1.2 allows to conclude that the latter set coincides with $\mathcal{E}_0$, hence the claim.*

iii) The local result given by i) and ii) can be naturally extended to all trajectories along which $\mathbf{Q}(\mathbf{x}_1(t), \boldsymbol{\xi}(t))$ is invertible, thus guaranteeing existence of the control law for all $t \geq 0$ and attractivity of $\mathcal{E}_0$.

iv) From (3.34), if $\mathbf{Q}(\mathbf{x}_1, \boldsymbol{\xi})$ is invertible for all $\mathbf{x}_1 \in S^N$, $\boldsymbol{\xi} \in \mathbb{R}^N$, then the control law $\mathbf{u}$ is globally well-defined. This fact, together with the properties of V, establishes the global asymptotic stability claim.

Remark 3.3.1. *If the equilibrium $\mathcal{E}$ (see Assumption 3.1.2) is not unique, but it is isolated, we can conclude from the analysis above that it is locally asymptotically stable. Moreover, for all initial conditions such that $\mathbf{Q}(\mathbf{x}_1(t), \boldsymbol{\xi}(t))$ is invertible, we have that $\mathbf{x}_1(t) \to \mathbf{0}$ and $\mathbf{x}_2(t) \to \mathbf{0}$.*

Remark 3.3.2. *The controller derived in Proposition 3.3.2 may be compared with the controller reported in [Casagrande et al., 2011b] that, as mentioned in the introduction, is too complex and does not respect the physical structure of the system. Moreover, as shown in the next section, the performance of the above control law for the transient stability problem is significantly better than the performance of the controller proposed in [Casagrande et al., 2011b].*

3.4 Simulation results

In this section we present simulation results using the well-known New England power system, which consists of 10 generators, 39 buses and 19 loads, as depicted in Figure 3.1. The system parameters are taken from [Pai, 1989]. The controller in equation (3.33) has been tested to stabilize the power system under different faults, this is

(i) Intermittent 3φ fault in bus number 16.

(ii) Permanent line switching between bus 17 and 18 followed by a full load trip in bus 18.

(iii) Permanent failure in generator 10.

To show the controller robustness we present two different simulation scenarios, first the power network is represented using the third order model (3.1)-(3.3) and second, the power system is presented by an eighth order model given below. In both scenarios the parameter D_i is 1 for all $i = 1, \ldots, n$, while the other parameters are given in Table 3.1. The initial condition is the equilibrium point also given in Table 3.1.

3.4.1 Third-order model

The power system is simulated using the aggregated (reduced) model given in equations (3.1)-(3.3). The matrices Y and α, which are related to the system admittance matrix, are given by equations (3.50) and (3.52). These matrices are obtained through (3.18) from the parameters G_{ij} and B_{ij} appearing in the reduced network admittance matrix, which has been obtained by eliminating all buses except the internal generator buses. According to the condition in (3.18), namely that $j \neq i$, the elements of the main diagonal of Y and α are set to zero. The values of the controller gains chosen taking into account the constrains pointed out in Section 3.3 and are listed in Table 3.2.

Intermittent 3φ fault in bus 16

This fault is introduced by connecting a small impedance to the ground at $t = 1$ (seconds) and disconnecting it after 0.15 seconds. In Figure 3.2 the time-histories of the states of the ten machines are depicted in error coordinate variables. Note that in this case, the state variable corresponding to the speed deviation, $\mathbf{x}_2$, increases for all the generators in a neighborhood of the time-instant in which the fault is introduced. Also, it can be noted that the convergence of the states to the corresponding equilibrium points, although rapid, is smooth, indicating that the controller injects low gains into the loop — a feature that is desirable in all practical applications. In addition, in Figure 3.3 the time history of the control inputs and of the Lyapunov function are plotted. Note that V is always decreasing except during the fault.

Permanent line switching between bus 17 and 18

This fault consists in a permanent disconnection of the transmission line between bus 17 and 18 followed by a full load trip in bus 18 at $t = 1$ (seconds). After 0.15 seconds the controller is updated and stabilizes the system to the new operation point. In Figures 3.4 and 3.5 the time-histories of the states of the ten machines, of the control inputs and of the Lyapunov function are depicted. It is noticeable that in this case the speed deviation $\boldsymbol{\omega}$ increase immediately right after the fault for exception of the machine #2 which results to be the more affected in this case.

Permanent failure in generator 10

In this case, the generator number 10 is suddenly (and permanently) disconnected from the network at $t = 1$, this causes a significant lack of electrical power injected into the system. Assuming all post-fault parameters and equilibrium points are known, at $t = 1.15$ seconds the controller is updated and stabilizes the system to the new operation point. Note that the power demand remains the same and the swing bus (number 2) provides the power that the generator 10 was contributing to the network. In order to show the change from the pre-fault equilibrium points to the post-fault equilibrium points, figures 3.6 and 3.7 illustrate the states variables in machine coordinates along with the control inputs and the Lyapunov function. In figures 3.6 the trajectories corresponding to machine number 10 diverge after the fault, while the trajectories corresponding to the remaining generators reach another equilibrium point smoothly. Also it is evident that the global asymptotic stability in the sense of Lyapunov is preserved.

i	P_i	E^*_{Fi}	G_i	$\bar{\delta}_i$	$\bar{E}_i$	$\bar{\xi}_i$
1	3.5726	1.1015	1.6574	0.1228	1.0523	3.3946
2	32.5842	1.9326	2.9407	0.3247	1.1705	27.83
3	34.1156	1.8643	3.5230	0.3606	1.1353	30.04
4	41.6173	1.5328	8.4329	0.3453	1.0588	39.3
5	36.8487	3.3334	2.4432	0.5685	1.3695	26.9
6	35.1766	1.9760	4.0012	0.3633	1.2047	29.19
7	39.9489	1.9192	4.4454	0.3718	1.1855	33.69
8	41.6606	1.5015	6.4950	0.3179	1.0914	38.17
9	45.3089	1.7204	8.1348	0.5498	1.1534	38.28
10	10.8425	1.2580	5.4062	0.0057	1.1129	9.74

Table 3.1: Parameters end equilibrium values used for the simulations.

$$Y = \begin{pmatrix} 0 & 1.5973 & 1.7025 & 0.8774 & 0.3035 & 0.7937 & 0.6606 & 1.4484 & 0.8518 & 2.8936 \\ 1.5973 & 0 & 1.7922 & 0.6323 & 0.2187 & 0.5720 & 0.4761 & 0.5379 & 0.4191 & 1.0062 \\ 1.7025 & 1.7922 & 0 & 0.8819 & 0.3049 & 0.7977 & 0.6641 & 0.6746 & 0.5465 & 1.2471 \\ 0.8774 & 0.6323 & 0.8819 & 0 & 1.9513 & 1.5890 & 1.3228 & 0.6871 & 0.7394 & 1.1378 \\ 0.3035 & 0.2187 & 0.3049 & 1.9513 & 0 & 0.5495 & 0.4574 & 0.2376 & 0.2557 & 0.3935 \\ 0.7937 & 0.5720 & 0.7977 & 1.5890 & 0.5495 & 0 & 3.0318 & 0.6215 & 0.6688 & 1.0292 \\ 0.6606 & 0.4761 & 0.6641 & 1.3228 & 0.4574 & 3.0318 & 0 & 0.5174 & 0.5566 & 0.8567 \\ 1.4484 & 0.5379 & 0.6746 & 0.6871 & 0.2376 & 0.6215 & 0.5174 & 0 & 1.2275 & 2.8730 \\ 0.8518 & 0.4191 & 0.5465 & 0.7394 & 0.2557 & 0.6688 & 0.5566 & 1.2275 & 0 & 1.4931 \\ 2.8936 & 1.0062 & 1.2471 & 1.1378 & 0.3935 & 1.0292 & 0.8567 & 2.8730 & 1.4931 & 0 \end{pmatrix} \tag{3.50}$$

(3.51)

$$\alpha = \begin{pmatrix} 0 & 0.4943 & 0.5087 & 0.6871 & 0.7689 & 0.6837 & 0.6855 & 0.3446 & 0.5908 & 0.4161 \\ 0.4943 & 0 & 0.2867 & 0.5610 & 0.6430 & 0.5575 & 0.5592 & 0.4497 & 0.6309 & 0.4893 \\ 0.5087 & 0.2867 & 0 & 0.5076 & 0.5894 & 0.5041 & 0.5059 & 0.4332 & 0.6021 & 0.4685 \\ 0.6871 & 0.5610 & 0.5076 & 0 & 0.2725 & 0.3841 & 0.3859 & 0.5009 & 0.5764 & 0.5013 \\ 0.7689 & 0.6430 & 0.5894 & 0.2725 & 0 & 0.4660 & 0.4677 & 0.5829 & 0.6581 & 0.5829 \\ 0.6837 & 0.5575 & 0.5041 & 0.3841 & 0.4660 & 0 & 0.1932 & 0.4975 & 0.5729 & 0.4979 \\ 0.6855 & 0.5592 & 0.5059 & 0.3859 & 0.4677 & 0.1932 & 0 & 0.4993 & 0.5747 & 0.4996 \\ 0.3446 & 0.4497 & 0.4332 & 0.5009 & 0.5829 & 0.4975 & 0.4993 & 0 & 0.4438 & 0.1184 \\ 0.5908 & 0.6309 & 0.6021 & 0.5764 & 0.6581 & 0.5729 & 0.5747 & 0.4438 & 0 & 0.3481 \\ 0.4161 & 0.4893 & 0.4685 & 0.5013 & 0.5829 & 0.4979 & 0.4996 & 0.1184 & 0.3481 & 0 \end{pmatrix} \tag{3.52}$$

i	$\beta_{1,i}$, $\beta_{4,i}$	$\beta_{2,i}$, $\beta_{3,i}$	$c_{1,i}$, $c_{3,i}$	$c_{2,i}$, $c_{4,i}$, $c_{5,i}$	ϵ_i
1	1.05	8.4	6	5.7143	0.6300
2	0.7	21	6	8.5714	0.2310
3	0.7	21	6	8.5714	0.1955
4	0.7	21	6	8.5714	0.2447
5	0.7	21	6	8.5714	0.2692
6	0.7	21	6	8.5714	0.2011
7	0.7	21	6	8.5714	0.2651
8	0.7	21	6	8.5714	0.2880
9	0.7	21	6	8.5714	0.2029
10	0.84	14	6	7.1429	0.6000

Table 3.2: Controller gains for scenario 1.

3.4.2 Eighth-order model with saturated input

The power system is simulated with the controller gains given in Table 3.3 and using a more complex dynamics than (3.1)-(3.3) to represent the machines, the transformers, the transmission lines and the loads (see [Kundur, 1994] and [Krause et al., 2002]). In

i	$\beta_{1,i}$, $\beta_{4,i}$	$\beta_{2,i}$, $\beta_{3,i}$	$c_{1,i}$, $c_{3,i}$	$c_{2,i}$, $c_{4,i}$,$c_{5,i}$	ϵ_i
1	0.45	15	5	11.11	0.6750
2	0.5	50	5	10	0.0495
3	0.5	50	5	10	0.0419
4	0.5	50	5	10	0.0524
5	0.5	50	5	10	0.0577
6	0.5	50	5	10	0.0431
7	0.5	50	5	10	0.0568
8	0.5	50	5	10	0.0617
9	0.5	50	5	10	0.0435
10	0.1	20	5	50	0.0714

Table 3.3: Controller gains for scenario 2.

particular, let I_d and I_q denote the direct and quadrature stator currents, I_{fd} the field current, I_{kd}, I_{kq1} and I_{kq2} the damper currents, R_s the stator resistance, R_{fd} the field resistance, R_{kd}, R_{kq1} and R_{kq2} the damper resistances, V_d and V_q the stator voltages, V_{fd} the field voltage, V_{kd}, V_{kq1} and V_{kq2} the damper voltages, L_d and L_q the stator inductances, L_{md} and L_{mq} the magnetizing inductances, L_{fd} the field inductance and L_{kd}, L_{kq1} and L_{kq2} the damper inductances. In the eighth-order model, equation (3.3) is replaced by the equation

$$\hat{R}J + \hat{L}\dot{J} = V\,, \tag{3.53}$$

where $J = (I_d\,, I_q\,, I_{fd}\,, I_{kd}\,, I_{kq1}\,, I_{kq2})^\top$, $V = (V_d\,, V_q\,, V_{fd}\,, V_{kd}\,, V_{kq1}\,, V_{kq2})^\top$,

$$\hat{L} = \begin{pmatrix} L_d & 0 & L_{md} & L_{md} & 0 & 0 \\ 0 & L_q & 0 & 0 & L_{mq} & L_{mq} \\ L_{md} & 0 & L_{fd} & L_{md} & 0 & 0 \\ L_{md} & 0 & L_{md} & L_{kd} & 0 & 0 \\ 0 & L_{mq} & 0 & 0 & L_{kq1} & 0 \\ 0 & L_{mq} & 0 & 0 & 0 & L_{kq2} \end{pmatrix}, \tag{3.54}$$

$$\hat{R} = \begin{pmatrix} \hat{R}_1 & \hat{R}_2 \\ \hat{R}_3 & \hat{R}_4 \end{pmatrix}, \tag{3.55}$$

with

$$\hat{R}_1 = \begin{pmatrix} R_s & -\omega_R L_q \\ \omega_R L_d & R_S \end{pmatrix}, \tag{3.56}$$

$$\hat{R}_2 = \begin{pmatrix} 0 & 0 & -\omega_R L_{mq} & -\omega_R L_{mq} \\ \omega_R L_{md} & \omega_R L_{md} & 0 & 0 \end{pmatrix}, \tag{3.57}$$

$$\hat{R}_4 = \mathrm{diag}\{R_{fd}, R_{kd}, R_{kq1}, R_{kq2}\} \tag{3.58}$$

and where $\hat{R}_3$ is a 4×2 matrix of zero entries.

The relation between equations (3.53) and (3.3) is given by the fact that the voltage V_{fd} of the i-th machine corresponds to the input ν_i appearing in (3.3) and by the fact that [Psillakis and Alexandridis, 2007], for $i = 1, \ldots, n$,

$$I_{qi}(t) = \sum_{j=1}^{N} E_j(t)(B_{ij}\sin(\delta_{ij}(t)) + G_{ij}\cos(\delta_{ij}(t)))\,, \tag{3.59}$$

where $\delta_{ij}(t) = \delta_i(t) - \delta_j(t) + \alpha_{ij}$.

To render the simulations more realistic, the control signal is limited to the range $\nu_i \in [-10\ \ 10]$ consistently with physically admissible ranges. We may reasonably expect that the control scheme, when applied to system (3.53) and constrained by a voltage saturation on the control signal, does not exhibit the same performance when applied to the third order model.

Intermittent 3φ fault in bus 16

In Figures 3.8 and 3.9 the time-histories of the states of the ten machines are shown for this scenario. It can be noted that the state trajectories shown in Figure 3.8 exhibit an oscillatory behavior; moreover, the speed of convergence of $\mathbf{x_1}$ and $\mathbf{x_3}$ is slow. On the other hand, $\mathbf{x_2}$ and $\boldsymbol{\nu}$ converge to their equilibrium rapidly. Note that $\mathbf{x_2}$ increase, for all the generators, after the fault. In Figure 3.9 the time-histories of the control inputs and of the Lyapunov function are plotted. In this case, the Lyapunov function is not strictly decreasing along the trajectories; this is due to the fact that the control designed for the third order model is applied to the eighth-order model. However, the Lyapunov function shows an overall decreasing behavior except during the period of the fault.

Permanent line switching between bus 17 and 18

Figures 3.10 and 3.11 show the time histories of the state variables, the saturated control signal and the Lyapunov function of the closed-loop system under permanent line switching between bus 17 and 18 and full load trip at bus 18. Moreover, the speed deviation ω is increasing immediately right after the fault. Again, the Lyapunov function exhibits an overall decreasing behavior and the state trajectories reach another equilibrium point. As presented before in third-order model case, the machine #2 results to be the more affected by this fault.

Permanent failure in generator 10

Figures 3.12 and 3.13 show the time histories of the state variables in machine coordinates, the saturated control input and the Lyapunov function of the closed-loop system under a permanent failure in generator 10. The trajectories corresponding to machine number 10 diverge after the fault, while the trajectories of the remaining generators reach another equilibrium point.

We conclude that despite the fact that the controller designed in this work is based on the simplified model (3.1)-(3.3) of a power system, it can be used to stabilize a more realistic model of the power system. The larger overshoot (notice the different scales), the higher oscillatory behaviour, the slow convergence and the non-strictly decreasing behaviour of the Lyapunov function in Scenario 2 are consequences of the fact that the controller is dealing with unmodeled dynamics.

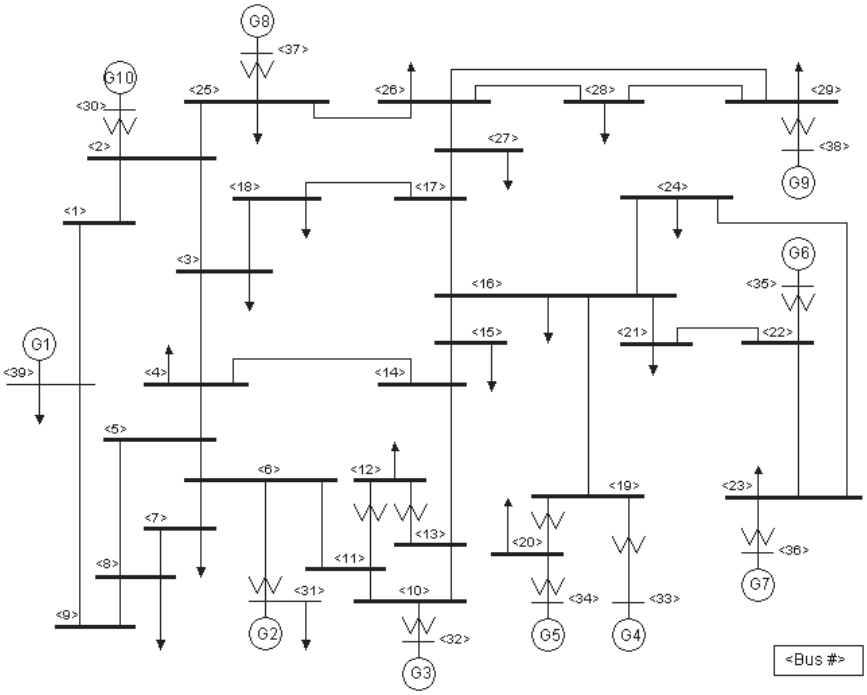

Figure 3.1: New England power system.

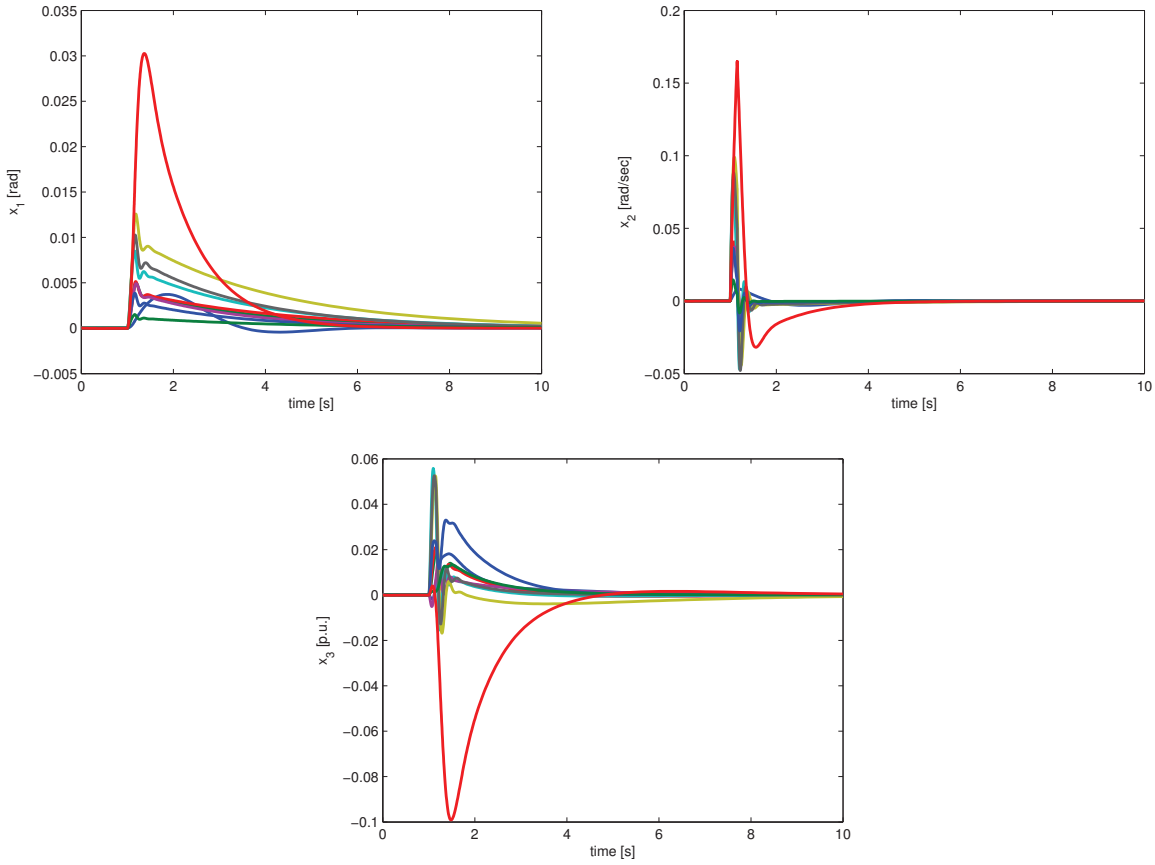

Figure 3.2: Time histories of the angle errors $\mathbf{x}_1$, of the angular speed deviations $\mathbf{x}_2$ and of the voltage errors $\mathbf{x}_3$ in the case of an intermittent 3φ fault in the third order model.

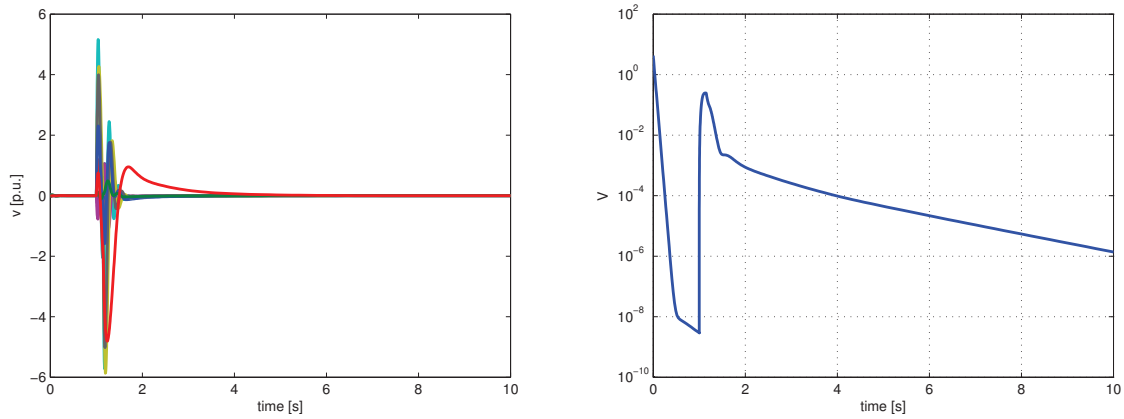

Figure 3.3: Time histories of the control signals $\boldsymbol{\nu}$ and of the Lyapunov function V in the case of an intermittent 3φ fault in the third order model.

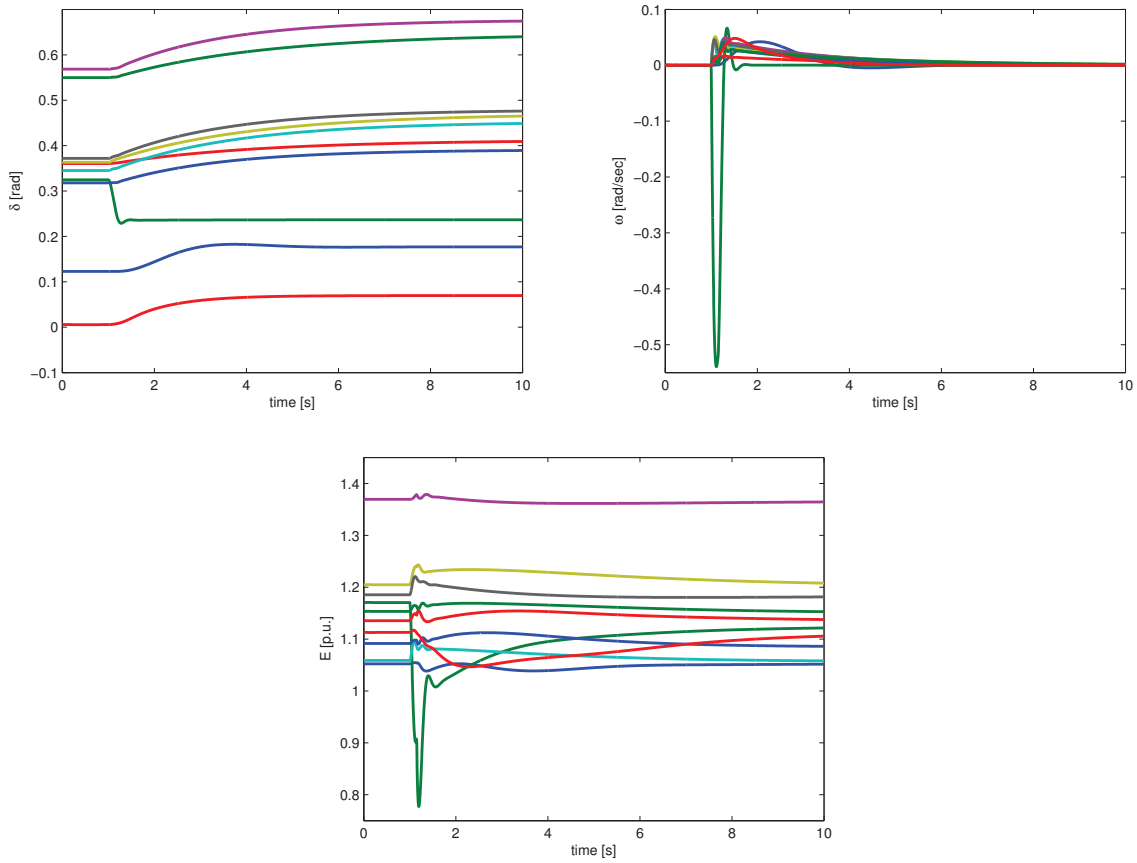

Figure 3.4: Time histories of the angles $\boldsymbol{\delta}$, of the angular speed deviations $\boldsymbol{\omega}$ and of the voltages $\mathbf{E}$ in the case of permanent line switching between buses 17-18 in the third order model.

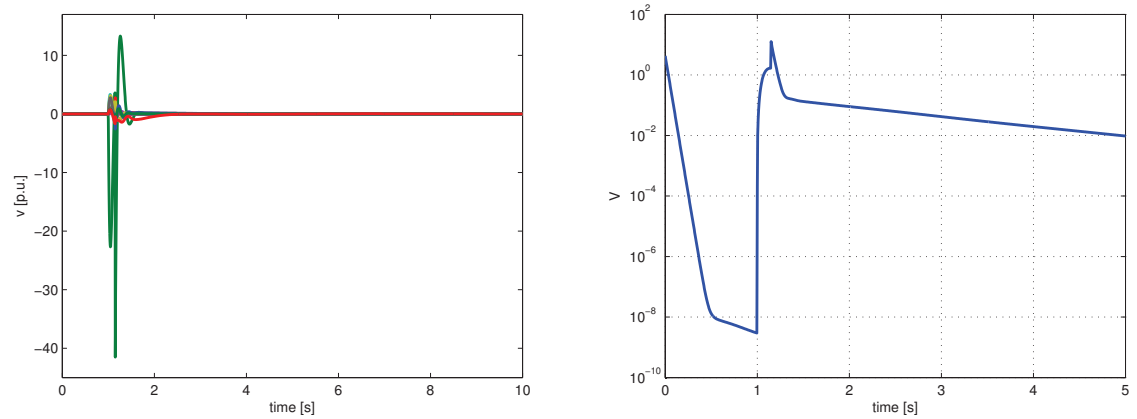

Figure 3.5: Time histories of the control signals $\boldsymbol{\nu}$ and of the Lyapunov function V in the case of permanent line switching between buses 17-18 in the third order model.

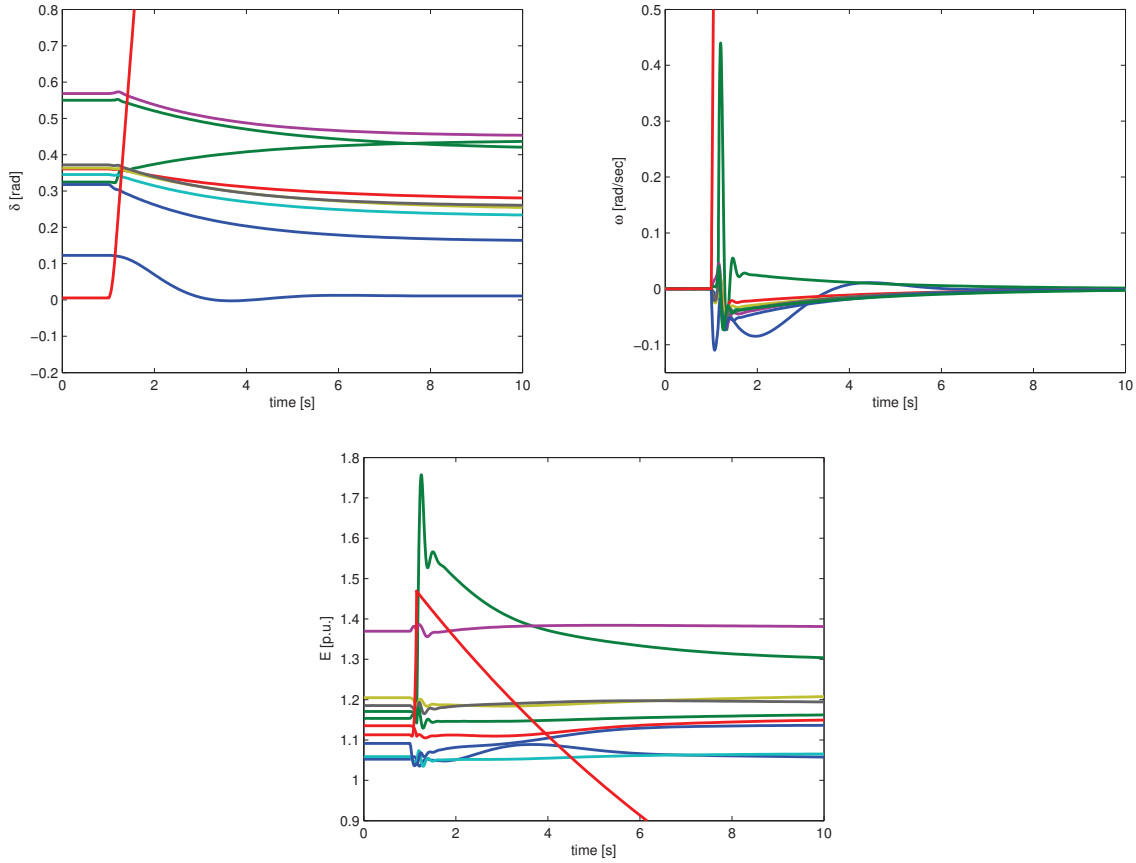

Figure 3.6: Time histories of the angles $\boldsymbol{\delta}$, of the angular speed deviations $\boldsymbol{\omega}$ and of the voltages $\mathbf{E}$ in the case of a permanent failure in one of the generators for the third order model.

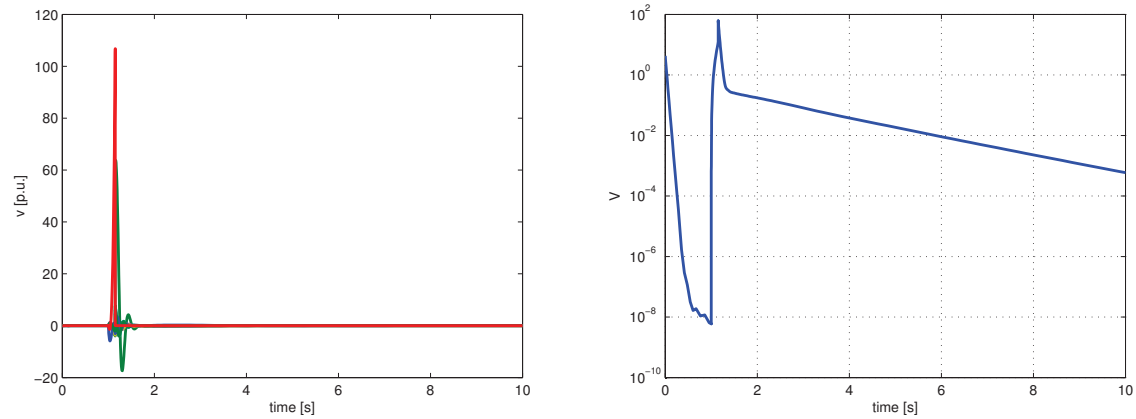

Figure 3.7: Time histories of the control signals $\boldsymbol{\nu}$ and of the Lyapunov function V in the case of a permanent failure in one of the generators for the third order model.

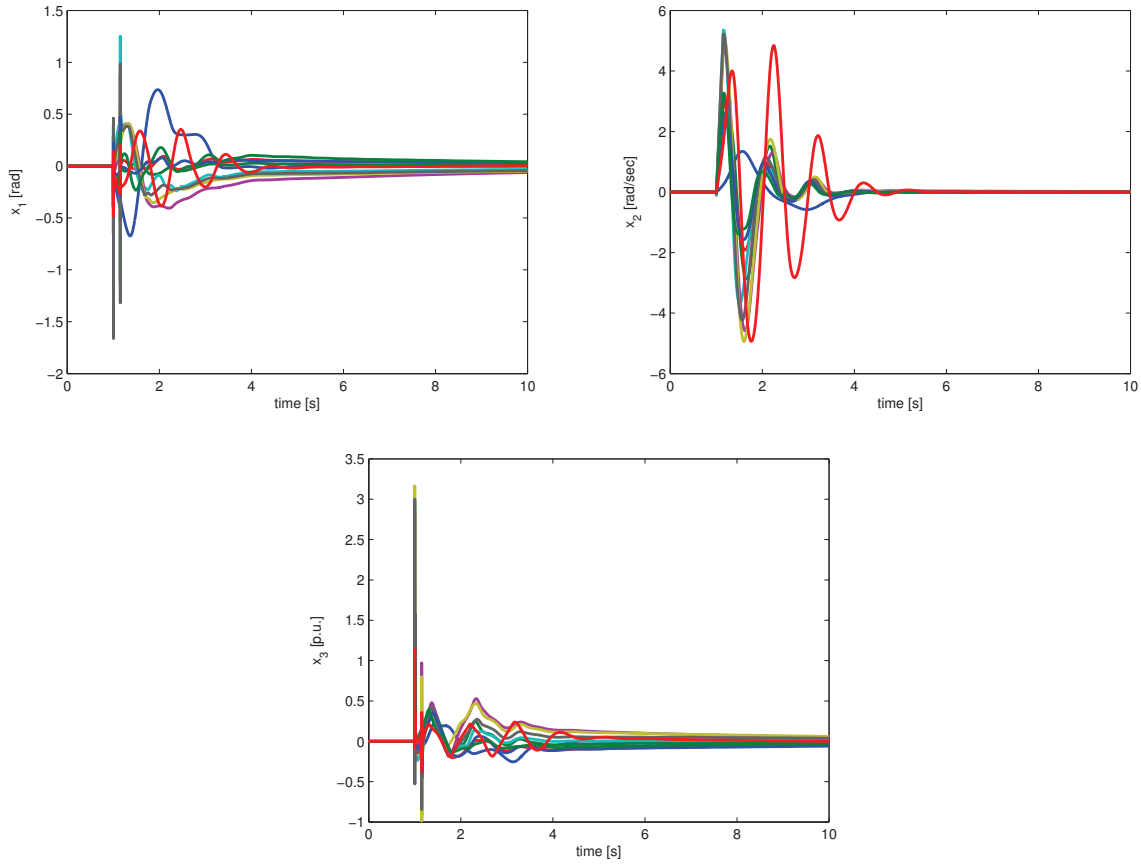

Figure 3.8: Time histories of the angle errors $\mathbf{x}_1$, of the angular speed deviations $\mathbf{x}_2$ and of the voltage errors $\mathbf{x}_3$ in the case of an intermittent 3φ fault for the eighth order model.

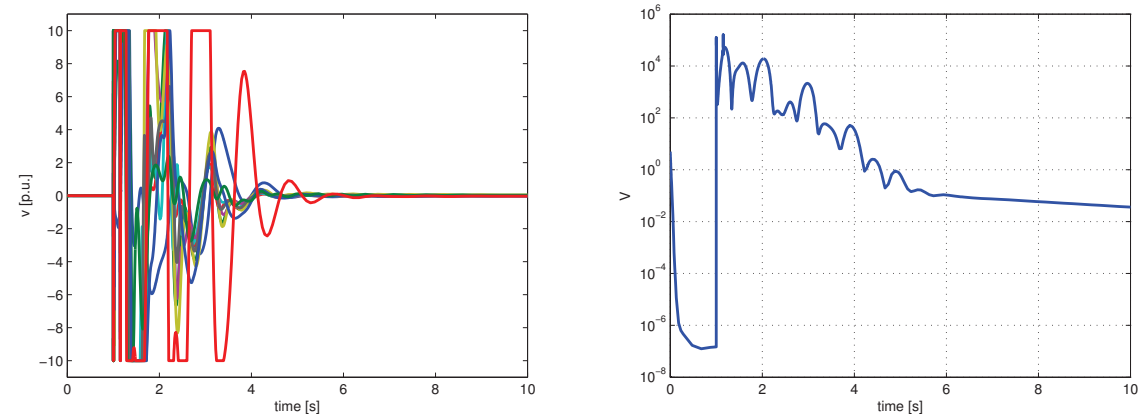

Figure 3.9: Time histories of the control signals $\boldsymbol{\nu}$ and of the Lyapunov function V in the case of an intermittent 3φ fault for the eighth order model.

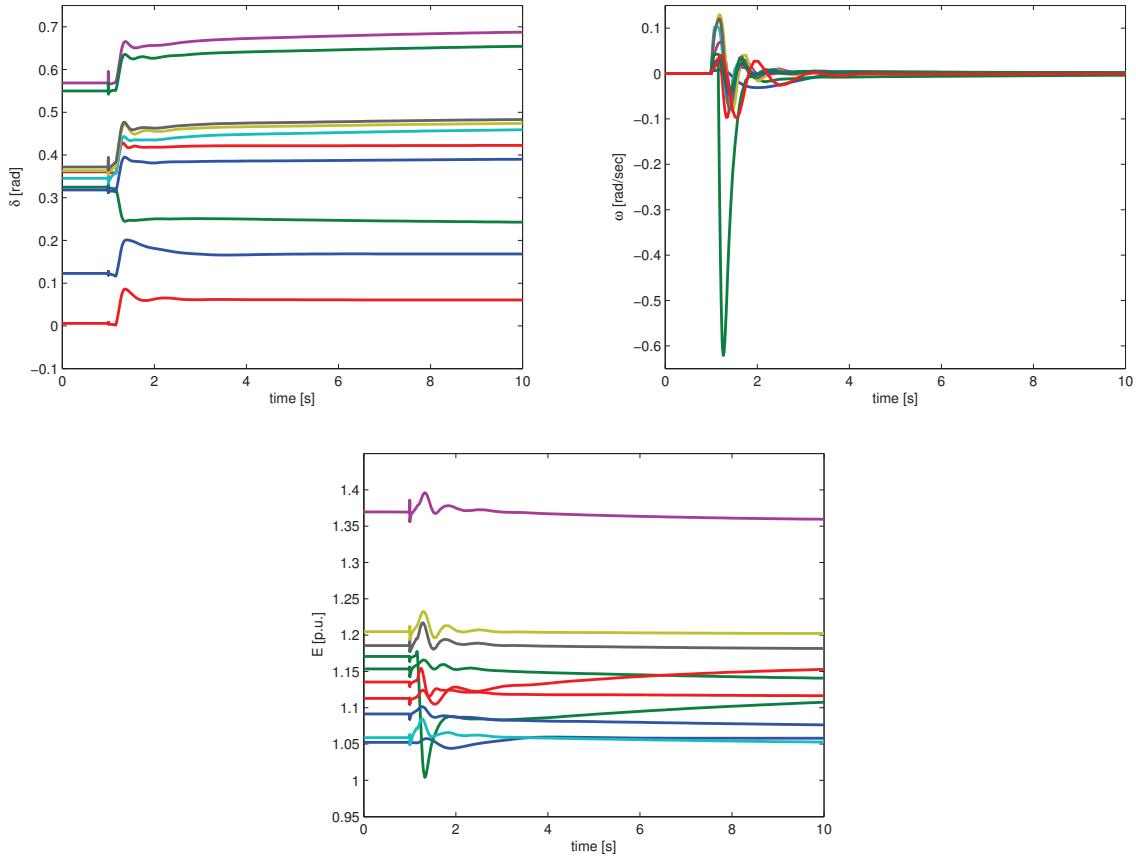

Figure 3.10: Time histories of the angles $\boldsymbol{\delta}$, of the angular speed deviations $\boldsymbol{\omega}$ and of the voltages $\mathbf{E}$ in the case of permanent line switching between buses 17-18 for the eighth order model.

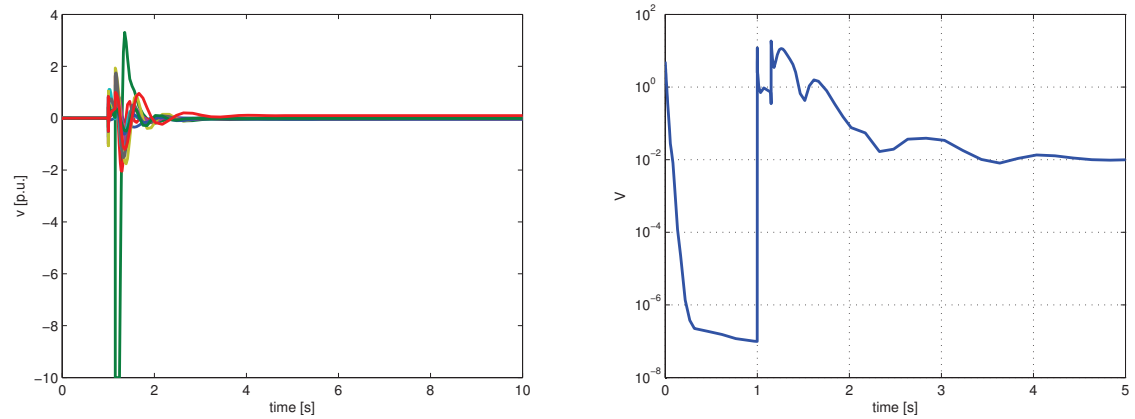

Figure 3.11: Time histories of the control signals $\boldsymbol{\nu}$ and of the Lyapunov function V in the case of permanent line switching between buses 17-18 for the eighth order model.

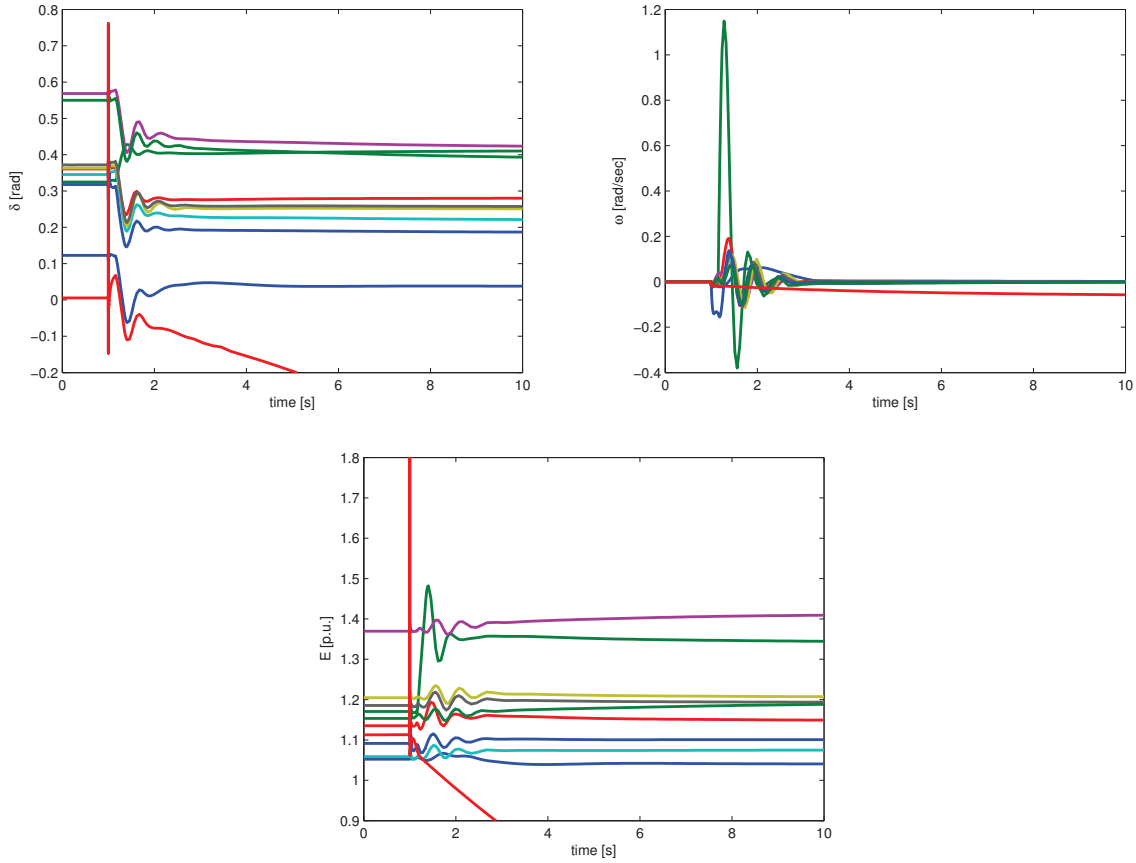

Figure 3.12: Time histories of the angles $\boldsymbol{\delta}$, of the angular speed deviations $\boldsymbol{\omega}$ and of the voltages $\mathbf{E}$ in the case of a permanent failure in one of the generators for the eighth order model.

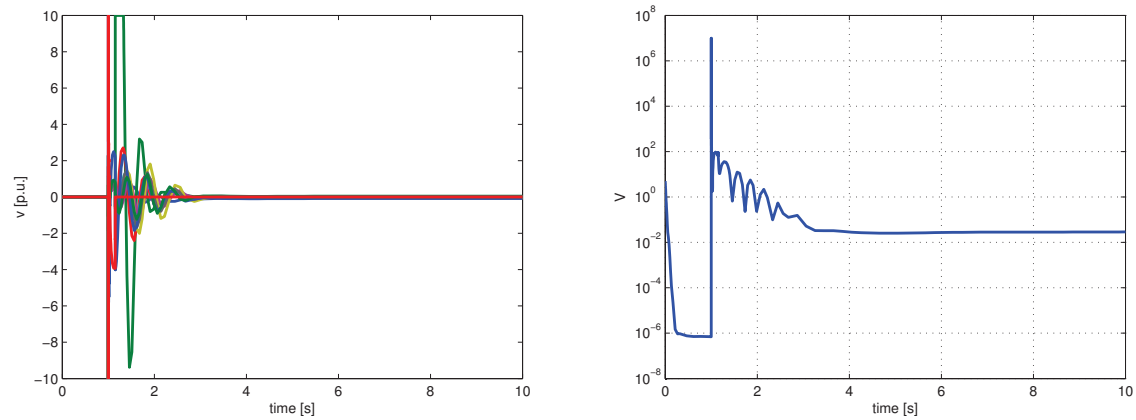

Figure 3.13: Time histories of the control signals $\boldsymbol{\nu}$ and of the Lyapunov function V in the case of a permanent failure in one of the generators for the eighth order model.

Chapter 4

Observer–Based Scheme for Decentralized Stabilization

An observer–based methodology for decentralized stabilization of large–scale linear time–invariant systems is presented in this chapter. The originality of this work relies on the fact that each local controller is provided with available local measurements, it implements a *deterministic* observer to reconstruct the state of the other subsystems and uses—in a *certainty–equivalent way*—these estimates in the control law. The observers are designed following the principles of immersion and invariance (I&I). Furthermore, the class of systems to which the design is applicable is identified via a linear matrix inequality solution, from which the observer gains are obtained. In addition, it is shown that the use of immersion and invariance observers, instead of standard Luenberger's observers, enlarges the class of stabilizable systems.

This chapter is then organized as follows. In Section 4.1 the decentralized stabilization problem is formulated and the main result is given. For ease of presentation, the proof of the main result is given first for a system composed of two subsystems in Section 4.2. Its generalization to $N > 2$ subsystems is discussed later. Finally, in section 4.3, the applicability of the proposed method is illustrated via two examples: a transient stabilization controller for a two–machine power system of 6th order and an academic case study of 12th order, where some simulation results are also given.

4.1 Problem formulation and main result

Consider the LTI large-scale system

$$\Sigma: \quad \dot{\mathbf{x}} = A\mathbf{x} + B\mathbf{u}, \tag{4.1}$$

where $\mathbf{x} = [x_1^\top, x_2^\top, \ldots, x_N^\top]^\top \in \mathbb{R}^{nN}$ is the total state vector, $x_i \in \mathbb{R}^n$ is the state vector corresponding to the i-th subsystem, $\mathbf{u} = [u_1^\top, u_2^\top, \ldots, u_N^\top]^\top \in \mathbb{R}^{mN}$ is the total input vector and $u_i \in \mathbb{R}^m$ is the input vector corresponding to the i-th subsystem. Also, it is defined the total system matrix

$$A = \begin{bmatrix} A_{11} & A_{12} & \ldots & A_{1N} \\ A_{21} & A_{22} & \ldots & A_{2N} \\ \vdots & \vdots & \ddots & \vdots \\ A_{N1} & A_{N2} & \ldots & A_{NN} \end{bmatrix} \in \mathbb{R}^{nN \times nN}$$

with $A_{ij} \in \mathbb{R}^{n\times n}$ and

$$B = \begin{bmatrix} B_1 & 0 & \dots & 0 \\ 0 & B_2 & \dots & 0 \\ \vdots & \vdots & \ddots & \vdots \\ 0 & 0 & \dots & B_N \end{bmatrix} \in \mathbb{R}^{nN\times mN},$$

with $B_i \in \mathbb{R}^{n\times m}$.

Remark To simplify the notation, and without loss of generality, we have assumed that the dimensions of all the subsystems states and inputs are the same. What's more, for future reference we partition the system (4.1) into N interconnected subsystems

$$\Sigma_i : \quad \dot{x}_i = A_{ii}x_i + B_i u_i + \sum_{j=1, j\neq i}^{N} A_{ij}x_j, \tag{4.2}$$

with $i \in \bar{N} := \{1, 2, \dots, N\}$. Unless indicated otherwise the subindex $(\cdot)_i$ ranges in the set $\bar{N}$. When clear from the context, this clarification is omitted. Then finally, it is assumed that each subsystem Σ_i has available for measurement the corresponding state x_i.

Assumption 4.1.1. *The pair (A, B) is controllable and we know a matrix $F \in \mathbb{R}^{mN\times nN}$ such that $A + BF$ is a Hurwitz matrix.*

Problem Formulation: Consider the system (4.2) satisfying Assumption 4.1.1. Design, if possible, an observer–based decentralized certainty–equivalent controller of the form

$$\begin{aligned} \dot{\xi}_{j\Sigma_i} &= W_{ij}(x_i, \xi_{j\Sigma_i}, \dots, \xi_{N\Sigma_i}, u_i) \\ \hat{x}_{j\Sigma_i} &= R_{ij}(x_i, \xi_{j\Sigma_i}, u_i) \\ u_i &= F_{ii}x_i + \sum_{j=1, j\neq i}^{N} F_{ij}\hat{x}_{j\Sigma_i},\ i, j \in \bar{N}, j \neq i, \end{aligned} \tag{4.3}$$

where $W_{ij} : \mathbb{R}^n \times \mathbb{R}^n \times ... \times \mathbb{R}^n \times \mathbb{R}^m \to \mathbb{R}^n$ and $R_{ij} : \mathbb{R}^n \times \mathbb{R}^n \times \mathbb{R}^m \to \mathbb{R}^n$ such that all trajectories are bounded and

$$\lim_{t\to\infty} \mathbf{x}(t) = 0,$$

for all initial conditions $(x_i(0), \xi_{j\Sigma_i}(0)) \in \mathbb{R}^n \times \mathbb{R}^n$.

The signal $\hat{x}_{j\Sigma_i}$ is the estimate of the state x_j generated with measurements of the subsystem Σ_i, whose state is the $(N-1)n$-dimensional vector $(\xi_{1\Sigma_i}^\top, ..., \xi_{N\Sigma_i}^\top)^\top$ excluding $\xi_{i\Sigma_i}^\top$.

Remark The proposed scheme is decentralized in the sense that there is no (on–line) information exchange between subsystems. Notice, however, that the matrix F is assumed to be known and is designed from knowledge of the matrices A and B.

The proposition below contains the main result of this chapter. Namely, the characterization, via an LMI, of a class of systems for which the aforementioned problem has a solution.

Proposition 4.1.1. *Define the matrices*

$$\begin{aligned} \Lambda &\in \mathbb{R}^{nN(N-1)\times nN(N-1)} \\ \Omega &\in \mathbb{R}^{nN(N-1)\times nN(N-1)} \end{aligned} \tag{4.4}$$

which are determined by elements of A, B and F. For instance, in the case of two interconnected subsystems ($N = 2$), they are defined as

$$\begin{aligned} \Lambda &= \begin{bmatrix} \bar{A}_{22} & -B_2F_{21} \\ -B_1F_{12} & \bar{A}_{11} \end{bmatrix} \\ \Omega &= \begin{bmatrix} A_{12} & 0 \\ 0 & A_{21} \end{bmatrix} \end{aligned} \tag{4.5}$$

where $\bar{A}_{ii} := A_{ii} + B_iF_{ii}$.

The decentralized stabilization problem stated above has a solution if there exists block diagonal matrices $P \in \mathbb{R}^{nN(N-1)\times nN(N-1)}$ and $U \in \mathbb{R}^{nN(N-1)\times nN(N-1)}$ solutions of the LMI

$$\begin{aligned} P &> 0 \\ P\Lambda + \Lambda^\top P - U\Omega - \Omega^\top U^\top &< 0. \end{aligned} \tag{4.6}$$

Furthermore, the mappings W_{ij}, R_{ij} are linear, that is the observer takes the form

$$\begin{aligned} \dot{\xi}_{j\Sigma_i} &= T^x_{ij}x_i + \sum_{k=1,k\neq i}^{N} T^\xi_{jk}\xi_{k\Sigma_i} + T^u_{ij}u_i \\ \hat{x}_{j\Sigma_i} &= H^x_{ij}x_i + H^\xi_{ij}\xi_{j\Sigma_i} + H^u_{ij}u_i,\ i,j \in \bar{N}, j \neq i, \end{aligned}$$

where $T^x_{ij}, T^\xi_{jk} \in \mathbb{R}^{n\times n}$, $T^u_{ij} \in \mathbb{R}^{n\times m}$, $H^x_{ij}, H^\xi_{ij} \in \mathbb{R}^{n\times n}$ and $H^u_{ij} \in \mathbb{R}^{n\times m}$.

4.2 Proof of the main result

For simplicity, we present first the proof for the case of two subsystems. The proof for the general case is given below in Subsection 4.2.2.

4.2.1 Two-subsystem case

Consider two-interconnected subsystems of the form

$$\begin{aligned} \Sigma_1 :&\ \dot{x}_1 = A_{11}x_1 + B_1u_1 + A_{12}x_2 \\ \Sigma_2 :&\ \dot{x}_2 = A_{22}x_2 + B_2u_2 + A_{21}x_1. \end{aligned} \tag{4.7}$$

Then, following (4.3), the certainty–equivalent decentralized control law is

$$\begin{aligned} u_1 &= F_{11}x_1 + F_{12}\hat{x}_{2\Sigma_1}, \\ u_2 &= F_{21}\hat{x}_{1\Sigma_2} + F_{22}x_2, \end{aligned} \tag{4.8}$$

where the state feedback gain matrix of Assumption 4.1.1 is partitioned as

$$F = \begin{bmatrix} F_{11} & F_{12} \\ F_{21} & F_{22} \end{bmatrix},$$

$\hat{x}_{2\Sigma_1}$ and $\hat{x}_{1\Sigma_2}$ represent the estimation of x_2 generated by Σ_1 and the estimation of x_1 generated by Σ_2, respectively.

Consequently, connecting (4.7) and (4.8), the closed–loop system takes the form

$$\begin{aligned} \dot{x}_1 &= \bar{A}_{11}x_1 + A_{12}x_2 + B_1F_{12}\hat{x}_{2\Sigma_1} \\ \dot{x}_2 &= \bar{A}_{22}x_2 + A_{21}x_1 + B_2F_{21}\hat{x}_{1\Sigma_2}, \end{aligned} \tag{4.9}$$

where we have defined $\bar{A}_{ii} := A_{ii} + B_iF_{ii}$.

The main thrust of the proof is the construction of a decentralized I&I observer for each subsystem Σ_i that, we recall, disposes of its corresponding state x_i. Towards this end, we follow the methodology of the I&I technique explicitly detailed in [Astolfi et al., 2008] and define the observed states as the sum of an integral and a proportional term.

More concisely, the estimate of x_2 generated by subsystem Σ_1 is defined as

$$\hat{x}_{2\Sigma_1} = \xi_{2\Sigma_1} + K_{2\Sigma_1}x_1,$$

where $\xi_{2\Sigma_1}$ is the integral part and $K_{2\Sigma_1} \in \mathbb{R}^{n\times n}$ is a matrix to be defined. Consequently, the estimation error is defined as

$$\tilde{x}_2 := \hat{x}_{2\Sigma_1} - x_2,$$

then computing its time derivative yields to the expression

$$\begin{aligned} \dot{\tilde{x}}_2 &= \dot{\xi}_{2\Sigma_1} + K_{2\Sigma_1}(A_{11}x_1 + B_1u_1 + A_{12}x_2) \\ &- (\bar{A}_{22}x_2 + A_{21}x_1 + B_2F_{21}\hat{x}_{1\Sigma_2}). \end{aligned}$$

Replacing the unmeasurable signal x_2 above by

$$x_2 = \xi_{2\Sigma_1} + K_{2\Sigma_1}x_1 - \tilde{x}_2,$$

and splitting into measurable and unmeasurable signals suggests the selection

$$\begin{aligned} \dot{\xi}_{2\Sigma_1} = &-(K_{2\Sigma_1}A_{12} - \bar{A}_{22})(\xi_{2\Sigma_1} + K_{2\Sigma_1}x_1) + \\ &+ (B_2F_{21} - K_{2\Sigma_1}A_{11} + A_{21})x_1 - K_{2\Sigma_1}B_1u_1. \end{aligned} \tag{4.10}$$

This yields the first observer error equation dynamics

$$\dot{\tilde{x}}_2 = (\bar{A}_{22} - K_{2\Sigma_1}A_{12})\tilde{x}_2 - B_2F_{21}\tilde{x}_1,$$

where we defined the observation error of the second subsystem as

$$\tilde{x}_1 := \hat{x}_{1\Sigma_2} - x_1.$$

Proceeding analogously with the derivative of $\tilde{x}_1$ and defining

$$\begin{aligned}\dot{\xi}_{1\Sigma_2} = &-(K_{1\Sigma_2}A_{21} - \bar{A}_{11})(\xi_{1\Sigma_2} + K_{1\Sigma_2}x_2)+ \\ &+ (B_1F_{12} - K_{1\Sigma_2}A_{22} + A_{12})x_2 - K_{1\Sigma_2}B_2u_2,\end{aligned} \tag{4.11}$$

we obtain the second observer error equation dynamics

$$\dot{\tilde{x}}_1 = (\bar{A}_{11} - K_{1\Sigma_2}A_{21})\tilde{x}_1 - B_1F_{12}\tilde{x}_2.$$

The two error equations can be compactly written as

$$\dot{\tilde{\mathbf{x}}} = \mathcal{A}\begin{bmatrix} \tilde{x}_2 \\ \tilde{x}_1 \end{bmatrix} \tag{4.12}$$

where

$$\mathcal{A} := \begin{bmatrix} \bar{A}_{22} - K_{2\Sigma_1}A_{12} & -B_2F_{21} \\ -B_1F_{12} & \bar{A}_{11} - K_{1\Sigma_2}A_{21} \end{bmatrix}.$$

Now, the closed–loop system (4.9) can be expressed in terms of the observation errors as

$$\dot{\mathbf{x}} = (A + BF)\mathbf{x} + \begin{bmatrix} B_1F_{12} & 0 \\ 0 & B_2F_{21} \end{bmatrix}\tilde{\mathbf{x}}. \tag{4.13}$$

Given *Assumption* 4.1.1 and the cascaded structure of (4.12) and (4.13) it is clear that the control objective is attained if the matrices $K_{2\Sigma_1}$, $K_{1\Sigma_2}$ are selected such that the matrix $\mathcal{A}$ is Hurwitz.

The matrix $\mathcal{A}$ can be written as

$$\mathcal{A} = \Lambda - K\Omega, \tag{4.14}$$

where the matrices

$$\begin{aligned}\Lambda &= \begin{bmatrix} \bar{A}_{22} & -B_2F_{21} \\ -B_1F_{12} & \bar{A}_{11} \end{bmatrix} \\ \Omega &= \begin{bmatrix} A_{12} & 0 \\ 0 & A_{21} \end{bmatrix}\end{aligned} \tag{4.15}$$

are given, and the unknown gain matrix is

$$K = \begin{bmatrix} K_{2\Sigma_1} & 0 \\ 0 & K_{1\Sigma_2} \end{bmatrix}.$$

To establish the proof we invoke a standard LMI argument given in [Boyd et al., 1994] that is detailed here for the sake of completeness. The matrix $\mathcal{A}$ is Hurwitz if and only if there exists a block diagonal symmetric matrix P such that

$$\begin{aligned}P &> 0 \\ P(\Lambda - K\Omega) + (\Lambda - K\Omega)^\top P &< 0.\end{aligned} \tag{4.16}$$

Defining the block diagonal matrix $U := PK$ the bilinear inequalities (4.16) becomes the standard LMI

$$\begin{aligned} P &> 0 \\ P\Lambda + \Lambda^\top P - U\Omega - \Omega^\top U^\top &< 0. \end{aligned} \tag{4.17}$$

that should be solved for P and U. The gain matrix K can be recovered using $K = P^{-1}U$.

The proof is completed identifying from the observer equations above the matrices of the proposition as

$$\begin{aligned} T_{12}^x &= B_2F_{21} - K_{2\Sigma_1}A_{11} + A_{21} - K_{2\Sigma_1}A_{12}K_{2\Sigma_1} + \\ &\quad + \bar{A}_{22}K_{2\Sigma_1} \\ T_{12}^\xi &= -(K_{2\Sigma_1}A_{12} - \bar{A}_{22}) \\ T_{12}^u &= -K_{2\Sigma_1}B_1 \\ H_{12}^x &= K_{2\Sigma_1} \\ H_{12}^\xi &= I_{n\times n} \\ H_{12}^u &= 0_{n\times n} \end{aligned}$$

and

$$\begin{aligned} T_{21}^x &= B_1F_{12} - K_{1\Sigma_2}A_{22} + A_{12} - K_{1\Sigma_2}A_{21}K_{1\Sigma_2} + \\ &\quad + \bar{A}_{11}K_{1\Sigma_2} \\ T_{21}^\xi &= -(K_{1\Sigma_2}A_{21} - \bar{A}_{11}) \\ T_{21}^u &= -K_{1\Sigma_2}B_2 \\ H_{21}^x &= K_{1\Sigma_2} \\ H_{21}^\xi &= I_{n\times n} \\ H_{21}^u &= 0_{n\times n}. \end{aligned}$$

In order to illustrate the ideas given by the proposed method above, the decentralized scheme diagram for two interconnected subsystems is presented in Fig. 4.1.

Remark Some simple calculations show that the standard reduced order Luenberger's observer in [Kailath, 1980]

$$\begin{aligned} \dot{\hat{x}}_{2\Sigma_1} &= A_{21}x_1 + \bar{A}_{22}\hat{x}_{2\Sigma_1} + B_2F_{21}x_1 \\ \dot{\hat{x}}_{1\Sigma_2} &= A_{12}x_2 + \bar{A}_{11}\hat{x}_{1\Sigma_2} + B_1F_{12}x_2, \end{aligned}$$

yields the error dynamics

$$\dot{\tilde{\mathbf{x}}} = \begin{bmatrix} \bar{A}_{22} & -B_2F_{21} \\ -B_1F_{12} & \bar{A}_{11} \end{bmatrix} \tilde{\mathbf{x}},$$

that coincides with (4.12) when $K_{2\Sigma_1} = K_{1\Sigma_2} = 0$. Hence, the set of stabilizable systems using this observer is strictly smaller than the one corresponding to the I&I observer. Similar derivations in [Cumming, 1969; Gopinath, 1971; Kailath, 1980] have been made to overcome the lack of the correction term in the Luenberger's reduced order observer

above. In addition, it can be shown that the error dynamics of a full order Luenberger's observer is of the form

$$\dot{\tilde{\boldsymbol{\chi}}} = \begin{bmatrix} \mathbf{L}_1 & A_{12} & 0 & 0 \\ 0 & \bar{A}_{22} & -B_2F_{21} & 0 \\ 0 & -B_1F_{12} & \bar{A}_{11} & 0 \\ 0 & 0 & A_{21} & \mathbf{L}_2 \end{bmatrix} \tilde{\boldsymbol{\chi}},$$

where $\tilde{\boldsymbol{\chi}} \in \mathbb{R}^{4n}$ is the observation error and $\mathbf{L}_i \in \mathbb{R}^{n\times n}$ are free matrices. From the structure of the matrix above it is obvious that a necessary condition for stability is that the matrix of the reduced order observer is Hurwitz. Hence, the use of a full order observer does not enlarge the class of stabilizable systems. □□□

Remark In the derivations above the full–state feedback stabilizing matrix F was supposed *fixed* to obtain an LMI in the observer gains $K_{j\Sigma_i}$. Posing the problem of finding both F and $K_{j\Sigma_i}$, for the given data A and B, results in a *nonlinear* matrix inequality. Indeed, using the standard reparametrization of the Lyapunov equation

$$Q > 0, \quad Q(A+BF) + (A+BF)^\top Q < 0$$

given in [Boyd et al., 1994]

$$S := Q^{-1}, \quad T := FQ^{-1},$$

shows that stability of $A+BF$ is equivalent to solvability of the LMI

$$\begin{aligned} S &> 0 \\ AS + BT + SA^\top + T^\top B^\top &< 0. \end{aligned}$$

On the other hand, the LMI (4.17) takes the form

$$\begin{aligned} P &> 0 \\ P(\Lambda_0 + \Lambda_1 TS) + (\Lambda_0 + \Lambda_1 TS)^\top P - U\Omega - \Omega^\top U^\top &< 0, \end{aligned}$$

where

$$\Lambda = \Lambda_0 + \Lambda_1 TS,$$

with Λ and Ω given in (4.15). Observe that we have split Λ into two to underscore that, since it depends *linearly* on the unknown F, it depends on TS. Notice also that Λ_0 and Λ_1 depend only on A and B. Taking together the two sets of inequalities yields a nonlinear equation in the unknowns S, T, P, U. Although numerical techniques are available to solve nonlinear matrix inequalities, for ease of presentation, we have preferred to avoid this complexity.

4.2.2 N-subsystem case

We now present the proof for the case of N subsystems. Consider (4.2) connected in closed-loop with u_i given in (4.3). The overall state feedback gain matrix is assembled as

$$F = \begin{bmatrix} F_{11} & F_{12} & \dots & F_{1N} \\ F_{21} & F_{22} & \dots & F_{2N} \\ \vdots & \vdots & \ddots & \vdots \\ F_{N1} & F_{N2} & \dots & F_{NN} \end{bmatrix},$$

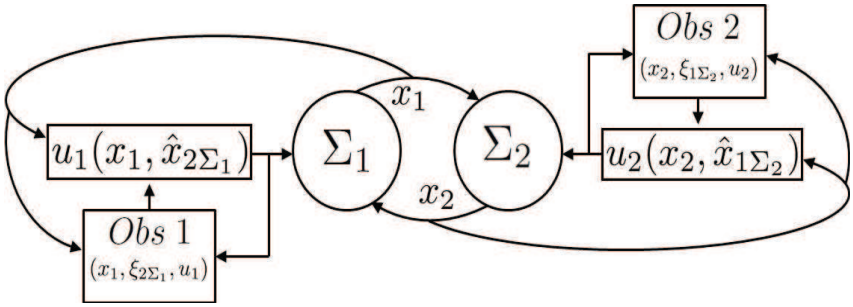

Figure 4.1: Decentralized stabilization scheme.

consequently, the closed-loop system takes the form

$$\Sigma_i : \quad \dot{x}_i = \bar{A}_{ii}x_i + \sum_{j=1, j\neq i}^{N} (A_{ij}x_j + B_i F_{ij}\hat{x}_{j\Sigma_i}).$$

The state estimation of the j-th subsystem provided to the i-th subsystem controller is

$$\hat{x}_{j\Sigma_i} = \xi_{j\Sigma_i} + K_{j\Sigma_i}x_i, \quad i, j \in \bar{N},\ j \neq i, \tag{4.18}$$

where $\xi_{j\Sigma_i}$ is the integral part and $K_{j\Sigma_i}x_i$ is the proportional part, $K_{j\Sigma_i} \in \mathbb{R}^{n\times n}$. We define the estimation error with the general form

$$\tilde{x}_{j\Sigma_i} = \hat{x}_{j\Sigma_i} - x_j, \tag{4.19}$$

where its time derivative results in

$$\begin{aligned}\dot{\tilde{x}}_{j\Sigma_i} = \dot{\xi}_{j\Sigma_i} + K_{j\Sigma_i}&\left(A_{ii}x_i + B_i u_i + \sum_{k=1, k\neq i}^{N} A_{ik}x_k\right) - \\ &- \left(\bar{A}_{jj}x_j + \sum_{k=1, k\neq j}^{N} (A_{jk}x_k + B_j F_{jk}\hat{x}_{k\Sigma_j})\right),\end{aligned}$$

and the unmeasurable signal x_j above is replacing by

$$x_j = \xi_{j\Sigma_i} + K_{j\Sigma_i}x_i - \tilde{x}_{j\Sigma_i}.$$

Separating into measurable and unmeasurable signals suggests the selection

$$\begin{aligned}\dot{\xi}_{j\Sigma_i} = &-(K_{j\Sigma_i}A_{ii} - A_{ji} - B_j F_{ji})x_i - \\ &- \sum_{k=1, k\neq i}^{N} (K_{j\Sigma_i}A_{ik} - A_{jk} - B_j F_{jk})\hat{x}_{k\Sigma_i} - \\ &- K_{j\Sigma_i}B_i u_i, \quad i, j, k \in \bar{N},\ j \neq i,\end{aligned} \tag{4.20}$$

which render the corresponding observer error dynamics

$$\begin{aligned}\dot{\tilde{x}}_{j\Sigma_i} = &- \sum_{k=1, k\neq i}^{N} (K_{j\Sigma_i}A_{ik} - A_{jk} - B_j F_{jk})\tilde{x}_{k\Sigma_i} - \\ &- \sum_{k=1, k\neq j}^{N} B_j F_{jk}\tilde{x}_{k\Sigma_j}, \quad i, j, k \in \bar{N},\ j \neq i.\end{aligned} \tag{4.21}$$

Notice the auxiliary subscript k follows $k \neq i$ and $k \neq j$ in the first and the second sum of (4.21), respectively. From the closed-loop system (4.2)–(4.3) and the estimation errors (4.19), we obtain

$$\dot{\mathbf{x}} = (A + BF)\mathbf{x} + \mathcal{I}\tilde{\mathbf{x}},$$

where $\tilde{\mathbf{x}} = [\tilde{\mathbf{x}}_{\Sigma_1}^\top, \tilde{\mathbf{x}}_{\Sigma_2}^\top, \ldots, \tilde{\mathbf{x}}_{\Sigma_n}^\top]^\top \in \mathbb{R}^{nN(N-1)}$, is the overall observation error vector formed by

$$\tilde{\mathbf{x}}_{\Sigma_1} = \begin{bmatrix} \tilde{x}_{2\Sigma_1} \\ \tilde{x}_{3\Sigma_1} \\ \vdots \\ \tilde{x}_{N\Sigma_1} \end{bmatrix}, \tilde{\mathbf{x}}_{\Sigma_2} = \begin{bmatrix} \tilde{x}_{1\Sigma_2} \\ \tilde{x}_{3\Sigma_2} \\ \vdots \\ \tilde{x}_{N\Sigma_2} \end{bmatrix}, \ \ldots, \ \tilde{\mathbf{x}}_{\Sigma_n} = \begin{bmatrix} \tilde{x}_{1\Sigma_N} \\ \tilde{x}_{2\Sigma_N} \\ \vdots \\ \tilde{x}_{N-1\Sigma_N} \end{bmatrix} \in \mathbb{R}^{n(N-1)}.$$

The interconnection matrix between the closed–loop system and the observer error dynamics is defined as

$$\mathcal{I} = \begin{bmatrix} \mathcal{I}_{11} & 0 & \ldots & 0 \\ 0 & \mathcal{I}_{22} & \ldots & 0 \\ \vdots & \vdots & \ddots & \vdots \\ 0 & 0 & \ldots & \mathcal{I}_{NN} \end{bmatrix} \in \mathbb{R}^{nN \times nN(N-1)},$$

formed by submatrices

$$\begin{aligned} \mathcal{I}_{11} &= [B_1F_{12}, B_1F_{13}, \ldots, B_1F_{1N}] \\ \mathcal{I}_{22} &= [B_2F_{21}, B_2F_{23}, \ldots, B_2F_{2N}] \\ \mathcal{I}_{NN} &= [B_NF_{N1}, B_NF_{N2}, \ldots, B_NF_{N(N-1)}]. \end{aligned}$$

The resulting observer error dynamics in (4.21) can be united as

$$\dot{\tilde{\mathbf{x}}} = \mathcal{A}\tilde{\mathbf{x}},$$

where

$$\mathcal{A} = \begin{bmatrix} \mathcal{A}_{11} & \mathcal{A}_{12} & \ldots & \mathcal{A}_{1N} \\ \mathcal{A}_{21} & \mathcal{A}_{22} & \ldots & \mathcal{A}_{2N} \\ \vdots & \vdots & \ddots & \vdots \\ \mathcal{A}_{N1} & \mathcal{A}_{N2} & \ldots & \mathcal{A}_{NN} \end{bmatrix} \in \mathbb{R}^{nN(N-1) \times nN(N-1)},$$

with sub-matrices $\mathcal{A}_{ii}$ defined by the first sum in (4.21) and the off-diagonal sub-matrices $\mathcal{A}_{ij}$ defined by the second sum. For convenience, the matrix $\mathcal{A}$ can be reformulated similar to (4.14). To this end, the resulting matrices $K_{j\Sigma_i}$ are placed in a diagonal formation leading to the overall observation gain matrix

$$\begin{aligned} K = &\text{diag}\{K_{2\Sigma_1}, K_{3\Sigma_1}, \ldots, K_{N\Sigma_1}, K_{1\Sigma_2}, K_{3\Sigma_2}, \ldots, K_{N\Sigma_2}, \\ &K_{1\Sigma_N}, K_{2\Sigma_N}, \ldots, K_{N-1\Sigma_N}\} \in \mathbb{R}^{nN(N-1) \times nN(N-1)}. \end{aligned}$$

According to proposition 4.1.1, it is possible to find a feasible matrix K by solving the LMI in (4.17). Moreover, the proof is completed identifying from the observer equations

above the matrices of the proposition as

$$\begin{aligned}
T^x_{ij} &= -(K_{j\Sigma_i}A_{ii} - A_{ji} - B_jF_{ji} + \sum_{k=1,k\neq i}^{N} T^\xi_{jk}K_{k\Sigma_i}) \\
T^\xi_{jk} &= -(K_{j\Sigma_i}A_{ik} - A_{jk} - B_jF_{jk}) \\
T^u_{ij} &= -K_{j\Sigma_i}B_i \\
H^x_{ij} &= K_{j\Sigma_i} \\
H^\xi_{ij} &= I_{n\times n} \\
H^u_{ij} &= 0_{n\times n}.
\end{aligned}$$

Finally, in the above description, each subsystem controller u_i is provided with $(N-1)$ local estimations and the total number of subsystem observers used by the whole scheme is $(N-1)N$.

4.3 Simulation results

The theory presented in this work is verified through two numerical simulation results. These results are obtained via Matlab as well as Yalmip-SeDuMi package [Lofberg, 2004] to compute the corresponding LMI's. Moreover, in both cases the controller robustness is tested introducing white noise in measurements.

4.3.1 Application example

The control law (4.8) is used to stabilize a nonlinear power system represented by two machines interconnected via a lossy transmission line as depicted in Figure (4.2). The dynamics of this system are (see [Ortega et al., 2005; Casagrande et al., 2011b, 2012])

$$\begin{aligned}
\dot\delta_1 &= \omega_1 \\
\dot\omega_1 &= -D_1\omega_1 + P_1 - G_1E_1^2 - E_1E_2Y_{12}\sin(\delta_1 - \delta_2 + \alpha_{12}) \\
\dot E_1 &= -a_1E_1 + b_1E_2\cos(\delta_1 - \delta_2 + \alpha_{12}) + \frac{1}{\tau_1}(E_{f_1} + \nu_1) \\
\dot\delta_2 &= \omega_2 \\
\dot\omega_2 &= -D_2\omega_2 + P_2 - G_2E_2^2 - E_2E_1Y_{21}\sin(\delta_2 - \delta_1 + \alpha_{21}) \\
\dot E_2 &= -a_2E_2 + b_2E_1\cos(\delta_2 - \delta_1 + \alpha_{21}) + \frac{1}{\tau_2}(E_{f_2} + \nu_2),
\end{aligned} \tag{4.22}$$

where $\delta_i \in \mathcal{S} := (-\pi/2, \pi/2)$, $\omega_i \in \mathbb{R}$ and $E_i \in \mathbb{R}_+$ are the states, $\nu_i \in \mathbb{R}$ are the control inputs, D_i,P_i, G_i, a_i, b_i, τ_i and E_{f_i} are positive constants depending on the physical parameters of the i-th machine, and Y_{ij} and α_{ij}, with $i, j \in \bar N$ and $j \neq i$, are constants depending on the topology, the physical properties of the network and the loads (admittance matrix). Moreover, we assume all parameters are exactly known. The equilibrium to be stabilized is

$$\mathcal{E} := (\bar{\boldsymbol{\delta}}, \mathbf{0}, \bar{\mathbf{E}}) \in \mathcal{S}^N \times \mathbb{R}^N \times \mathbb{R}^N_+, \tag{4.23}$$

Table 4.1: System parameters.

Parameter	Machine 1	Machine 2
D	0.0781	0.1661
P	11.4412	29.4031
G	9.4542	12.9505
a	0.3854	0.4906
b	0.2168	0.3220
τ	6	5.89
E_F^*	1.0456	1.0421
$\bar{\delta}$	0.0460	0.1031
$\bar{E}$	1.0321	1.0314
Y_{12}	49.3799	
Y_{21}	104.9939	
α_{12}	0.0832	
α_{21}	0.0832	

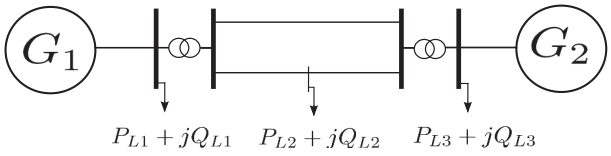

Figure 4.2: Two generator system with three active and reactive power loads.

with $\bar{\boldsymbol{\delta}} := \text{col}(\bar{\delta}_i)$ and $\bar{\mathbf{E}} := \text{col}(\bar{E}_i)$. $\bar{\boldsymbol{\delta}}$ is such that (4.22), with $\omega_i = 0$ and $\delta_i = \bar{\delta}_i$, has a unique solution in $\mathbf{E} = \text{col}(E_i)$, with $E_i > 0$ for all i.

The system parameters are grouped in Table 4.1. In the same way, initial conditions for the nonlinear model in (4.22) are gathered in Table 4.2. They have been selected to be around $\pm 20\%$ of the equilibrium points. The initial condition for the state of the observers (4.10) and (4.11) are settled to zero.

The matrices A and B resulting from the linearization of (4.22) and the controller gain matrices F_{11}, F_{12}, F_{21}, F_{22} are given below. The spectrum of the closed-loop systems is $\lambda(A + BF) = \{-0.31 \pm 12.76i, -0.66 \pm 1.45i, -0.83, -0.71\}$. The LMI (4.17) is feasible and the resulting matrix K places all eigenvalues of $\mathcal{A}$ at the left hand side of the complex plane. However it is needed to assign the spectrum of $\mathcal{A}$ at the left hand side of the spectrum of $A + BF$ to provide the observer with a faster dynamics than the closed-loop dynamics. The spectrum of $\mathcal{A}$ can be placed in a desired disk region in the complex plane if the LMI [Ostertag, 2011]

$$\begin{aligned} P = P^\top > 0 \\ L \otimes P + M \otimes (\Lambda^\top P - \Omega^\top U^\top) + M^\top \otimes (P\Lambda - U\Omega) < 0 \end{aligned} \tag{4.24}$$

holds, where $\otimes$ defines de Kronecker product and

$$L = \begin{bmatrix} -r & q \\ q & -r \end{bmatrix}, \quad M = \begin{bmatrix} 0 & 1 \\ 0 & 0 \end{bmatrix},$$

characterize a disk region D with center $-q$ and radius r in the complex plane. Under this consideration, the observer gain matrices $K_{2\Sigma_1}$ and $K_{1\Sigma_2}$ given below, are obtained from the solution of (4.24) where all the eigenvalues of $\mathcal{A}$ lie within the disc $D(-15, 5)$.

In Figs. 4.3 to 4.5, the evolution of the states variables of the machines 1 and 2 are depicted together with the corresponding estimations, the latter are expressed in the machine coordinates $[\hat{\delta}_{1\Sigma_2}, \hat{\omega}_{1\Sigma_2}, \hat{E}_{1\Sigma_2}]^\top = \hat{x}_{1\Sigma_2} + [\bar{\delta}_1, 0, \bar{E}_1]^\top$ and $[\hat{\delta}_{2\Sigma_1}, \hat{\omega}_{2\Sigma_1}, \hat{E}_{2\Sigma_1}]^\top = \hat{x}_{2\Sigma_1} + [\bar{\delta}_2, 0, \bar{E}_2]^\top$, respectively. A good performance is observed in both objectives: stabilization and estimation of the unknown states trajectories.

Table 4.2: Initial conditions.

State	Value
$\delta_1(0)$	$0.80\bar{\delta}_1$
$\delta_2(0)$	$1.20\bar{\delta}_2$
$\omega_1(0)$	0.10
$\omega_2(0)$	0.10
$E_1(0)$	$1.20\bar{E}_1$
$E_2(0)$	$0.80\bar{E}_2$

$$A_{11} = \begin{bmatrix} 0 & 1 & 0 \\ -52.5474 & -0.0781 & -20.8423 \\ -0.0058 & 0 & -0.3854 \end{bmatrix}$$

$$A_{12} = \begin{bmatrix} 0 & 0 & 0 \\ 52.5474 & 0 & -1.3277 \\ 0.0058 & 0 & 0.2168 \end{bmatrix}$$

$$A_{21} = \begin{bmatrix} 0 & 0 & 0 \\ 110.6683 & 0 & -15.1441 \\ 0.0465 & 0 & 0.3188 \end{bmatrix}$$

$$A_{22} = \begin{bmatrix} 0 & 1 & 0 \\ -110.6683 & -0.1661 & -41.8686 \\ -0.0465 & 0 & -0.4906 \end{bmatrix}$$

$$B_1 = [0 \quad 0 \quad 0.1667]^\top$$
$$B_2 = [0 \quad 0 \quad 0.1698]^\top$$

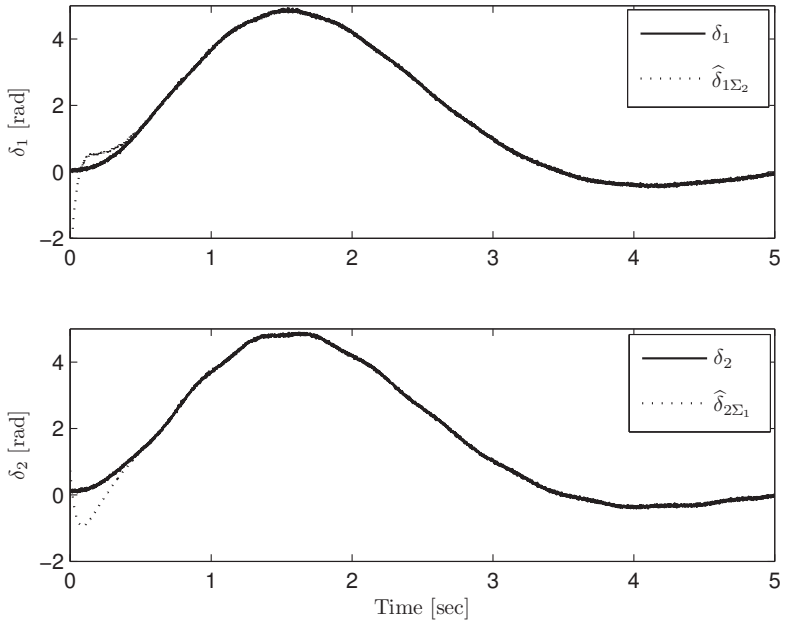

Figure 4.3: Time histories of δ_1, δ_2 and their estimations $\hat{\delta}_{1\Sigma_2}$ and $\hat{\delta}_{2\Sigma_1}$.

$$F_{11} = \begin{bmatrix} -1.4777 & 0.54763 & -9.7568 \end{bmatrix}$$
$$F_{12} = \begin{bmatrix} 2.0369 & 0.35803 & -6.7931 \end{bmatrix}$$
$$F_{21} = \begin{bmatrix} 11.236 & 0.13086 & -1.8999 \end{bmatrix}$$
$$F_{22} = \begin{bmatrix} -11.081 & 0.10006 & -4.4729 \end{bmatrix}$$

$$K_{2\Sigma_1} = \begin{bmatrix} 0 & 0.4100 & 3.3388 \\ 0 & 0.0922 & -183.5872 \\ 0 & -0.0382 & 44.7519 \end{bmatrix}$$
$$K_{1\Sigma_2} = \begin{bmatrix} 0 & 0.1721 & 10.9143 \\ 0 & 0.3902 & -19.6936 \\ 0 & -0.0049 & 25.0726 \end{bmatrix}$$

4.3.2 Academic example

A twelve-order LTI system formed by 4 interconnected subsystems, is parametrized with the overall matrices A and B as in (4.26) and (4.27) given below. Moreover, each subsystem has three states and one control signal, resulting in $N = 4$, $n = 3$ and $m = 1$. The system initial conditions are $x_1(0) = [20,\ 5,\ -13]^\top$, $x_2(0) = [-40,\ 25,\ 90]^\top$, $x_3(0) = [12,\ -50,\ 16]^\top$ and $x_4(0) = [-7,\ 1\ -1]^\top$. In addition, the initial conditions of the observer in (4.20) are set to zero. The state feedback matrix F is specified in (4.25) below. The LMI (4.17) results feasible and the estimation gain matrices are recovered as

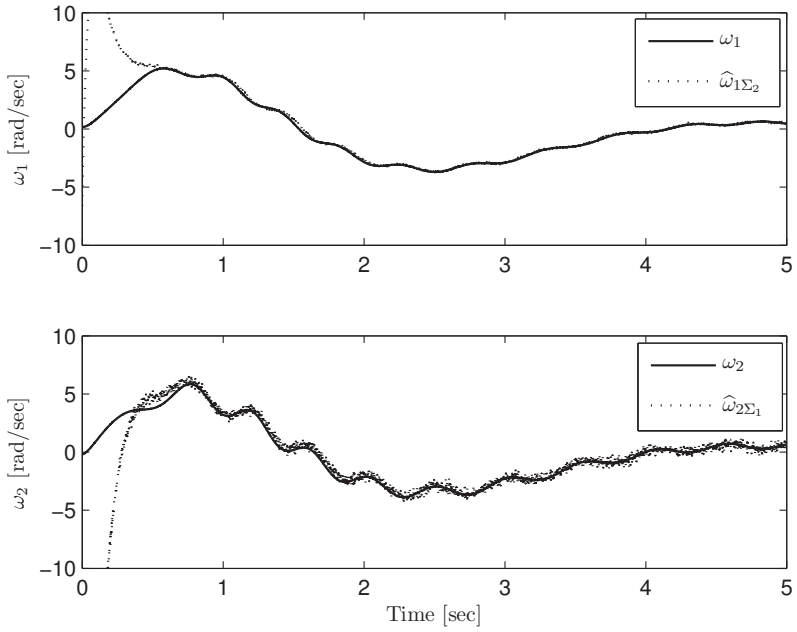

Figure 4.4: Time histories of ω_1, ω_2 and their estimations $\hat{\omega}_{1\Sigma_2}$ and $\hat{\omega}_{2\Sigma_1}$.

in (4.28), below.

The Figures 4.6 to 4.9 show the time history of the state variables and their corresponding estimations. System trajectories reach equilibrium after 5 seconds, meanwhile, all estimations converge around 3 seconds, proving the effectiveness of the proposed scheme for a large-sacle LTI system.

$$F = \left[\begin{array}{rrr|rrr|rrr|rrr} 14.95 & -31.80 & 27.75 & 2.17 & 1.56 & -9.59 & 0.67 & -13.15 & -7.48 & 0.35 & 0.20 & -2.14 \\ -0.65 & 1.39 & -0.98 & -2.13 & 4.50 & -0.26 & -0.57 & 1.00 & -0.11 & 3.00 & -0.35 & -2.47 \\ \hline -1.05 & 1.35 & -0.95 & -0.08 & -0.83 & -1.14 & 1.55 & -4.40 & -7.95 & -2.00 & 0.33 & 1.67 \\ 1.06 & -1.63 & 1.16 & -3.92 & 4.18 & 6.27 & 1.29 & -3.97 & -2.06 & 26.02 & -3.97 & -18.25 \end{array}\right] \tag{4.25}$$

$$A = \left[\begin{array}{rrr|rrr|rrr|rrr} -4 & 6 & -4 & 0.4 & 0.25 & 0.25 & -0.45 & 0.4 & 0 & -0.1 & 0.05 & 0 \\ 2 & -9 & 3 & -0.15 & 0.1 & -0.035 & 0.1 & 0.025 & -0.25 & 0.05 & 0.005 & -0.1 \\ 1 & -7 & 1 & 0.79 & -0.35 & 0.45 & 0.35 & -0.5 & 0.6 & 0.2 & -0.15 & 0.35 \\ \hline 0.4 & 0.25 & 0.25 & 0.4 & 12 & 8.8 & 0.05 & -0.075 & -0.15 & -0.05 & -0.2 & -0.1 \\ -0.15 & 0.1 & -0.035 & -4 & -1 & 8 & 0.2 & -0.5 & 0.4 & -0.1 & -0.05 & 0.15 \\ 0.79 & -0.35 & 0.45 & 7 & 0.5 & -2 & 0.15 & -0.4 & -0.2 & 0.25 & -0.3 & -0.05 \\ \hline -0.45 & 0.4 & 0 & 0.05 & -0.075 & -0.15 & 7 & -14 & 4 & -0.135 & -0.07 & 0.215 \\ 0.1 & 0.025 & -0.25 & 0.2 & -0.5 & 0.4 & 5 & -2 & 7 & 0.485 & -0.15 & -0.25 \\ 0.35 & -0.5 & 0.6 & 0.15 & -0.4 & -0.2 & -9 & -6 & 5 & -0.2 & 0.05 & 0 \\ \hline -0.1 & 0.05 & 0 & -0.05 & -0.2 & -0.1 & -0.135 & -0.07 & 0.215 & -5 & -1 & 7 \\ 0.05 & 0.005 & -0.1 & -0.1 & -0.05 & 0.15 & 0.485 & -0.15 & -0.25 & 12 & -7 & 5 \\ 0.2 & -0.15 & 0.35 & 0.25 & -0.3 & -0.05 & -0.2 & 0.05 & 0 & -2 & -1 & 3 \end{array}\right] \tag{4.26}$$

$$B = \left[\begin{array}{c|c|c|c} 1 & 0 & 0 & 0 \\ 1 & 0 & 0 & 0 \\ 1 & 0 & 0 & 0 \\ \hline 0 & 1 & 0 & 0 \\ 0 & 1 & 0 & 0 \\ 0 & 1 & 0 & 0 \\ \hline 0 & 0 & 1 & 0 \\ 0 & 0 & 1 & 0 \\ 0 & 0 & 1 & 0 \\ \hline 0 & 0 & 0 & 1 \\ 0 & 0 & 0 & 1 \\ 0 & 0 & 0 & 1 \end{array}\right] \tag{4.27}$$

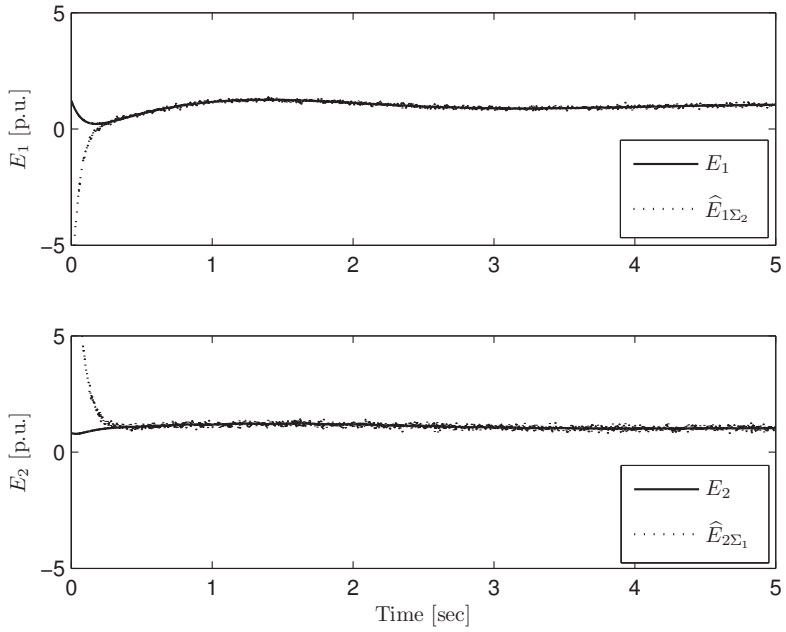

Figure 4.5: Time histories of E_1, E_2 and their estimations $\hat{E}_{1\Sigma_2}$ and $\hat{E}_{2\Sigma_1}$.

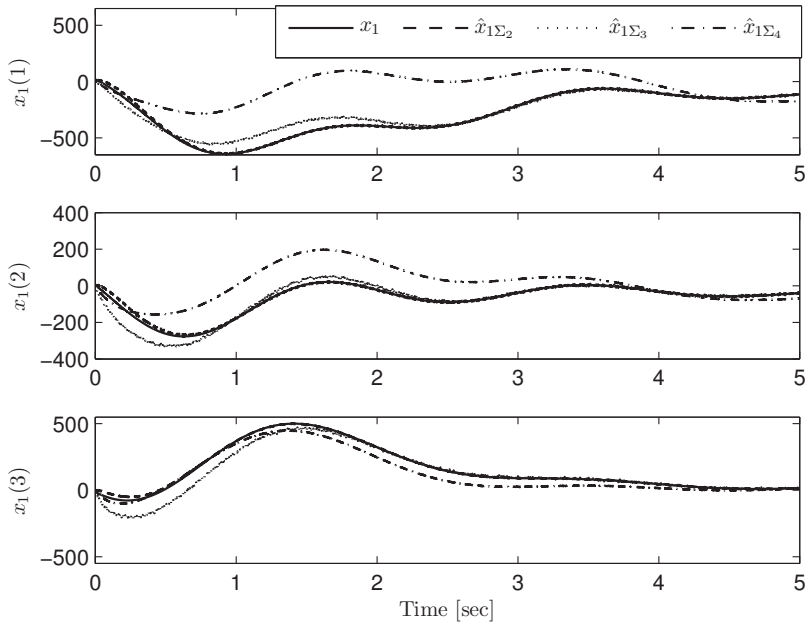

Figure 4.6: Time histories of x_1 and its estimations.

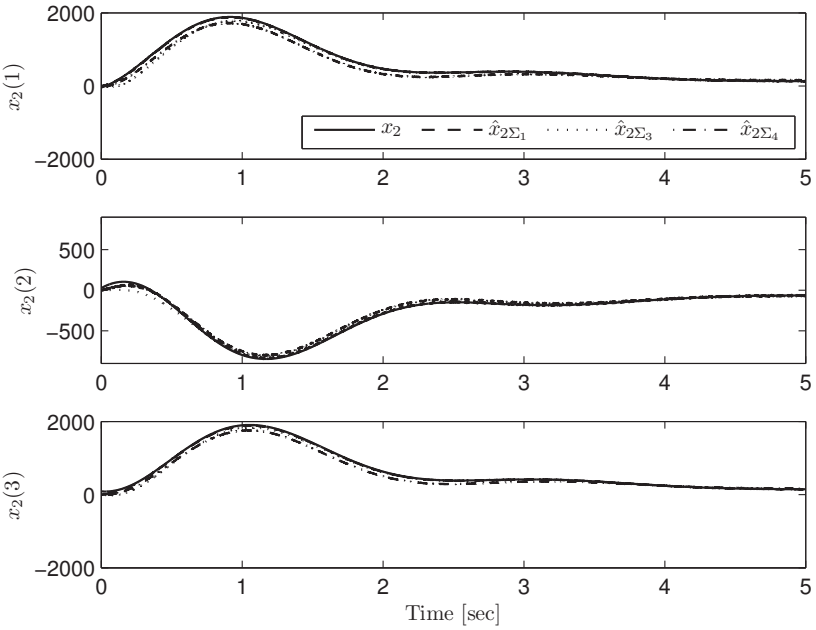

Figure 4.7: Time histories of x_2 and its estimations.

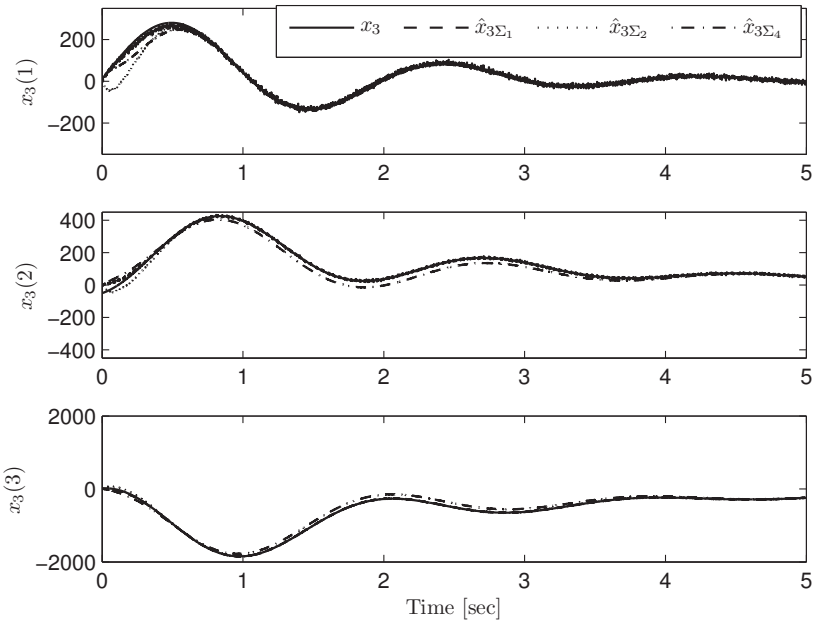

Figure 4.8: Time histories of x_3 and its estimations.

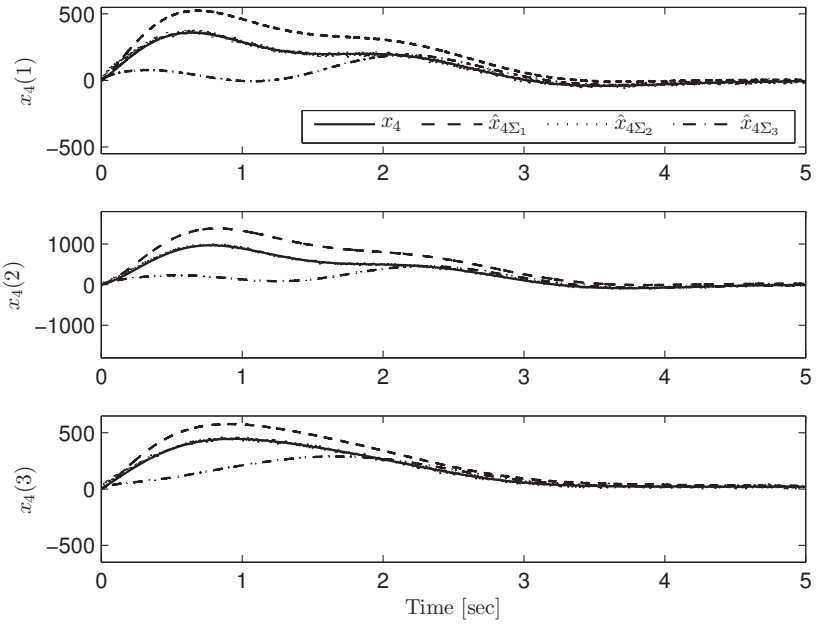

Figure 4.9: Time histories of x_4 and its estimations.

$$
\begin{aligned}
K_{2\Sigma_1} &= \begin{bmatrix} 39.85 & 78.75 & 25.12 \\ 27.45 & 70.79 & 15.67 \\ 19.07 & 37.95 & 12.27 \end{bmatrix}, \; K_{3\Sigma_1} = \begin{bmatrix} -22.53 & 115.17 & 28.06 \\ -2.03 & 70.49 & 5.45 \\ -6.34 & -97.86 & -4.48 \end{bmatrix}, \; K_{4\Sigma_1} = \begin{bmatrix} 4.60 & 22.96 & 22.35 \\ 5.70 & 25.92 & 26.99 \\ 4.22 & 9.90 & 19.12 \end{bmatrix}, \\
K_{1\Sigma_2} &= \begin{bmatrix} -20.62 & 2.80 & 65.33 \\ -8.71 & 1.81 & 45.95 \\ -4.16 & 3.20 & 34.26 \end{bmatrix}, \; K_{3\Sigma_2} = \begin{bmatrix} 2.76 & -50.80 & -8.09 \\ 5.50 & -36.86 & -9.80 \\ -9.27 & 75.17 & 16.20 \end{bmatrix}, \; K_{4\Sigma_2} = \begin{bmatrix} -116.75 & -12.31 & 111.66 \\ -167.27 & -22.15 & 158.26 \\ -110.48 & -11.65 & 106.36 \end{bmatrix}, \\
K_{1\Sigma_3} &= \begin{bmatrix} -48.46 & -4.10 & 62.93 \\ 0.77 & -1.17 & 68.61 \\ 41.51 & 6.70 & 75.56 \end{bmatrix}, \quad K_{2\Sigma_3} = \begin{bmatrix} 21.77 & 63.87 & 25.65 \\ -1.42 & -0.09 & -1.24 \\ 13.38 & 38.85 & 15.97 \end{bmatrix}, \; K_{4\Sigma_3} = \begin{bmatrix} -8.02 & -4.55 & -16.44 \\ -33.75 & -13.40 & -27.06 \\ -3.63 & -2.25 & -14.76 \end{bmatrix}, \\
K_{1\Sigma_4} &= \begin{bmatrix} -16.40 & 10.76 & 45.60 \\ 12.43 & 15.30 & 54.25 \\ 23.81 & 18.70 & 62.21 \end{bmatrix}, \; K_{2\Sigma_4} = \begin{bmatrix} -99.51 & -16.94 & 16.71 \\ -64.29 & -32.85 & -26.83 \\ -52.90 & -1.87 & 19.54 \end{bmatrix}, \; K_{3\Sigma_4} = \begin{bmatrix} 20.62 & 73.34 & 2.66 \\ -8.28 & 19.13 & 0.03 \\ 42.05 & -3.18 & 0.41 \end{bmatrix},
\end{aligned}
\tag{4.28}
$$

Chapter 5

Nonlinear Decentralized Solution

A global solution to the problem of transient stabilization of multimachine power system with non–negligible transfer conductances was introduced in chapter 3. The proposed scheme is a *centralized* nonlinear dynamic controller that ensures global asymptotic stability of the desired operating point. Due to technological and reliability considerations the exchange of information between generators is restricted, and in some cases undesirable, hence the need for *decentralized* controllers. The main contribution of this part of the research is the proof that, using local measurements available with existing technology, it is possible to transform our previous centralized controller into a truly decentralized one, provided that the derivative of the active power at each generator can be suitably estimated. Some simulation results using the 10-machine New England benchmark show that transient stability enhancement and voltage regulation under different fault scenarios is effectively achieved.

This chapter is ordered in the following manner. In Section 5.1 the standard power system model is briefly reviewed and the decentralized transient stabilization problem is formulated. In Section 5.2 the centralized controller of [Casagrande et al., 2012] is outlined. The decentralized scheme and its stability analysis are presented in Section 5.3. Finally, an illustrative example is given in Section 5.4, where a comparison between centralized and decentralized schemes is made.

5.1 System model and problem formulation

In this section the N–machine power system model considered in this work is presented. The behavior of the interconnected generators can be described using the classical third order model with flux decay dynamics reported in [Pai, 1989; Kundur, 1994; Bergen and Vital, 2000; Anderson and Fouad, 2003]. This model includes the voltage angle (considered equal to the shaft angle), the speed deviation and the voltage behind the transient reactance. In addition, all the electrical network has been reduced to an internal bus representation. The dynamical model of the i–th generator is given by

$$\begin{aligned}
\dot{\delta}_i &= \omega_i \\
\dot{\omega}_i &= -\frac{D_{mi}}{M_i}\omega_i + \frac{\omega_0}{M_i}(P_{mi} - P_{ei}) \\
\dot{E}_i &= \frac{1}{\tau_i}(-E_{qi} + E_{fi} + \nu_i), \quad i \in \bar{N} := \{1, ..., N\}
\end{aligned} \tag{5.1}$$

where the states variables of this subsystem are the rotor angle $\delta_i \in \mathbb{S} := [0, 2\pi)$, rad, the speed deviation $\omega_i \in \mathbb{R}$ in rad/sec and the generator quadrature internal voltage $E_i \in \mathbb{R}_+$ in p.u.. D_{mi} is the damping constant in p.u., $M_i = 2H$, where H is the inertia constant in seconds, P_{mi} is the constant mechanical input power and P_{ei} is the electromagnetic power, both in p.u., τ_i is the direct axis transient short circuit time constant. The voltages E_{qi}, E_{fi} and ν_i, expressed in p.u., are the electromotive force in the quadrature axis, the control constant voltage component applied to the field winding, and the control voltage input, respectively. To simplify the notation, whenever clear from the context, the qualifier "$i \in \bar{N}$" will be omitted in the sequel.

The active P_{ei} and reactive Q_{ei} power as well as the voltage E_{qi} are defined as

$$\begin{aligned} P_{ei} &= E_i I_{qi} \\ Q_{ei} &= E_i I_{di} \\ E_{qi} &= E_i + (x_{di} - x'_{di}) I_{di} = x_{adi} I_{fi} \end{aligned} \tag{5.2}$$

where I_{qi} and I_{di} are the quadrature and direct axis currents, x_{di} is the direct axis reactance and x'_{di} the direct axis transient reactance, where we have that $x_{di} > x'_{di}$. I_{fi} is the field winding current and x_{adi} is the mutual reactance between the excitation and stator coils. All the latter quantities are expressed in p.u. system.

The interconnections between machines are given by the currents

$$\begin{aligned} I_{qi} &= \sum_{j=1}^{N} E_j (G_{mij} \cos \delta_{ij} + B_{mij} \sin \delta_{ij}) \\ I_{di} &= \sum_{j=1}^{N} E_j (G_{mij} \sin \delta_{ij} - B_{mij} \cos \delta_{ij}) \end{aligned} \tag{5.3}$$

where $\delta_{ij} = \delta_i - \delta_j$, G_{mij} is the conductance and B_{mij} is the susceptance, both in p.u.. resulting from the computation of the network admittance matrix. Developing the sums when $j = i$ and recalling the identities [Ortega et al., 2005]

$$\begin{aligned} Y_{ij} &= \sqrt{G_{mij}^2 + B_{mij}^2} \\ \alpha_{ij} &= \arctan\left(\frac{G_{mij}}{B_{mij}}\right) \\ G_{mij} \cos \delta_{ij} + B_{mij} \sin \delta_{ij} &= Y_{ij} \sin(\delta_{ij} + \alpha_{ij}) \\ G_{mij} \sin \delta_{ij} - B_{mij} \cos \delta_{ij} &= -Y_{ij} \cos(\delta_{ij} + \alpha_{ij}) \end{aligned}$$

yields

$$\begin{aligned} I_{qi} &= G_{mii}E_i + \sum_{j=1,j\neq i}^{N} E_j Y_{ij}\sin(\delta_{ij}+\alpha_{ij}) \\ I_{di} &= -B_{mii}E_i - \sum_{j=1,j\neq i}^{N} E_j Y_{ij}\cos(\delta_{ij}+\alpha_{ij}). \end{aligned} \tag{5.4}$$

Finally, combining (5.1) and (5.4) results in the well–known compact form [Chiang et al., 1995a; Lu et al., 2001; Ortega et al., 2005; Casagrande et al., 2012]

$$\begin{aligned} \dot{\delta}_i &= \omega_i \\ \dot{\omega}_i &= -D_i\omega_i + P_i - G_{ii}E_i^2 - d_iE_i \sum_{j=1,j\neq i}^{N} E_j Y_{ij}\sin(\delta_{ij}+\alpha_{ij}) \\ \dot{E}_i &= -a_iE_i + b_i \sum_{j=1,j\neq i}^{N} E_j Y_{ij}\cos(\delta_{ij}+\alpha_{ij}) + \frac{1}{\tau_i}(E_{f_i}+\nu_i) \end{aligned} \tag{5.5}$$

with the positive constants

$$D_i = \frac{D_{mi}}{M_i}, \quad P_i = d_iP_{mi}, \quad G_{ii} = d_iG_{mii}, \quad d_i = \frac{\omega_0}{M_i},$$

$$a_i = \frac{1}{\tau_i}(1-(x_{di}-x'_{di})B_{mii}), \quad b_i = \frac{1}{\tau_i}(x_{di}-x'_{di}).$$

Similarly to [Casagrande et al., 2012] we assume that all parameters are exactly known with exception to the difference $x_{di}-x'_{di}$ which is assumed to be unknown, then we make the following practically reasonable assumption.

Assumption 5.1.1. *The equilibrium to be stabilized*

$$\mathcal{E} := (\bar{\boldsymbol{\delta}}, \mathbf{0}, \bar{\mathbf{E}}) \in \mathbb{S}^N \times \mathbb{R}^N \times \mathbb{R}_+^N,$$

where $\bar{\boldsymbol{\delta}} := col(\bar{\delta}_i)$ *and* $\bar{\mathbf{E}} := col(\bar{E}_i)$*, is such that (5.5), with* $\omega_i = 0$ *and* $\delta_i = \bar{\delta}_i$*, has a unique solution in* $\mathbf{E} = \mathrm{col}(E_i)$*, with* $E_i > 0$*.*

To develop a decentralized version of the one presented in chapter 3 and published in [Casagrande et al., 2012] we make, following [Guo et al., 2000; Yan et al., 2010], the additional assumptions.

Assumption 5.1.2. *The signals* δ_i*,* ω_i*,* E_i*,* P_{ei} *and* Q_{ei} *are measurable at each generating unit.*

Remark 5.1.1. *Although the voltage behind the transient reactance E_i is an artificial quantity, is often approximated via phasorial operations between the P_{ei}, Q_{ei} and the generator terminal voltage [Anderson and Fouad, 2003]. However, the state variable E_i can be suitable computed from the combination of the last two equations in (5.2), and recalling that $E_i > 0$, we obtain the quadratic equation*

$$E_i^2 - x_{adi} I_{fi} E_i + (x_{di} - x'_{di}) Q_{ei} = 0.$$

In order for (5.2) to make physical sense, this equation most admit a positive real solution, hence

$$x_{adi}^2 I_{fi}^2 \geq 4(x_{di} - x'_{di}) Q_{ei},$$

and the solution is given by

$$E_i = \frac{x_{adi} I_{fi}}{2} \pm \frac{\sqrt{x_{adi}^2 I_{fi}^2 - 4(x_{di} - x'_{di}) Q_{ei}}}{2}, \tag{5.6}$$

Since the solution has to match the equilibrium value $\bar{E}_i$ in steady–state, the sign of the square root term is determined computing (5.6) and using the steady–state values of I_{fi} and Q_{ei}. Note that I_{fi} is the rotor field current, hence measurable.

Assumption 5.1.3. *An estimate of the signal $\dot{P}_{ei}$, denoted $\dot{P}_{ei}^f$, satisfying*

$$\dot{P}_{ei}^f = \dot{P}_{ei} + \varepsilon_i,$$

with ε_i exponentially decaying signals, can be computed from the measurable signals.

Problem Formulation: Consider the system (5.5), verifying Assumptions 5.1.1–5.1.3. Find an adaptive decentralized dynamic control law such that the equilibrium of the extended closed loop system is GAS.

Remark 5.1.2. *In [Guo et al., 2000] and [Yan et al., 2010] , it is furthermore assumed that $x_{di} - x'_{di}$ is known. As shown below, this assumption can be obviated.*

5.2 Centralized controller review

A review of the centralized stabilization scheme described in chapter 3 is presented in this section for convenience. The derivation of this controller is based on a new methodology for stabilization of non–globally feedback linearizable triangular systems. Applied to the power system model (5.5) leads to a centralized dynamic state–feedback controller that ensures the equilibrium of the extended closed loop system is GAS. That is, it solves the problem formulated above replacing Assumption 5.1.2 by the assumption of full state measurement at each generating unit.

To begin with the centralized controller derivation, the partial linearizing control law

$$\nu_i = \tau_i \left(u_i + a_i E_i - b_i \sum_{j=1, j\neq i}^{N} E_j Y_{ij} \cos(\delta_{ij} + \alpha_{ij}) \right) - E_{fi} \tag{5.7}$$

is applied to the system (5.5), where $u_i \in \mathbb{R}$, are the new control inputs.

Using the error coordinates

$$x_{1,i} := \delta_i - \bar{\delta}_i, \;\; x_{2,i} := \omega_i, \;\; x_{3,i} := E_i - \bar{E}_i, \tag{5.8}$$

the compact model (5.5) can be expressed as

$$\begin{array}{rcl} \dot{x}_{1,i} & = & x_{2,i} \\ \dot{x}_{2,i} & = & -D_i x_{2,i} + P_i - (x_{3,i} + \bar{E}_i) h_i(\mathbf{x}_1, \mathbf{x}_3) \\ \dot{x}_{3,i} & = & u_i \end{array} \tag{5.9}$$

where for $k = 1, 2, 3$, then we have defined the vectors

$$\mathbf{x}_k = \mathrm{col}(x_{k,1}, x_{k,2}, \ldots, x_{k,N}),$$

and introduced the functions

$$\begin{array}{rcl} h_i(\mathbf{x}_1, \mathbf{x}_3) & := & G_{ii}(x_{3,i} + \bar{E}_i) + d_i \sum_{j=1, j\neq i}^{N} (x_{3,j} + \bar{E}_j) Y_{ij} \sin(\mu_{ij}(\mathbf{x}_1)) \\ \mu_{ij}(\mathbf{x}_1) & := & x_{1,i} + \bar{\delta}_i - x_{1,j} - \bar{\delta}_j + \alpha_{ij}, \; i \neq j. \end{array} \tag{5.10}$$

The dynamic nonlinear stabilizing control law is then defined as

$$u_i = \dot{x}^d_{3,i} + \beta_{1,i} \; h_i x_{2,i} - \beta_{2,i} \; (x_{3,i} - x^d_{3,i}) + \epsilon_i \xi_i \sin(x_{1,i}), \tag{5.11}$$

where $\beta_{1,i} > 0$, $\beta_{2,i} > 0$ and $\epsilon_i > 0$, ξ_i is the controller state whose dynamics are defined by

$$\dot{\xi}_i = \beta_{3,i} \; (h_i - \xi_i) - \beta_{4,i} \; (x^d_{3,i} + \bar{E}_i) x_{2,i} + \dot{h}_i - \epsilon_i (x_{3,i} + \bar{E}_i) \sin(x_{1,i}) \tag{5.12}$$

with $\beta_{3,i} > 0$, $\beta_{4,i} > 0$, and the auxiliary signal

$$x^d_{3,i} = \frac{1}{\xi_i} [\sin(x_{1,i}) + P_i] - \bar{E}_i. \tag{5.13}$$

It is important to note that the signals $\dot{x}^d_{3,i}$ and $\dot{h}_i$, used in the controller equations (5.11), (5.12), can be computed without differentiation as

$$\dot{x}^d_{3,i} = \frac{1}{\xi_i} [x_{2,i} \cos(x_{1,i})] - \frac{1}{\xi_i^2} [\sin(x_{1,i}) + P_i] \dot{\xi}_i \,, \tag{5.14}$$

$$\dot{h}_i = G_i u_i + d_i \sum_{j=1, j\neq i}^{N} [u_j Y_{ij} \sin(\mu_{ij}(x_{1,i})) + (x_{3,j} + \bar{E}_j) Y_{ij} (x_{2,i} - x_{2,j}) \cos(\mu_{ij}(x_{1,i}))]. \tag{5.15}$$

The complete centralized stabilization scheme is given by the set of equations (5.7) and (5.10)–(5.13). We should underscore that the computation of ν_i and h_i and its time derivative, require the exchange of information between generating units, rendering the controller naturally centralized.

Remark 5.2.1. *Note that the control signal u_i is present explicitly in equations (5.11) and (5.15) and implicitly in (5.12) and (5.14) producing an algebraic loop in the computation of the control signal. The last issue is solved in chapter 3 imposing some additional conditions on the physical parameters, namely, Assumption 3.1.3. It is interesting to note that this assumption is obviated in the new decentralized controller proposed below.*

5.3 Decentralized stabilization scheme

To obtain a decentralized version of the controller equations (5.7) and (5.10)–(5.13) we will use the algebraic relations (5.2) that involve the measurable signals P_{ei}, Q_{ei} and E_i.

First, we observe that the centralized partial linearizing term (5.7) can be rendered decentralized using E_{qi}. Indeed, from the third equation in (5.1) we have that (5.7) is equivalent to

$$\nu_i = \tau_i u_i + E_{qi} - E_{fi},$$

and from (5.2), the last expression can be formulated as

$$\nu_i = \tau_i u_i + E_i + \theta_i I_{di} - E_{fi}, \tag{5.16}$$

with $\theta_i = x_{di} - x'_{di}$ as unknown parameter. To render robust the current decentralized version, we now invoke the Immersion and Invariance (I&I) methodology described in detail in [Astolfi et al., 2008] to develop an adaptive law to estimate θ_i and use —in a certainty–equivalent way—this estimate in the control law. Accordingly to [Astolfi et al., 2008], the estimation error can be defined as

$$z_i = \hat{\theta}_i - \theta_i + \eta_i(E_i), \tag{5.17}$$

where $\hat{\theta}_i \in \mathbb{R}$ and $\eta_i(E_i) \in \mathbb{R}$, and its time derivative as

$$\dot{z}_i = \dot{\hat{\theta}}_i + \frac{1}{\tau_i}\frac{\partial \eta_i}{\partial E_i}\Big(- E_i - \big(\hat{\theta}_i + \eta_i(E_i) - z_i\big) I_{di} + E_{fi} + \nu_i\Big). \tag{5.18}$$

Then selecting

$$\dot{\hat{\theta}}_i = -\frac{1}{\tau_i}\frac{\partial \eta_i}{\partial E_i}\Big(- E_i - \big(\hat{\theta}_i + \eta_i(E_i)\big) I_{di} + E_{fi} + \nu_i\Big), \tag{5.19}$$

yields to the error dynamics

$$\dot{z}_i = \frac{1}{\tau_i}\frac{\partial \eta_i}{\partial E_i} I_{di} z_i, \tag{5.20}$$

moreover, selecting

$$\eta_i(E_i) = -\sigma_i \tau_i E_i, \quad \sigma_i > 0 \tag{5.21}$$

render the estimation error dynamics as

$$\dot{z}_i = -\sigma_i I_{di} z_i. \tag{5.22}$$

Since each generator is producing reactive power Q_{ei}, I_{di} is assumed to be positive for all time. In addition the total Lyapunov function in this case is defined as

$$\mathcal{V}(\mathbf{z}) = \sum_{i=1}^{N} \frac{1}{2} z_i^2 \tag{5.23}$$

where $\mathbf{z} = \text{col}(z_i)$ and the time derivative along the trajectories of (5.22) is

$$\dot{\mathcal{V}} = -\sum_{i=1}^{N} \sigma_i I_{di} z_i^2 \leq 0, \tag{5.24}$$

hence, the error dynamics have a globally stable equilibrium point.

Remark the Lyapunov function (5.23) corresponding to the adaptive scheme will be added to the general Lyapunov function W given below.

Second, the function h_i is related with the quadrature axis current I_{qi}, which can be determined from the measurement of the active power P_{ei} and the voltage E_i as follows

$$h_i = d_i I_{qi} = d_i \frac{P_{ei}}{E_i}. \tag{5.25}$$

At this point we make the important observation that the state equation (5.12) of the centralized control law contains the term $\dot{h}_i$ that, as seen in (5.15), requires the exchange of information between generators. To avoid this problem we note that

$$\dot{h}_i = \frac{d_i}{E_i^2}(\dot{P}_{ei} E_i - P_{ei} u_i),$$

where we have used the fact that $\dot{E}_i = u_i$ in the computation of the derivative. Invoking Assumption 5.1.3 it is clear that $\dot{h}_i$ can be asymptotically estimated without exchange of information between generators.

Although it is possible to estimate directly $\dot{P}_{ei}$—via, *e.g.*, approximate differentiation of P_{ei}—and then replace $\dot{h}_i$ in (5.12), this generates and algebraic loop in the computation of u_i. Instead, we propose to estimate directly $\dot{h}_i$ using its approximate differentiation, denoted $\dot{h}_i^f$ and computed via

$$\dot{h}_i^f = -\gamma_i h_i^f + \kappa_i h_i, \tag{5.26}$$

where γ_i, κ_i are arbitrary positive constants. See Fig. 5.1. In this way, the aforementioned algebraic loop is avoided and Assumption 5.1.3 is replaced by the following.

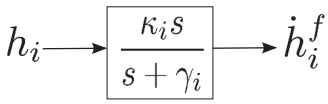

Figure 5.1: Block diagram of the approximate differentiator (5.26).

Assumption 5.3.1. *Consider the signal h_i defined in* (5.25) *and its approximate differentiation $\dot{h}_i^f$ computed via* (5.26)*. Then,*

$$\dot{h}_i^f = \dot{h}_i + \varepsilon_i, \tag{5.27}$$

with ε_i exponentially decaying signals.

Finally, using (5.19), (5.25) and the filtered signal (5.26), the adaptive decentralized dynamic nonlinear stabilizing control law is then defined as

$$\begin{aligned}
\nu_i &= \tau_i u_i + E_i + (\hat{\theta}_i + \eta_i(E_i))I_{di} - E_{fi} \\
u_i &= \dot{x}_{3,i}^d + \beta_{1,i}\, h_i x_{2,i} - \beta_{2,i}\, (x_{3,i} - x_{3,i}^d) + \epsilon_i \xi_i \sin(x_{1,i}) \\
\dot{\xi}_i &= \beta_{3,i}\, (h_i - \xi_i) - \beta_{4,i}\, (x_{3,i}^d + \bar{E}_i) x_{2,i} + \dot{h}_i^f - \epsilon_i (x_{3,i} + \bar{E}_i) \sin(x_{1,i})
\end{aligned} \tag{5.28}$$

with the auxiliary signal $x_{3,i}^d$ defined by (5.13). Notice the use of the term $\dot{h}_i^f$, generated via (5.27), instead of $\dot{h}_i$. Taking into account (5.27) it is clear that the only difference between the centralized and the decentralized control is the presence of the additive, exponentially decaying term ε_i in $\dot{\xi}_i$.

We are in position to present the main result of the paper, whose proof follows immediately from the proof of the centralized scheme reported in [Casagrande et al., 2012] (and also detailed in chapter 3) and Assumption 5.3.1.

Proposition 5.3.1. *Consider the multimachine power system (5.5), verifying Assumptions 5.1.1, 5.1.2 and 5.3.1. The decentralized dynamic control law (5.13), (5.19),* (5.25)–(5.28) *ensures that the desired equilibrium $\mathcal{E}$ is GAS.*

Proof 5.3.1. *Mimicking chapter 3, we propose the Lyapunov function candidate below, which includes two new terms corresponding to the new features adaptive and decentralized.* $W : \mathbb{S}^N \times \mathbb{R}^{3N} \times \mathbb{R} \times \mathbb{R}_+ \to \mathbb{R}$

$$W(\mathbf{x}, \boldsymbol{\xi}, \mathbf{z}, t) = V(\mathbf{x}, \boldsymbol{\xi}) + \mathcal{V}(\mathbf{z}) + \sum_{i=1}^{N} \left(\frac{c_{4,i}}{2\beta_{3,i}} \int_t^\infty \varepsilon_i^2(\eta) \mathrm{d}\eta \right), \tag{5.29}$$

where

$$\begin{aligned}
V(\mathbf{x}, \boldsymbol{\xi}) = \sum_{i=1}^{N} \Bigg(& c_{1,i} \int_0^{x_{1,i}} \sin(\eta) \mathrm{d}\eta + c_{2,i} \epsilon_i x_{2,i} \sin(x_{1,i}) \\
& + \frac{1}{2} \left(c_{3,i} x_{2,i}^2 + c_{4,i} (\xi_i - h_i)^2 + c_{5,i} (x_{3,i} - x_{3,i}^d)^2 \right) \Bigg),
\end{aligned}$$

with $\boldsymbol{\xi} = col(\xi_1, \cdots, \xi_N)$ *and* $c_{k,i}$, *for* $k = 1, 2, \ldots, 5$, *are positive constants. Notice the addition of the integral term, which is required to take into account the presence of the exponential term in* (5.27).
In [Casagrande et al., 2012] it is shown that V *is positive definite in the set*

$$\{\mathbf{x}_1 = \mathbf{0}, \mathbf{x}_2 = \mathbf{0}, \mathbf{x}_3 = \mathbf{x}_3^d, \boldsymbol{\xi} = \mathbf{h}(\mathbf{0}, \mathbf{0})\},$$

since $W \geq V$ *we also have that* W *is positive definite. The time derivative of* W *is*

$$\begin{aligned}\dot{W} = \sum_{i=1}^{n} \Bigg(& c_{1,i} \sin(x_{1,i}) x_{2,i} + c_{2,i}\epsilon_i x_{2,i}^2 \cos(x_{1,i}) + \\ & + c_{2,i}\epsilon_i \dot{x}_{2,i} \sin(x_{1,i}) + c_{3,i} x_{2,i} \dot{x}_{2,i} + \\ & + c_{4,i}(\xi_i - h_i)(\dot{\xi}_i - \dot{h}_i) + \\ & + c_{5,i}(x_{3,i} - x_{3,i}^d)(\dot{x}_{3,i} - \dot{x}_{3,i}^d) - \sigma_i I_{di} z_i^2 - \frac{c_{4,i}}{2\beta_{3,i}} \varepsilon_i^2 \Bigg),\end{aligned}$$

where the term $(\dot{x}_{3,i} - \dot{x}_{3,i}^d)$ *is obtained recalling that* $\dot{x}_{3,i} = u_i$ *and the fact that*

$$\dot{x}_{3,i} - \dot{x}_{3,i}^d = \beta_{1,i}\ h_i^f x_{2,i} - \beta_{2,i}\ (x_{3,i} - x_{3,i}^d) + \epsilon_i \xi_i \sin(x_{1,i}),$$

which follows from (5.28). *The term* $(\dot{\xi}_i - \dot{h}_i)$ *is obtained from (5.28) and (5.27) as*

$$\dot{\xi}_i - \dot{h}_i = \beta_{3,i}\ (h_i - \xi_i) - \beta_{4,i}\ (x_{3,i}^d + \bar{E}_i) x_{2,i} - \epsilon_i (x_{3,i} + \bar{E}_i) \sin(x_{1,i}) + \varepsilon_i.$$

Now, selecting

$$\begin{aligned}\beta_{1,i} =& \beta_{4,i}, \\ c_{1,i} =& c_{3,i} \\ c_{2,i} =& c_{4,i} = c_{5,i}, \\ c_{1,i} =& c_{2,i}\beta_{1,i},\end{aligned}$$

the time-derivative of W *can be written as*

$$\begin{aligned}\dot{W} = \sum_{i=1}^{n} \Bigg(& - c_{4,i}\beta_{3,i}(\xi_i - h_i)^2 - c_{5,i}\beta_{2,i}(x_{3,i} - x_{3,i}^d)^2 - \\ & - [x_{2,i}\ \ \sin(x_{1,i})] M_i(x_{1,i}) \begin{bmatrix} x_{2,i} \\ \sin(x_{1,i}) \end{bmatrix} \\ & + c_{4,i}(\xi_i - h_i)\varepsilon_i - \sigma_i I_{di} z_i^2 - \frac{c_{4,i}}{2\beta_{3,i}} \varepsilon_i^2 \Bigg),\end{aligned} \tag{5.30}$$

where we defined the matrices

$$M_i(x_{1,i}) := \begin{bmatrix} c_{3,i} D_i - c_{2,i}\epsilon_i \cos(x_{1,i}) & \frac{c_{2,i}\epsilon_i D_i}{2} \\ \frac{c_{2,i}\epsilon_i D_i}{2} & c_{2,i}\epsilon_i \end{bmatrix}.$$

The time derivative of W can be expressed as

$$\begin{aligned}\dot{W} = \sum_{i=1}^{n} \Bigg(& -\frac{1}{2}c_{4,i}\beta_{3,i}(\xi_i - h_i)^2 - c_{5,i}\beta_{2,i}(x_{3,i} - x_{3,i}^d)^2 - \\ & -[x_{2,i} \ \ \sin(x_{1,i})] M_i(x_{1,i}) \begin{bmatrix} x_{2,i} \\ \sin(x_{1,i}) \end{bmatrix} - \\ & -\sigma_i I_{di} z_i^2 - \frac{c_{4,i}}{2}\left(\sqrt{\beta_{3,i}}(\xi_i - h_i) - \frac{1}{\sqrt{\beta_{3,i}}}\varepsilon_i\right)^2\Bigg).\end{aligned} \tag{5.31}$$

The proof of GAS is completed selecting the free parameter ϵ_i verifying

$$0 < \epsilon_i < \frac{4c_{3,i}D_i}{c_{2,i}(4 + D_i)},$$

which ensures $M_i(x_{1,i}) > 0$, and invoking the arguments used in [Casagrande et al., 2012].

Remark 5.3.1. *It is well–known that an approximate differentiator asymptotically reconstructs the derivative of a signal provided the frequency range of the signal's spectrum is concentrated in the "good" range of the bandwidth of the filter. Hence, Assumption 5.3.1 essentially requires that the tuning parameters κ_i, γ_i of the filter (5.26) be selected in accordance with the frequency content of h_i.*

Remark 5.3.2. *Due to the use of the filter (5.26) the computation of the proposed decentralized scheme does not involve the algebraic loop that appears in the centralized controller of [Casagrande et al., 2012]—see Remark 5.2.1. Besides the advantage of removing this assumption, since there is no need for the matrix inversion, the computation of the decentralized control law is considerably simplified. Of course, the new scheme requires the additional measurements P_{ei} and Q_{ei} while the stability analysis relies on the (*a priori *unverifiable) Assumption 5.3.1.*

5.4 Simulation results

The performance of the proposed decentralized controller given by the set of equations (5.13), (5.19), (5.25)–(5.28) has been tested with the New England Power system benchmark, which consists of 10 generators, 39 buses and 19 loads. All system parameters are taken from [Pai, 1989].

For comparison purposes, we present also the simulation results of the centralized controller in chapter 3 selecting, in both cases, the same controller gains given in Table 5.1. The gains of the filters (5.26) are selected as $\gamma_i = \kappa_i = 100$, and the estimation gains in (5.21) are selected $\sigma_i = 5$.

To assess the controller robustness we present three different simulation cases.

Table 5.1: Controller gains.

i	$\beta_{1,i}$, $\beta_{4,i}$	$\beta_{2,i}$, $\beta_{3,i}$	$c_{1,i}$, $c_{3,i}$	$c_{2,i}$, $c_{4,i}$, $c_{5,i}$	ϵ_i
1	1.05	8.4	6	5.7143	0.6300
2	0.7	21	6	8.5714	0.2310
3	0.7	21	6	8.5714	0.1955
4	0.7	21	6	8.5714	0.2447
5	0.7	21	6	8.5714	0.2692
6	0.7	21	6	8.5714	0.2011
7	0.7	21	6	8.5714	0.2651
8	0.7	21	6	8.5714	0.2880
9	0.7	21	6	8.5714	0.2029
10	0.84	14	6	7.1429	0.6000

(i) Intermittent 3φ fault in bus number 16.

(ii) Permanent line switching between bus 17 and 18.

(iii) Permanent failure in generator 10.

5.4.1 Intermittent 3φ fault in bus 16

This fault is introduced connecting a small impedance to ground at $t = 1$ (seconds) and cleared after 0.15 (seconds). Figures 5.2, 5.3 and 5.4 show the angle error $x_{1,i}$, the speed deviation $x_{2,i}$ and the voltage error $x_{3,i}$, respectively. It is noticeable that the decentralized controller largely outperforms the centralized one.

Figure 5.5 depicts the control signals ν_i for both cases. It is important to observe that the control signals of the decentralized controller case are almost twice as large as those in the centralized case, which partially explains the transient performance improvement—remaining within physically reasonable values. This behavior is a consequence of the direct measurement of the active and reactive power: since the fault is propagated among the controller internal signals, it allows the control system to react more vigorously than the centralized controller. This behavior is prevalent in all the remaining cases.

Figure 5.6 depicts the Lyapunov function for both cases showing, again, that the decentralized controller reacts faster to the fault than the centralized one. In both cases, except during the fault, V is monotonically decreasing as predicted by the theory. To assess the validity of the estimation of θ_i and of the Assumption 5.3.1 Figures 5.7–5.8 shows the estimation error z_i and the difference $\dot{h}_i^f - \dot{h}_i$, where both errors converge to zero rapidly. The same behavior for these errors was observed in the other simulations, hence the plots are omitted for brevity. Note that for all the simulations the initial value of $\hat{\theta}_i + \eta_i(E_i)$ is selected to be 0.1 p.u. over the nominal value of $x_{di} - x'_{di}$.

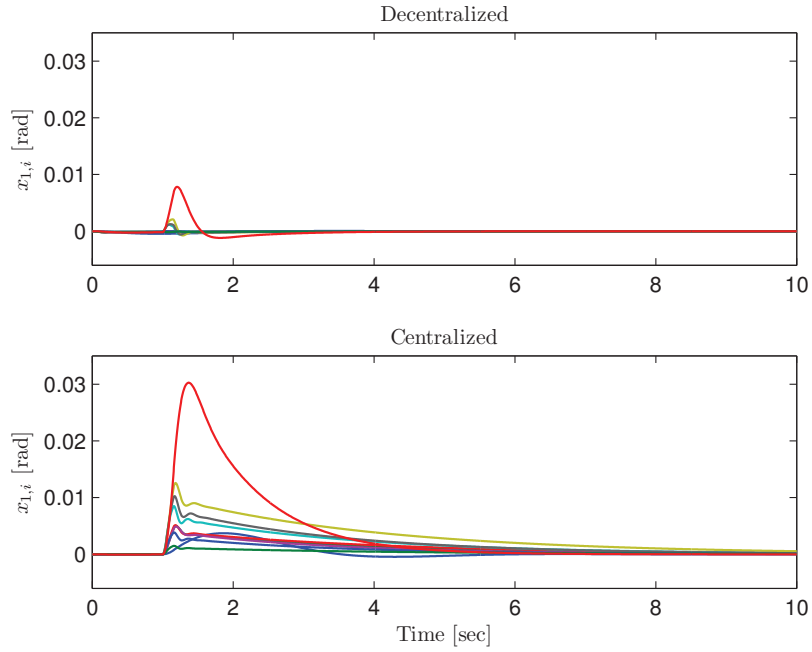

Figure 5.2: Angle errors $x_{1,i}$ for the case of intermittent 3φ fault.

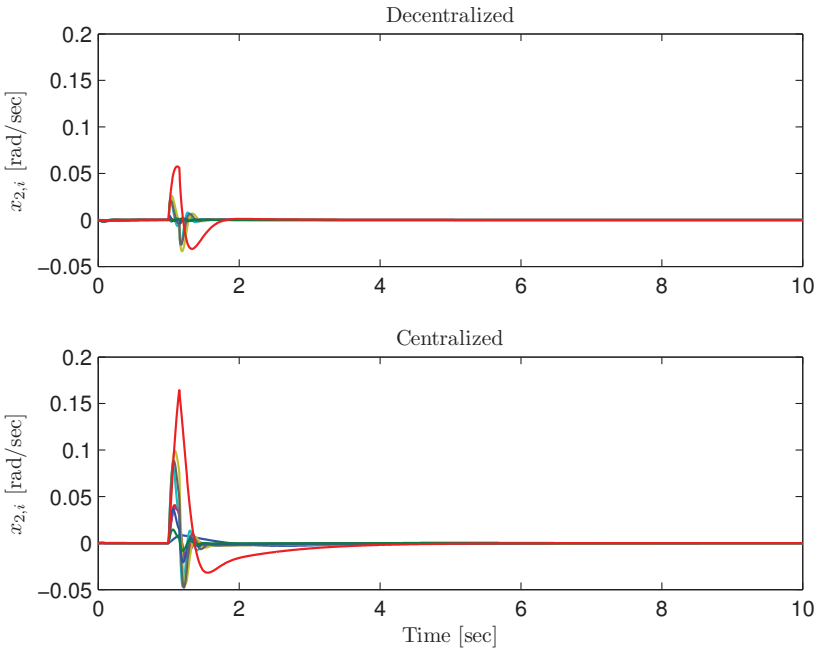

Figure 5.3: Angular speed deviations $x_{2,i}$ for the case of intermittent 3φ fault.

5.4.2 Permanent line switching between bus 17 and 18

This fault consists in a permanent disconnection of the transmission line between bus 17 and 18 followed by a full load trip in bus 18 at $t = 1$ (seconds). After 0.15 seconds the controller is updated and stabilizes the system to the new operating point. In Figures 5.9

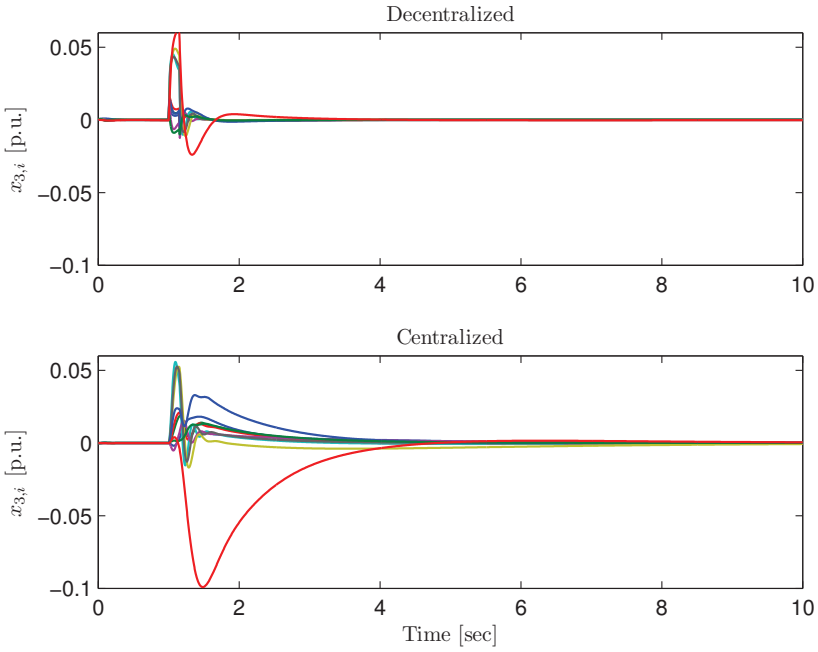

Figure 5.4: Voltage errors $x_{3,i}$ for the case of intermittent 3φ fault.

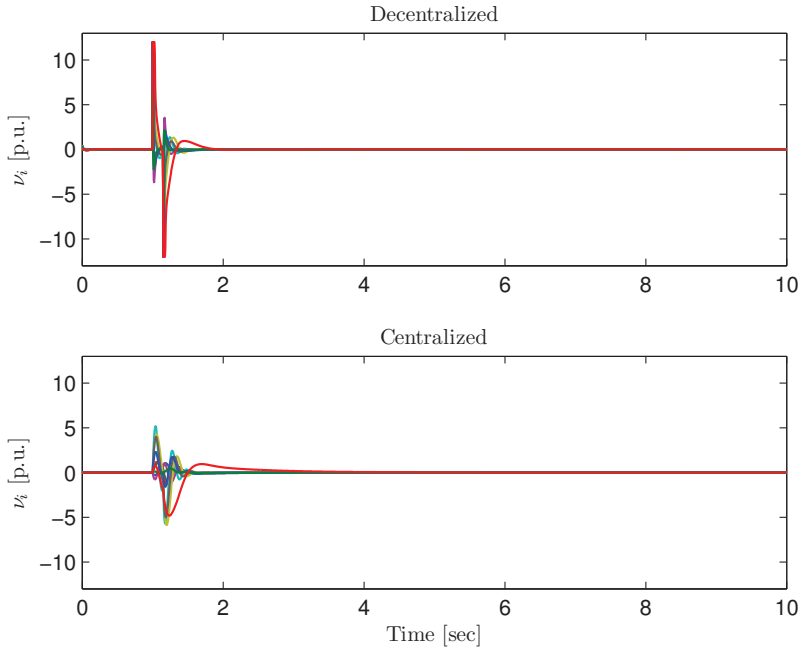

Figure 5.5: Control signals ν_i for the case of intermittent 3φ fault.

to 5.13 the time histories of the state errors of the ten machines, the control inputs and the Lyapunov function are depicted.

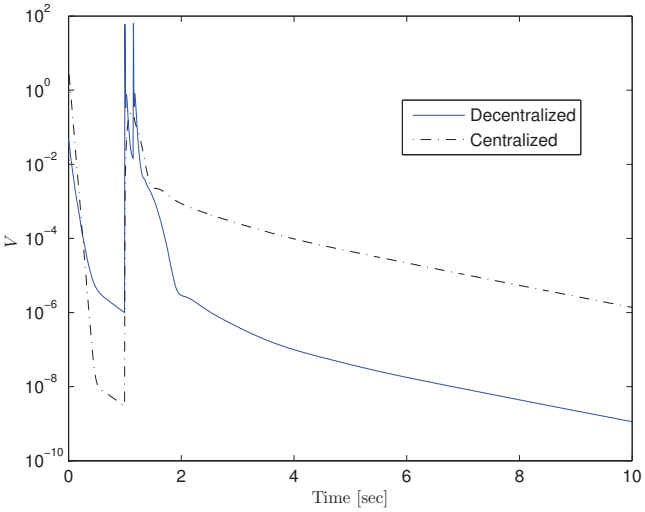

Figure 5.6: Lyapunov functions for the case of intermittent 3φ fault.

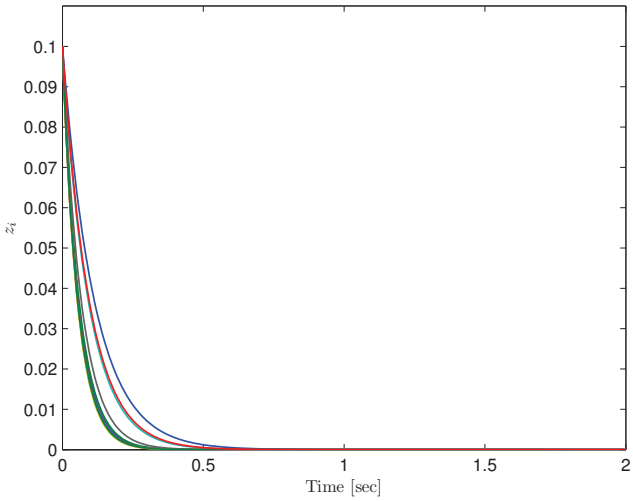

Figure 5.7: Estimation error z_i for the case of intermittent 3φ fault.

5.4.3 Permanent failure in generator 10

In this case, the generator number 10 is suddenly disconnected from the network at $t = 1$ (seconds), this causes a significant lack of electrical power injected into the system. Assuming all post–fault parameters and equilibrium points are known, at $t = 1.15$ (seconds) the controller is updated and stabilizes the system to the new operating point. Note that the power demand remains the same and the swing bus number 2 provides the power that the generator 10 was contributing to the network. Figures 5.14 to 5.18 show the state errors, the control inputs and the Lyapunov function for both decentralized and centralized cases. In these figures the voltage of machine number 10, which is disconnected after the fault, diverges while the remaining machines reach another equilibrium point.

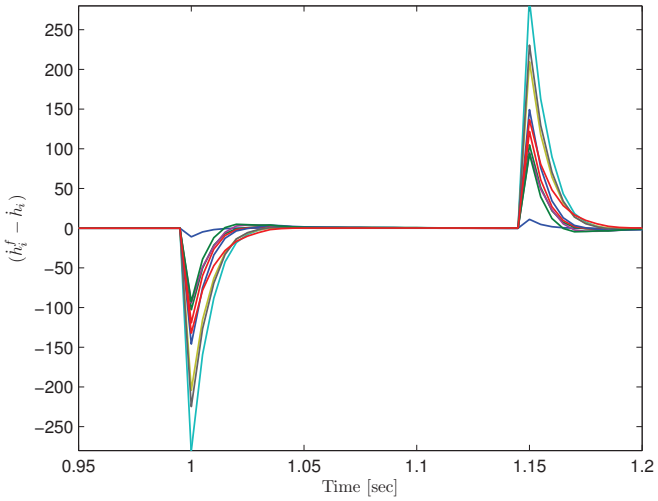

Figure 5.8: Difference $\dot{h}_i^f - \dot{h}_i$ for the case of intermittent 3φ fault.

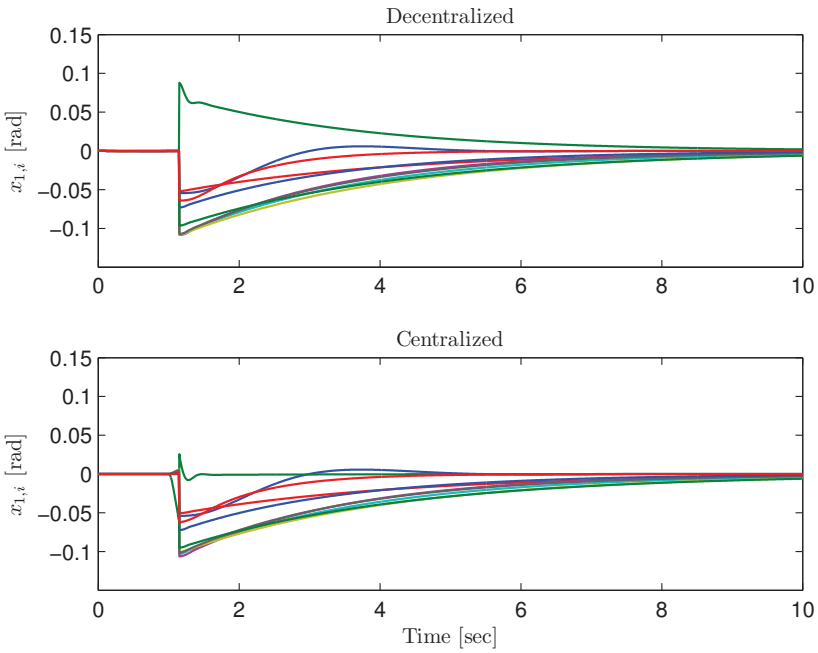

Figure 5.9: Angle errors $x_{1,i}$ for the case of permanent line switching between buses 17-18.

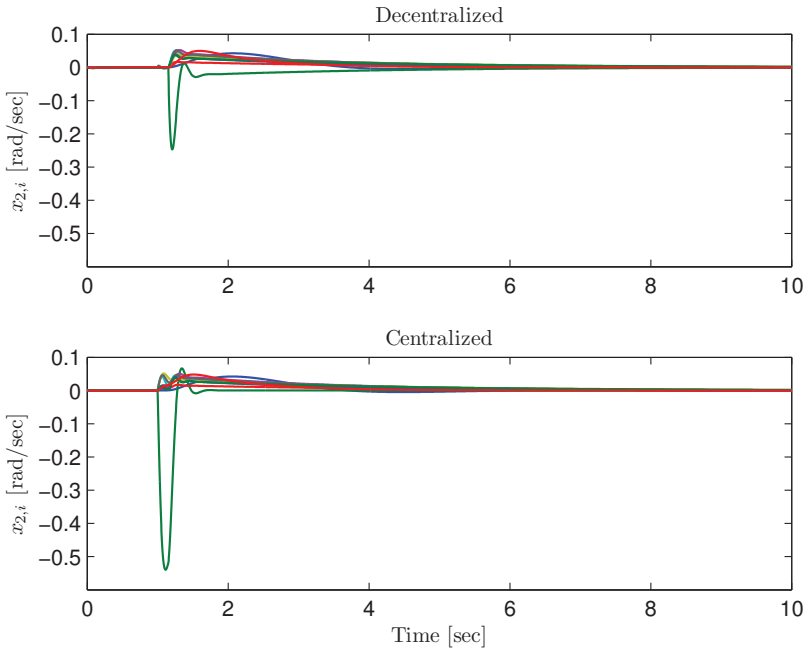

Figure 5.10: Angular speed deviations $x_{2,i}$ for the case of permanent line switching between buses 17-18.

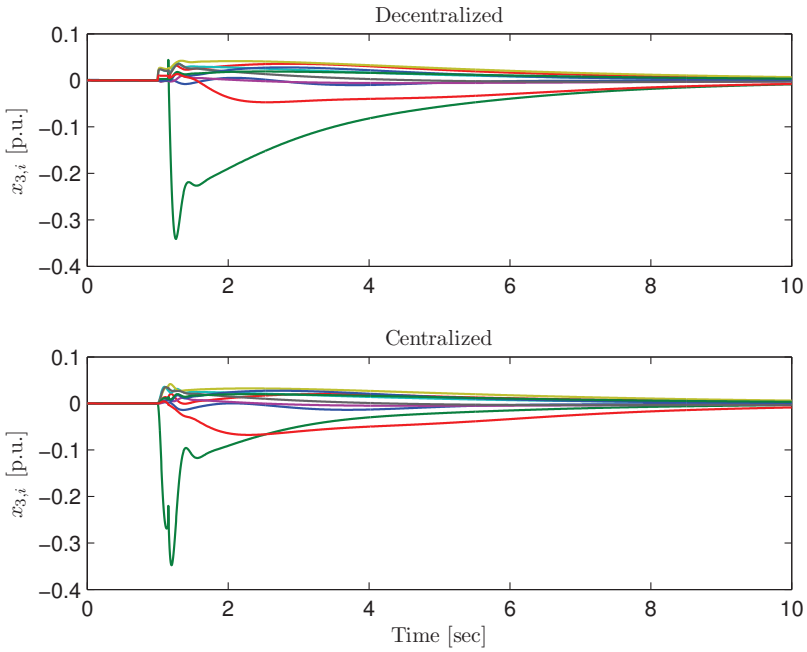

Figure 5.11: Voltage errors $x_{3,i}$ for the case of permanent line switching between buses 17-18.

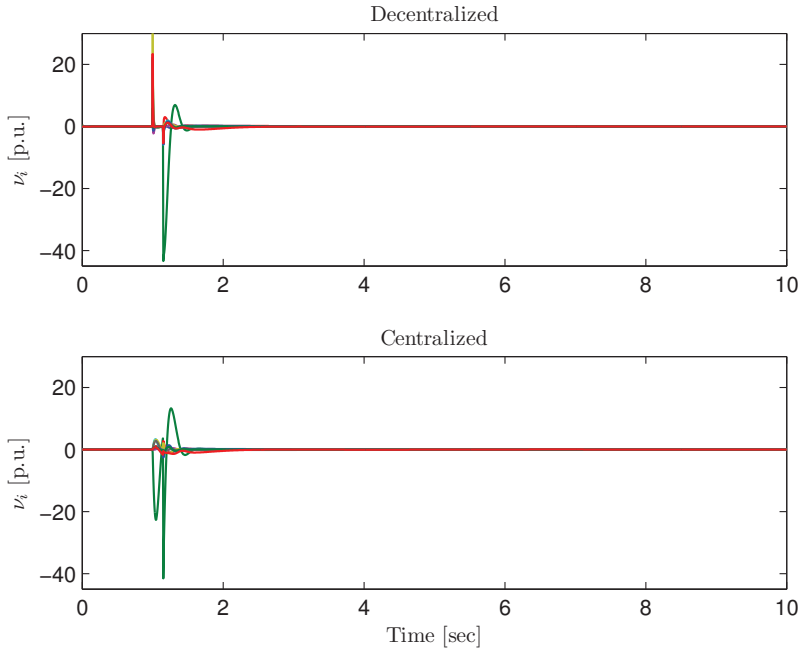

Figure 5.12: Control signals ν_i for the case of permanent line switching between buses 17-18.

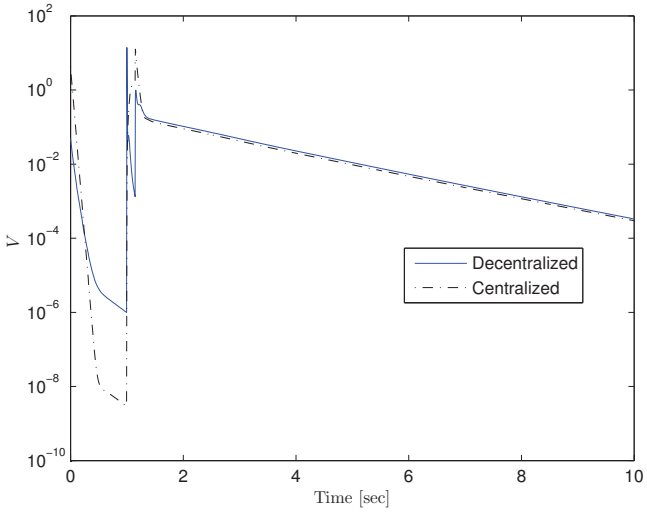

Figure 5.13: Lyapunov functions for the case of permanent line switching between buses 17-18.

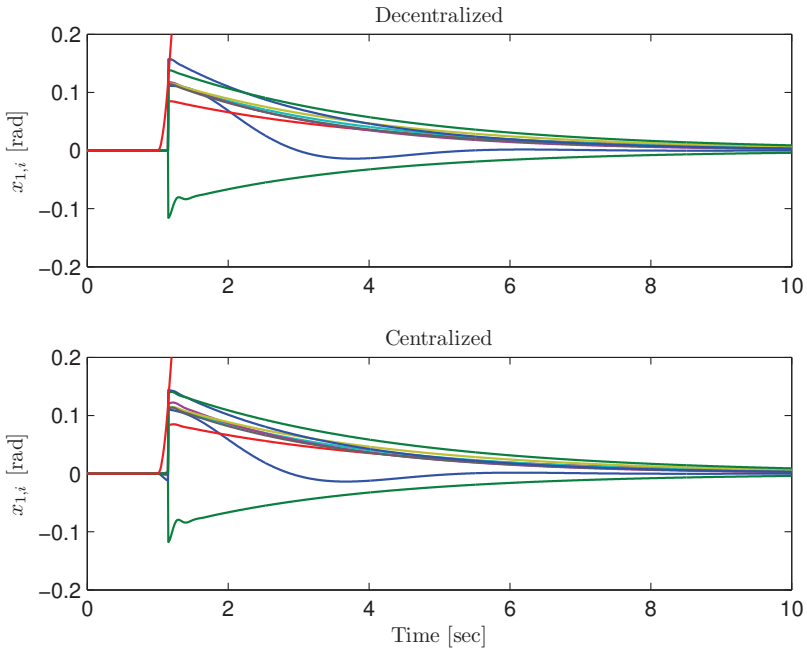

Figure 5.14: Angle errors $x_{1,i}$ for the case of permanent failure in generator.

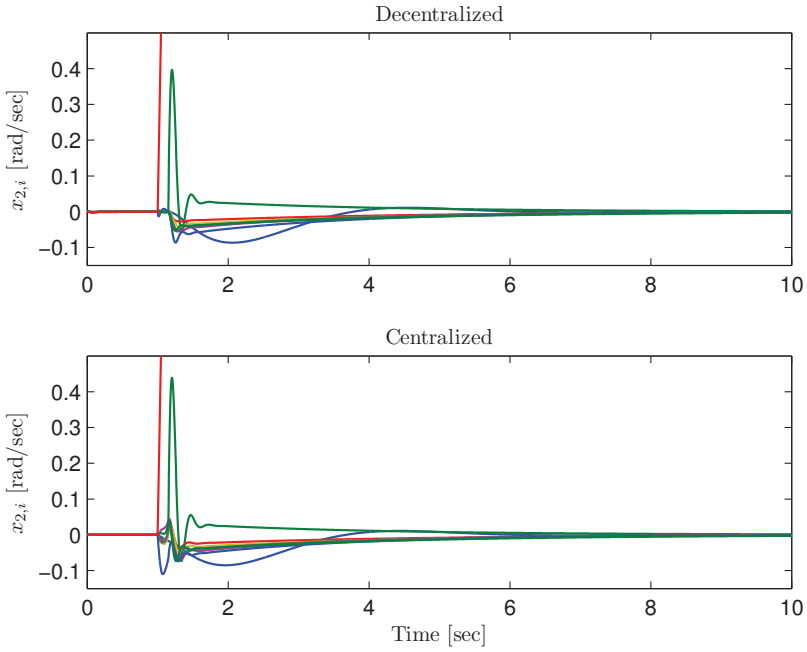

Figure 5.15: Angular speed deviations $x_{2,i}$ for the case of permanent failure in generator.

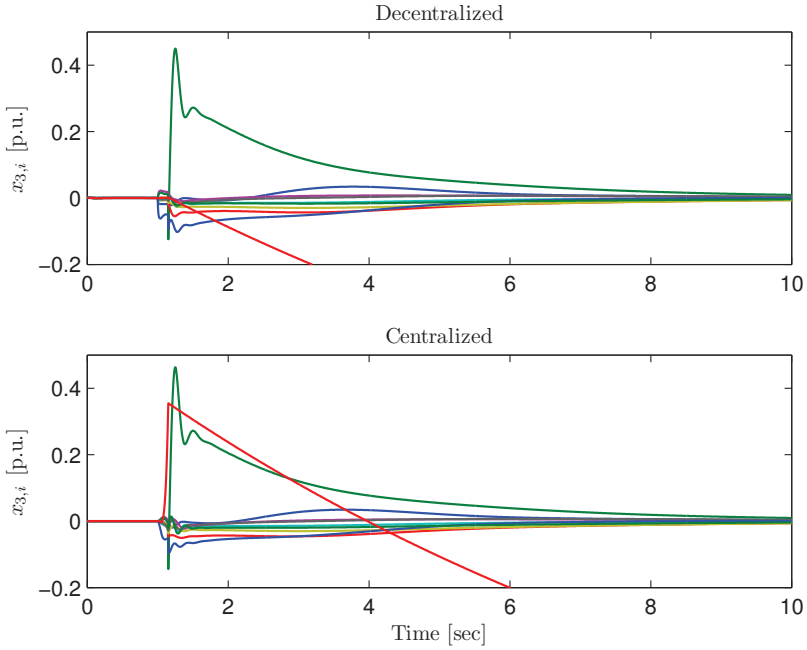

Figure 5.16: Voltage errors $x_{3,i}$ for the case of permanent failure in generator.

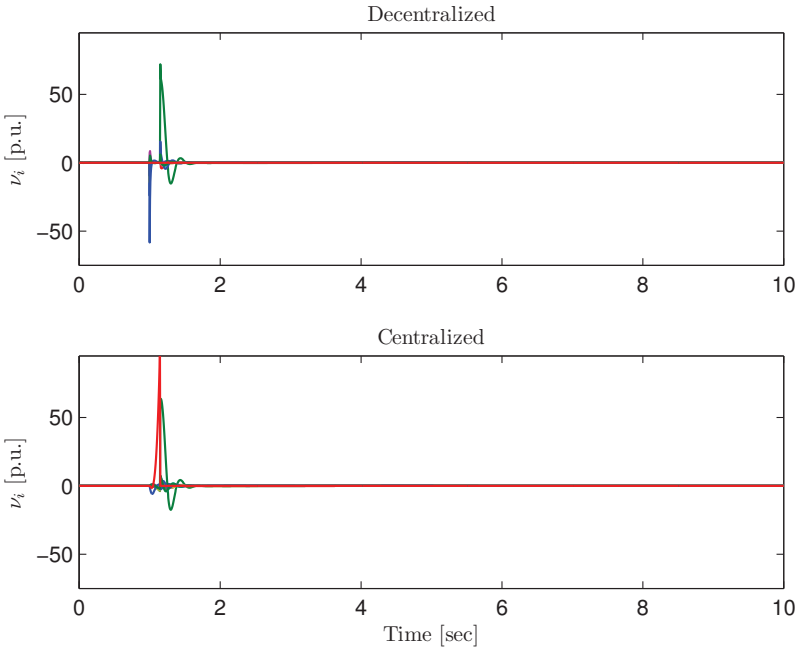

Figure 5.17: Control signals ν_i for the case of permanent failure in generator.

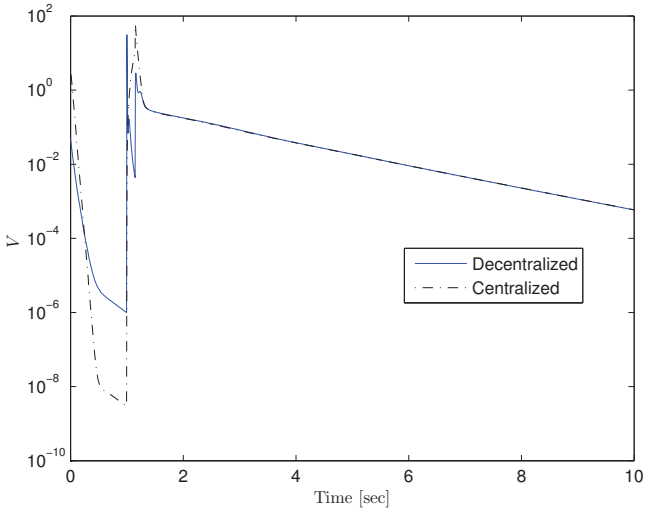

Figure 5.18: Lyapunov functions for the case of permanent failure in generator.

Chapter 6

Conclusions and Future Work

6.1 Concluding remarks

This thesis research deals with three schemes for transient stabilization of power systems, namely, a nonlinear *centralized* controller, a linear *decentralized* controller and finally a nonlinear *decentralized* controller given in chapter 3, 4 and 5 respectively.

The aforementioned controllers are based on the classical three-dimensional flux decay EPS model with lossy transmission lines. This model, concisely represents the dynamics of N generator interconnected through transformers, transmission lines and loads. The states are the angle δ, the speed deviation ω and the voltage behind the transient reactance E. In some sense this representation is considered artificial but despite this fact, it has been largely used by both power systems and control communities. We make special emphasis on the electromagnetic power P_{ei}, which is the link between the electrical and the mechanical part of the generator and highly nonlinear. As a result, both nonlinear controllers are naturally design to cope this nonlinearity aiming attractiveness of a given equilibrium point. Other nonlinearities are presented in the electrical part, *i.e.* the dynamical equation of E, but in this case a partial linearizing control laws (see equations (3.6) and (5.28)) are used to cope them. This design step is not robust since parameter variation can exist in modeling. Either way, Chapter 5 intends to relax this assumption employing I&I adaptive theory to estimate the difference $(x_d - x'_d)$ and consequently robustify (5.28).

In Chapter 3, we have presented a solution to the longstanding problem of designing a globally asymptotically stabilizing controller for multi-machine power systems with non-negligible transfer conductances, this means, considering lossy transmission fulfilling the algebraic condition (3.20), which is inspired from Gershgorin's circle theorem. However, these results involve some assumptions that stymies its practical applicability, these are: full state measurement availability (centralized feature involving no information exchange constraints), full knowledge on system parameters, matrix invertibility (which is computationally expensive). Note that, a central controller for power systems is justified just by the use of phasor measurement units (PMU), which allows real time knowledge of interest variables like current, voltage frequency and angles at specific network locations. Similarly to most developments reported by the control theory community on the transient stability problem, this kind of work in within the framework of fundamental research where basic issues, like solvability of the problem, are addressed. However, differently

from the studies showing only the existence of stabilizing control laws, this nonlinear scheme proves, through a constructive proof, that a globally asymptotically stabilizing controller can indeed be explicitly designed. Moreover, the required conditions to select the control gains are founded via stability analysis in the sense of Lyapunov.

On the other hand, the proposed control scheme detailed in chapter 5, contrasts with its *centralized* counter part, since the on–line information exchange between machine controllers is no longer required. The *decentralization* process is carried out using the local measurements of the local state variables, the active and the reactive power , which are available with existing technology and an approximate differentiator used to estimate the time derivative of the function h_i. Additionally, the proposed scheme uses—in a certainty–equivalent way—the estimation of the difference between the direct axis reactance and the direct axis transient reactance $(x_d - x'_d)$ in the control law, providing robustness to the inner–loop partial linearizing control term. Besides the fundamental feature of being implementable with local measurements, the new controller is less computationally demanding than the *centralized* controller, since there is no need to compute a matrix inversion. Furthermore, the stability analysis of the new scheme add two new terms to the (*centralized*) Lyapunov function, corresponding to the new *adaptive* and *decentralized* features. Unfortunately, this analysis relies on the (a priori unverifiable) assumption of availability of an asymptotically convergent estimate of the time derivative of the signal h_i made by the approximate differentiator. Finally in this part is presented a new way to reconstruct the internal generator voltage E which to the date is a new result.

Comparing simulation results between nonlinear controller considering various fault scenarios show that, due to the direct measurement of local variables, *the decentralized* scheme outperforms the *centralized* one, alas, requiring faster control signals with larger amplitudes. It has also been verified that the approximate differentiator (5.26) is indeed doing its job, hence the critical Assumption 5.3.1 is actually verified.

In contrast to the above results, a methodology to stabilize large-scale interconnected LTI systems via *decentralized* observer-based control has been presented in Chapter 4. These scheme represents a new result since to the date different approaches have been considered for the same purpose. The restriction of limited exchange of information between subsystem has been overcome using I&I observers that, as is well–known [Astolfi et al., 2008], have a novel structure consisting of an integral part and a proportional part. A similar construction has been proposed in [Cumming, 1969] and [Gopinath, 1971] to include a correction term in standard Luenberger's reduced order observer. The proposed procedure, however, seems more involved and less systematic than the I&I observer given here. Finally, the proof of existence of the observer gains that stabilize the system reduces to a simple LMI test, in addition a circumference LMI region was used to located the eigenvalues of the observer.

The validity of the theory presented in here has been tested through numerical simulation. For instance, both nonlinear *centralized/decentralized* controllers are applied to the 10-machine New England benchmark which is widely used by the community to validate results. For the control scheme presented in Chapter 4, despite its linear nature, a two

machine nonlinear system has been used for the same purpose. These simulations comprise several realistic scenarios, these are: *a)* intermittent 3φ fault in bus number 16, *b)* permanent line switching between bus 17 and 18 followed by a full load trip in bus 18, and finally *c)* permanent failure in generator 10. What's more, the *centralized* nonlinear controller is tested facing higher dynamics since the power network was build using Matlab power system toolbox blocks where larger and more complex dynamics than the reduced model are considered.

6.2 Future work

The results obtained in this work have motivated further research on the following issues.

- The nonlinear decentralized scheme can be improved considering the reconstruction of the voltage E via (5.6), and the estimation of the parameters τ and $(x_d - x'_d)$, simultaneously.
- The relaxation of Assumption 5.3.1 by using a switching strategy reported [Casagrande et al., 2011a] could provide the time derivative of h_i in a more suitable way.
- Since the equilibrium of a given power system might not be known in practice, an estimator for both $\bar{\delta}_i$ and $\bar{E}_i$ could provide an interesting feature to the proposed controllers.
- For the linear scheme, would be interesting to use other LMI regions to locate the observer eigenvalues, these could be a half plane with $\mathrm{R}(z) < -q$ with q positive or a conic sector at the origin with pre-specified opening angle.
- Validate the theory in Chapter 4 with other type of systems like communications channels.
- For the same purpose as the one detailed in Chapter 4, it would be interesting to develop a nonlinear scheme.

Bibliography

Anderson, P. and Fouad, A. (2003). *Power System Control and Stability*. Wiley-Interscience.

Astolfi, A., Karagiannis, D., and Ortega, R. (2008). *Nonlinear and Adaptive Control with Applications*. Springer.

Bergen, A. and Vital, V. (2000). *Power System Analysis*. Prentice-Hall.

Bollobas, B. (1998). *Modern Graph Theory*. Springer, New York.

Boyd, S., Ghaoui, L. E., Feron, E., and Balakrishnan, V. (1994). *Linear Matrix Inequalities in System and Control Theory*. SIAM.

Casagrande, D., Astolfi, A., Langarica, D., and Ortega, R. (2014). Solution to the multimachine transient stability problem and simulated validation in realistic scenarios. *IET Generation, Transmission & Distribution*.

Casagrande, D., Astolfi, A., and Ortega, R. (2011a). Asymptotic stabilization of passive systems without damping injection: A sampled integral technique. *Automatica*, 47:262–271.

Casagrande, D., Astolfi, A., and Ortega, R. (2011b). Global stabilization of non–globally linearizable triangular systems: Application to transient stability of power systems. *50th IEEE Conference on Decision and Control and European Control Conference, Orlando, FL, USA*.

Casagrande, D., Astolfi, A., Ortega, R., and Langarica, D. (2012). A solution to the problem of transient stability of multimachine power systems. *51th IEEE Conference on Decision and Control and European Control Conference, Maui, HI, USA*.

Chiang, H., Chu, C., and Cauley, G. (1995a). Direct stability analysis of electric power systems using energy functions: Theory, applications, and perspective. *Proc. IEEE,*, 83(11):1497–1529.

Chiang, H., Chu, C., and Cauley, G. (1995b). Direct stability analysis of electric power systems using energy functions: Theory, applications, and perspectives. *Proceedings of the IEEE*, 83(11):1497–1529.

Cumming, D. (1969). Design of observers of reduced dynamics. *Electron. Lett.*, 5(10):213–214.

Dib, W. (2009). *Transient Stability of Multi-Machine Power Systems.* Université Paris-sud XI, LSS.

Dib, W., Astolfi, A., and Ortega, R. (2009a). A state observer for multimachine power systems based on model reduction by moment matching. *European Control Conference, Budapest, Hungary,.*

Dib, W., Kenné, G., and Lamnabhi-Lagarrigue, F. (2009b). An application of immersion and invariance to transient stability and voltage regulation of power systems with unknown mechanical power. *Joint 48th IEEE Conference on Decision and Control and 28th Chinese Control Conference, Shanghai, China.*

Dib, W., Ortega, R., Astolfi, A., and Hill, D. (2011). Improving transient stability of multi-machines power systems: Synchonization via immersion and invariance. *American Control Conference, San Francisco, California, USA.*

Dib, W., Ortega, R., Barabanov, A., and Lamnabhi-Lagarrigue, F. (2009c). A "globally" convergent controller for transient stability of multi–machine power systems using the structure-preserving models. *IEEE Transactions on Automatic Control*, 54(9):2179–2184.

El-Hawary, M. (2008). *Introduction to Electrical Power Systems.* Wiley-IEEE Press.

Elgerd, O. (1982). *Electric Energy Systems Theory.* Mcgraw-hill.

et al, V. D. (2009). *Modeling and Control of Complex Physical Systems: The Port-Hamiltonian Approach.* Springer-Verlag, Berlin.

Evans, L. (2010). Partial differential equations: Graduate studies in mathematics. *American Mathematical Society*, 19.

Fardo, S. and Patrick, D. (2009). *Electrical Power Systems Technology.* The Fairmont Press.

Fu, J. and Zhao, J. (2005). Robust nonlinear excitation control based on a novel adaptice back-stepping design for power systems. *American Control Conference, Portland, OR, USA.*

Fusco, G. and Russo, M. (2011). Nonlinear control design for excitation controller and power system stabilizer. *Control Engineering Practice*, 19.

Galaz, M. (2003). *Nonlinear Control of Power Systems.* Université Paris-sud XI, LSS.

Galaz, M., Ortega, R., and Bazanella, A. (2004). On parameter estimation for excitation control of synchronous generators. *International Journal of Adaptive Control and Signal Processing*, 18.

Galaz, M., Ortega, R., Bazanella, A., and Stankovic, A. (2001). An energy-shaping approach to the design of excitation control of synchronous generators. *Automatica*, 39(1).

Gopinath, B. (1971). On the control of linear multiple input-output system. *Bell Syst. Tech. J.*, 50:1063–1081.

Guo, Y., Hill, D., and Wang, Y. (2000). Nonlinear decentralized control of large-scale power systems. *Automatica*, 36:1275–1289.

IEEE/CIGRE (2004). Joint task force on stability terms and definitions: Definition and classification of power system stability. *IEEE Transactions on Power Systems*, 19:1387–1401.

Isidori, A. (1995). *Nonlinear Control Systems*. Springer.

Janković, M., Sepulchre, R., and Kokotović, P. (1997). *Constructive Nonlinear Control*. Springer-Verlag.

Kailath, T. (1980). *Linear Systems*. Prentice-Hall.

Karlsson, D., Hemmingsson, M., and Lindahl, S. (2004). Wide area system monitoring and control. *IEEE Power & Energy Magazine*, 2(5):68–76.

Khalil, H. (2000). *Nonlinear Systems*. Prentice-Hall.

Korobov, V. and Pavlichkov, S. (2008). Global properties of the triangular systems in the singular case. *Journal of Mathematical Analysis and Applications*, 342.

Krause, P., Wasynczuk, O., and Sudhoff, S. (2002). *Analysis of Electric Machinery and Drive Systems*. IEEE Press.

Krstić, M., Kanellakopoulos, I., and Kokotović, P. (1995). *Nonlinear and Adaptive Control Design*. John Wiley & and Sons.

Kundur, P. (1994). *Power System Stability and Control*. McGraw-Hill.

Lam, S. and Davison, E. (2010). The real decentralized fixed mode radius of lti systems. *In Proceedings of the 50th IEEE Conference on Decision and Control, New Orleans, LA, USA*, pages 3036–3041.

Lavaei, J. and Aghdam, A. (2008). Control of continuous-time lti systems by means of structurally constrained controllers. *Automatica*, 44:141–148.

Lin, W. and Qian, C. (2002). Adaptive control of nonlinearly parametrized systems. *IEEE Transactions on Automatic Control*, 47(8).

Lofberg, J. (2004). Yalmip: A toolbox for modeling and optimization in matlab. *IEEE International Symposium on Computer Aided Control Systems Design, Taipei*, pages 284–289.

Loukianov, A., Canedo, J., Friedman, L., and Soto-Cota, A. (2011). High-order block sliding-mode controller for a synchronous generator with an exciter system. *IEEE Transactions on Industrial Electronics*, 58(1).

Lu, Q., Sun, Y., and Mei, S. (2001). *Nonlinear Control Systems and Power System Dynamics Synchronous Generators*. Kluwer Academic Publishers.

Lunze, J. (1992). *Feedback Control of Large-Scale Systems*. Prentice-Hall.

Manjarekar, N., Banavar, R., and Ortega, R. (2012). Stabilization of a synchronous generator with a controllable series capacitor via immersion and invariance. *Int. J. Robust Nonlinear Control*, 22.

Marquez, H. (2003). *Nonlinear Control Systems*. Wiley.

Miller, D. and Davison, E. (2012). An algebraic characterization of quotient decentralized fixed modes. *Automatica*, 48:1639–1644.

Ortega, R., Galaz, M., Astolfi, A., Sun, Y., and Shen, T. (2005). Transient stabilization of multimachine power systems with nontrivial transfer conductances. *IEEE Transactions on Automatic Control*, 50(1):60–75.

Ortega, R., Galaz, M., Bazanella, A., and Stankovic, A. (2001). Excitation control of synchronous generators via total energy-shaping. *American Control Conference, Arlington, VA, USA*.

Ostertag, E. (2011). *Mono- and Multivariable Control and Estimation: Linear, Quadratic and LMI Methods*. Springer.

Pai, M. (1989). *Energy Function Analysis for Power System Stability*. Kluwer Academic Publishers.

Pavella, M., Ernst, D., and Ruiz-Vega, D. (2000). *Transient Stability of Power Systems: A Unified Approach to Assesment and Control*. Springer.

Pavlichkov, S. and Ge, S. (2009). Global stabilization of the generalized mimo triangular systems with singular input-output links. *IEEE Transactions on Automatic Control*, 54(8).

Prioste, F. and e Silva, A. S. (2007). Power system stability improvement by feedback of state and algebraic variables. In *Proceedings of the IEEE Powertech*.

Psillakis, H. and Alexandridis, A. (2007). A simple nonlinear adaptive-fuzzy passivity-based control of power systems. *Nonlinear Dynamics and Systems Theory*, 7(1):51–67.

Qian, C. and Lin, W. (2001). A continuous feedback approach to global strong stabilization of nonlinear systems. *IEEE Transactions on Automatic Control*, 46(7).

Song, C., Feng, G., and Wang, Y. (2013). Decentralized dynamic coverage control for mobile sensor networks in a non-convex environment. *Asian Journal of Control*, 15(2):512–520.

Sun, L., Feng, J., Dimirovski, G., and Zhao, J. (2009). Adaptive robust h_∞ control of the generator excitation system. *American Control Conference, St. Louis, MO, USA*.

Tsinias, J. (1997). Triangular systems: A global extension of the coron-praly theorem on the existence of feedback-integrator stabilizer. *European Jornal of Control*, 3.

Tsinias, J. and Karafyllis, I. (1999). Iss property for time-varying systems and application to partial-static feedback stabilization and asymptotic tracking. *IEEE Transactions on Automatic Control*, 44(11).

van der Schaft, A. (2010). Characterization and partial synthesis of the behavior of resistive circuits at their terminals. *Systems and Control Letters*, 59:423–428.

Varga, R. (2009). *Matrix Iterative Analysis*. Springer Series in Computational Mathematics. Springer.

Čelikovský, S. and Arande-Bricaire, E. (1999). Constructive nonsmooth stabilization of triangular systems. *Systems & Control Letters*, 36.

Čelikovský, S. and Nijmijer, H. (1996). Equivalence of nonlinear systems to triangular form: the singular case. *Systems & Control Letters*, 27.

Šiljak, D. (1991). *Decentralized Control of Complex Systems*. Academic Press.

Šiljak, D. and Zečević, A. (2005). Control of large-scale systems: Beyond decentralized feedback. *Elsevier Annual Reviews in Control*, 29:169–179.

Wang, S. and Davison, E. (1973). On the stabilization of decentralized control systems. *IEEE Transactions on Automatic Control*, AC-30(1):473–478.

Yan, R., Dong, Z., Saha, T., and Majumder, R. (2010). A power system nonlinear adaptive decentralized controller design. *Automatica*, 46:330–336.

Zečević, A. and Šiljak, D. (2010). *Control of Complex Systems: Structural Constraints and Uncertainty*. Springer.

Zonetti, D. (2011). An hamiltonian approach to power systems modeling. *Université de Paris-Sud XI*.

Zonetti, D., Fiaz, S., Ortega, R., Schaft, A. V. D., Langarica, D., and Scherpen, J. (2012). Du bond graph au modèle hamiltonien à ports d'un système de puissance. *Conférence Internationale Francophone d'Automatique, Grenoble, France, July*.

.